SPSE

Photographic

SCIENCE AND ENGINEERING

C. E. Kenneth Mees, 1882–1960 313

On the Relation between Color Correction and Frequency Response in the Central Part of the Image of a Group of Photographic Systems *T. Malinowski and W. Mandler* 317

Spread Function and Contrast Transfer Function of Photographic Layers • *H. Frieser* 324

The Effect of the Variables of a Photographic System on Detail Rendition, with Special Reference to Camera Motion • *Robert N. Wolfe and Sam A. Tuccio* 330

Theoretical Considerations Concerning the Relationship between Characteristic Curves of Elementary and Thick Layers • *E. Klein* 341

A Photographic Process Using Persistent Internal Polarization in Phosphors *H. P. Kallmann, J. Rennert, and M. Sidran* 345

Rapid-Drying Characteristics of Several Films for Aerial Photography • *James W. Boyd* 354

Book and Journal Reviews 359

New Products and Developments • *Frank Smith* 365

Annual Index 367

Erratum — The Effect of Gamma-Ray Exposure on Camera Films, *by G. M. Corney*, facing page 367

Coming Technical and Scientific Meetings 353

1961 ANNUAL CONFERENCE ANNOUNCEMENT 329

Volume 4 · Number 6

NOVEMBER-DECEMBER · 1960

Editorial Policy

Photographic Science and Engineering is dedicated to the advancement of the knowledge and application of photography and other directly related sciences. Its pages are open to all who wish to report on new studies dealing with the theory of photosensitive systems, the design of photographic instruments and apparatus useful in the treatment of photographic materials, photographic optics and illuminants, the use of photography for scientific or engineering measurement or recording, and photographic instrumentation and data recording. Only original papers should be submitted except on special invitation.

Manuscripts should be typed double-spaced on white bond paper with $1\frac{1}{4}$-inch margins all around. Literature references should be exact, and should include titles of journals, names of authors, numbers of volumes and pages, and year of publication. Book references should include title of volume, names of authors, publisher, number of edition, year of publication, and chapter and pages cited.

Graphs, charts, and other line illustrations should conform to good usage such as given in the American Standards Association Document Y-15, "A Guide for Preparing Technical Illustrations for Publication and Projection." Continuous-tone photographs should be made on 8 by 10-inch glossy paper and should show pertinent image detail sufficiently clearly to permit reduction to fit a 3-inch column in this journal. All illustrations should be numbered in soft blue pencil on the back to correspond with captions typed on a separate page. Tables should also be submitted on separate pages appropriately identified. An abstract should accompany each manuscript.

Papers intended for publication (two copies) and books for review should be submitted to the editor, T. H. James, Research Laboratories, Eastman Kodak Co., Rochester 4, N.Y. Correspondence regarding proofs and reprints should be directed to Jennie H. Allen, 94 Hastings Ave., Croton-on-Hudson, N.Y. All papers submitted for publication will be reviewed by members of the Editorial Review Board and if not accepted will be returned to the author. Published papers become the property of the Society and are protected by appropriate copyrights. Each author receives one copy of the issue in which his contribution appears. Authors may order reprints of their papers at the time they return the galley proofs. The Society does not assume responsibility for material in transit, nor guarantee publication of unsolicited material.

Photographic
SCIENCE AND ENGINEERING

official publication of the
Society of Photographic Scientists and Engineers

November–December 1960
Volume 4, Number 6

EDITORIAL STAFF

T. H. James, *Editor*
Jennie H. Allen, *Managing Editor*
H. F. Nitka, *Associate Editor*
Norman A. Exley, *Assistant Editor*
S. C. Goddard, *Feature Editor*
Frank Smith, *Feature Editor*

EDITORIAL REVIEW BOARD

J. H. Altman	Marilyn Levy
R. S. Barrows	C. S. McCamy
Richard L. Bent	J. A. Maurer
B. R. Harriman	F. W. H. Mueller
John H. Jacobs	H. F. Nitka
R. Clark Jones	W. S. Shoemaker
Peter Krause	Thos. D. Smith
John H. Ladd	William West
K. G. Leistner	Deane R. White

Photographic Science and Engineering is published six times a year by the Society of Photographic Scientists and Engineers.

• Address remittances, orders for subscriptions and for single copies, claims for missing numbers, and notices of change of address to the Society at Box 1609, Main Post Office, Washington, D. C. Subscription to nonmembers of the Society, $12.00 per year; subscription cost to members included in $8.00 annual dues; single copies, $2.00 each.

• The publication office is at 20th and Northampton Streets, Easton, Pa. Second-class mail privileges authorized at Easton, Pa. This publication is authorized to be mailed at the special rates of postage prescribed by Section 132.122.

• The Society is not responsible for the accuracy of statements made by authors and does not necessarily subscribe to their views.

© Copyright 1961 by the Society of Photographic Scientists and Engineers, Inc. Permission to reprint any part of the contents, except in reviews and abstracts, must be obtained in writing from the Editorial Vice President.

PHOTOGRAPHIC SCIENCE AND ENGINEERING
Volume 4, Number 6, November–December 1960

C. E. Kenneth Mees, 1882–1960

Dr. C. E. Kenneth Mees died August 15, 1960, in Honolulu, Hawaii, where he had lived since his retirement in 1955. He was 78. Internationally known for his contribution to the literature and theory of the photographic process and for his pioneering activities in industrial research, he was an outstanding figure in the growth of photography during this century.

Charles Edward Kenneth Mees was born at Wellingborough, England, on May 26, 1882, the son of a Wesleyan minister. Although his early schooling was of the conventional classical type, his interest in chemistry was aroused when, at the age of ten, he watched the schoolmaster prepare chlorine and later was allowed to repeat the experiment himself. "I began to see at once, it seemed to me, what a marvelous thing science was," Dr. Mees recalled.

"From there I went to a school in England which didn't approve of science . . . . . but, in spite of their classical views, they had a laboratory. Now, laboratories need keeping clean, and before long I had made a bargain with the science master that if I kept the laboratory clean, I could have a key to it. I could escape there from the hordes of ruffians outside who wanted to play football and things of that sort, and I could enjoy myself in the laboratory."

After a course of studies at St. Dunstan's College, Mees entered University College, London, where the professor of chemistry was the great experimentalist, Sir William Ramsay. At the same time, another St. Dunstan student, S. E. Sheppard, entered University College. Ramsay felt that both were well advanced in chemistry and arranged for them to start at once on some elementary research. Mees was assigned to work with E. C. C. Baly, who was photographing the spectra of the newly discovered noble gases. "I started to photograph the red end of the iron arc spectrum, using plates which were bathed in Alizarin Blue to make them sensitive to the red. I simply followed the textbooks there. Looking back on the results, I can only conclude I wasn't very good at sensitizing plates"—a deficiency that was remedied most effectively in later years.

The major field of interest in Ramsay's laboratory at that time was the study of the noble gases which had been isolated from the atmosphere by Ramsay and his associates. Mees and Sheppard, however, had become interested in photography and, inspired by a classic paper written in 1890 by Hurter and Driffield, started a research program on the photographic process. Ramsay was enthusiastic about this program, and arranged for Mees and Sheppard to present the work to the University as a thesis for the B. Sc. degree in 1903. For the next three years they continued to work on sensitometry, statics and kinetics of development, microscopic structure of the developed image, the theory of fixation, and the effects of oxidizing agents on the latent image. The results were published in a series of papers between 1904 and 1907, and were presented jointly as their thesis for the degrees of Doctor of Science in 1906. The thesis was published in 1907 as a book, *Investigations on the Theory of the Photographic Process*, which in later years became generally known as "Sheppard and Mees."

Mees was interested in an academic career, but Ramsay, who had a very clear vision of the part that science should play in industry, persuaded him to enter the photographic industry. He joined the firm of Wratten and Wainwright as a partner and joint managing director. During his six years with this firm, he manufactured a successful series of light-filters, darkroom safelights, and dye-sensitized plates (he had discovered that much improved dye-sensitization could be obtained if the shredded emulsion were bathed in the dye solution before coating, instead of bathing the coated plates, the customary procedure at that time). He also introduced special plates for the photoengravers and spectroscopists, carried out research on theory, including the first measurements of the resolving power of photographic materials, and pioneered in the publication of technical instructional booklets.

In 1912, Mees accepted George Eastman's invitation to join the Kodak Company to organize and direct a research laboratory. He now had the opportunity of realizing his two dreams: he would be able to experiment in the field of industrial research on a large scale, and he would have a staff to conduct fundamental research on the science of photography. The very task of organizing a research laboratory of this kind was a research project in itself, since an industrial research laboratory was a rarity at that time. The laboratory he organized was one of the first in America and his pioneering efforts in the field have had an important part in the remarkable growth of industrial research in the following years.

During World War I, all efforts of the laboratory under Mees's direction were concentrated on prob-

lems of military importance, and the first school of aerial photography was founded under his direction at Kodak Park. A serious shortage of organic chemicals for research, previously obtained from Germany, was met by the addition to the research laboratory of a synthetic organic chemistry department. This department has since become a major source of organic chemicals for university and industrial research in this country.

At the close of the war, Mees organized a department for the development of photographic apparatus and became Director of Research and Development. Through his efforts, other new departments were added as needed, including one for emulsion research in 1931 and one for research on cellulose ester yarn and plastics in 1934. Mees was made a director of the company in 1923 and vice-president in charge of research and development in 1934.

Dr. Mees saw the fulfillment of both his dreams. The success of his direction of large scale industrial research was evidenced by the rapid growth in the size and scope of the laboratories and by the contributions which they made to the photographic industry. These contributions include a method of making x-ray emulsions, the reversal process of amateur cinematography, improved cellulose acetate film base, a series of important sensitizing dyes, panchromatic film of high sensitivity for motion-picture work, Verichrome film, the first Kodacolor process (a lenticular film process marketed in 1928), a series of color films based on the dye-forming coupler principle (starting with the Kodachrome process of color motion pictures in 1935), a wide range of special plates and films, including the modern high-speed materials for spectrography and astronomy, and improved equipment for high-vacuum distillation.

The fundamental research program also was highly successful. An important share of the world's research on the theory of the photographic process was carried out in the Kodak laboratories in Rochester, Harrow (England), and Vincennes (France). The theory of tone reproduction was developed, and methods were worked out for the measurement and interpretation of the sensitometric properties of photographic materials. Extensive investigations also were made on the structure of the developed image and its relation to the photographic properties of the image, on the nature of photographic gelatin and its effects upon photographic sensitivity, on the nature of the latent photographic image and the mechanism of its formation and development, on the mechanism of spectral sensitization by dyes, on the relation between the color and constitution of dyes, and on the mechanism of evaporation of liquids in high vacuum. Mees encouraged publication of the results of these fundamental researches and sought to make them available to as widespread a group as possible both by publication in scientific journals throughout the world and by subsequent publications, in shortened form, in the *Abridged Scientific Publications of the Kodak Research Laboratories*. He also encouraged the general dissemination of scientific information—an end to which his own publications have made a substantial contribution. In 1915, at a time when war restricted free exchange among the scientists of the world, he founded the *Monthly Abstract Bulletin* now in its 46th year of coverage of the scientific photographic literature of the world.

By 1942, knowledge of photographic theory had reached a stage where Mees and his associates were able, as he stated, "to put the whole thing together in a book, a very fat and heavy book, in which the whole theory of the photographic process had been put into a form where it made a comprehensible whole." This book, *The Theory of the Photographic Process*, helped to stimulate work in photographic theory in the following years. When it was revised twelve years later, it was necessary to rewrite the entire book and change about one third of its contents.

Dr. Mees was an inspiring director. His colleague, L. A. Jones, said of him: "While he has been successful as an individual research worker... his great success and his great contribution lie in the ability and sagacity he has shown as director.... His unbounded enthusiasm, his vivid imagination, and his uncanny ability to suggest the most fruitful experiments to perform have been a constant source of inspiration and encouragement to the members of his staff. His preeminent fairness to those working under him, his kindliness, and his humanity have endeared him to the hearts of his associates."

His achievements have received formal recognition on many occasions. He was elected a member of the National Academy of Sciences (1950) and a Fellow of the Royal Society of London (1939), a combination of honors accorded to very few scientists. Among the awards given him are: the Henderson Medal of the Royal Photographic Society in 1907, the Silver Medal of the Royal Society of Arts in 1908 (for a paper on color photography), the Progress Medal of the Royal Photographic Society in 1913 and again in 1953, the John Scott Medal and Award of the City of Philadelphia in 1921, the Janssen Medal of the Société Française de Photographie in 1924, the Hurter and Driffield Medal in 1924, the Progress Medal of the Society of Motion Picture Engineers in 1936, the Henry Draper Medal of the National Academy of Sciences in 1936, the Rumford medals of the American Academy of Arts and Sciences in 1943, the Adelskold Medal of the Swedish Photographic Society in 1948, the Progress Medal of the Photographic Society of America (initial award) in 1948, and the Franklin Medal in 1954. In awarding him the first Honorary Membership of the Society of Photographic Engineers (1954), Leo Pavelle said "The task [of choosing the first Honorary Member] was disarmingly simple... no second choice was anywhere in sight."—*T. H. James*

Publications by C. E. K. Mees

This bibliography lists the more important scientific papers and those concerned with the general problems of research.

Schrötter's Carbonic Acid Apparatus. *Chem. News*, **85:** 251 (1902).

On the Development Factor. *Phot. J.*, **43:** 48 (1903) (with S. E. Sheppard).

On the Highest Development Factor Attainable in Any Plate. *Phot. J.*, **43:** 199 (1903) (with S. E. Sheppard). Gamma infinity introduced for the first time.

Instruments for Sensitometric Investigation, with an Historical Résumé *Phot. J.*, **44:** 200 (1904) (with S. E. Sheppard).

The Sensitometry of Photographic Plates. *Phot. J.*, **44:** 282 (1904) (with S. E. Sheppard).

Die Chemischen Reaktionen im Hydrochinonentwickler. *Z. wiss. Phot.*, **2:** 5 (1904) (with S. E. Sheppard).

The Theory of Photographic Processes—On the Chemical Dynamics of Development. *Proc. Roy. Soc.*, **74:** 447 (1904) (with S. E. Sheppard).

On Some Points in Modern Chemical Theory and their Bearing on Development. *Phot. J.*, **45:** 241 (1905) (with S. E. Sheppard).

On the Properties of Homocol as a Sensitizer. *Phot. J.*, **45:** 264 (1905) (with A. J. Newton and S. E. Sheppard).

The Theory of Photographic Processes—II: On the Chemical Dynamics of Development, including the Microscopy of the Image. *Proc. Roy. Soc.*, **76A:** 217 (1905). *Phot. J.*, **45:** 281, 319 (1905) (with S. E. Sheppard).

A Small Concave Grating Spectroscope. *Phot. J.*, **45:** 401 (1905).

The Molecular Condition in Solution of Ferrous Oxalate. *J. Chem. Soc.*, **87-I:** 189 (1905) (with S. E. Sheppard).

Modern Chemistry for Photographic Workers. *Brit. J. Phot.*, **52:** 345, 364, 386, 406, 443 (1905).

Estimation of the Colour Sensitiveness of Plates. *Phot. J.*, **46:** 110 (1906) (with S. E. Sheppard).

Theory of Fixation and the Action of Thiosulphate on Development. *Phot. J.*, **46:** 235 (1906) (with S. E. Sheppard).

A Note on a Panchromatic Emulsion of Silver Erythrosinate. *Phot. J.*, **46:** 300 (1906) (with S. H. Wratten).

Interpretation of Sensitometric Tests. *Brit. J. Phot.*, **53:** 104, 126, 143 (discussion, 179, 617, 636, 797, 857, 899) (1906).

Orthochromatic Plates and Filters. *Brit. J. Phot.*, **53:** 430 (1906) (with W. J. Smith).

Filter Yellow K. *Brit. J. Phot.*, **53:** 765 (1906) (with S. H. Wratten).

Printing and Copying from Screen-Plate Colour Negatives and Positives. *Brit. J. Phot.*, Col. Suppl., **54:** 75 (1907) (with J. H. Pledge).

The Action of Substances upon the Latent Image. *Phot J.*, **47:** 65 (1907) (with S. E. Sheppard).

A Measurement of the Efficiency of Dark Room Filters. *Phot. J.*, **47:** 267 (1907) (with J. K. Baker).

Rapid Filter Blue. *Brit. J. Phot.*, Col. Suppl., **54:** 62 (1907) (with S. H. Wratten).

Development with Insufficient Reducer. *Brit. J. Phot.*, **54:** 172 (1907) (with S. H. Wratten).

The Wedge Spectrograph. *Brit. J. Phot.*, **54:** 384 (1907) (with S. H. Wratten).

Variations in the Watkins Factor. *Brit. J. Phot.*, **54:** 560 (1907) (with S. H. Wratten).

Preparing Colour Duplicates by the Warner-Powrie Process. *Brit. J. Phot.*, **54:** 707 (1907).

Plates Sensitized with Dicyanin and Photography of the Infrared. *Phot. J.*, **48:** 25 (1908) (with S. H. Wratten).

Silver Acetylide Emulsion. *Phot. J.*, **48:** 338 (1908) (with S. H. Wratten).

Screen Plate Colour Photography. *J. Roy. Soc. Arts*, p. 195 (1908) (Society of Arts Medal Award).

The Photography of Coloured Objects in Principle and Practice. *Brit. J. Phot.*, **55:** 735, 754, 770, 788 (1908).

The Construction of One-Exposure Cameras for Three-Colour Photography. *Brit. J. Phot.*, Col. Suppl., **55:** 58 (1908).

On the Resolving Powers of Photographic Plates. *Proc. Roy. Soc.*, **83A:** 10 (1909).

A Report on the Present Condition of Sensitometry. *Brit. J. Phot.*, **56:** 685 (1909).

Absorption Spectra. *Phot. J.*, **49:** 235 (1909) (with S. H. Wratten).

On Some Experimental Methods Employed in the Examination of Screen Plates. *Phot. J.*, **50:** 197 (1910) (with J. H. Pledge).

Time Development. *Phot. J.*, **50:** 403 (1910).

New Investigations on Standard Light Sources. *Phot. J.*, **50:** 287 (1910). *Brit. J. Phot.*, **57:** 627 (1910) (with S. E. Sheppard).

On the Fogging Power of Developers—I. General Introduction and the Hydroquinone Developer. *Phot. J.*, **51:** 226 (1911). *Brit. J. Phot.*, **58:** 491, 515 (1911) (with C. Welborne Piper).

On the Ratio between Diameter of the Photographic Image of a Point and the Exposure which Produced It. *Astrophys. J.*, **33:** 81 (1911).

On the Fogging Power of Developers—II. Sulphite Fog and Solubility of Silver Bromide in Sulphite Solutions. *Phot. J.*, **52:** 221 (1912) (with C. Welborne Piper).

The Photographic Industry. *J. Soc. Chem. Ind.*, **31:** 307 (1912). *Brit. J. Phot.*, **59:** 326 (1912).

A New Laboratory for Research in Optics and Photography. *Sci. American*, Supplement, **76:** 56 (1913). *Phot. Rundschau.*, **51:** 200 (1914).

The Physical Chemistry of Photographic Development. *J. Am. Chem. Soc.*, **35:** 1727 (1913). *Brit. J. Phot.*, **60:** 935 (1913).

The Sensitometry of Process Plates. *Penrose's Pictorial Annual*, **19:** 105 (1913–14).

The Calculation of Exposure *Wilson's Phot. Mag.*, **50:** 561 (1913), *Brit. J. Phot.*, **61:** 21 (1914).

The Future of Scientific Research. *Brit. J. Phot.*, **61:** 692 (1914).

Light Filters for Use in Photometry. *Trans. Ill. Eng. Soc.*, **9:** 990 (1914).

The Effect of Humidity on the Sensitiveness of the Photographic Plate. *Astrophys. J.*, **40:** 236 (1914).

The Triple Projection Process of Colour Photography. *Brit. J. Phot.*, Col. Suppl., **61:** 14 (1914).

The Sensitometry of Photographic Papers. *Phot. J.*, **54:** 342 (1914). *Brit. J. Phot.*, **62:** 9 (1915) (with L. A. Jones and P. G. Nutting).

Artificial Illuminants for Use in Practical Photography. *Trans. Ill. Eng. Soc.*, **10:** 947 (1915).

Physics of the Photographic Process. *J. Franklin Inst.*, **179:** 141 (1915). *Brit. J. Phot.*, **62:** 165, 183, 221 (1915).

The Organization of Industrial Scientific Research. *Science*, **43:** 763 (1916). *Nature*, **97:** 411, 431 (1916).

The Kodachrome Process of Color Portraiture. *Sci. American*, **112:** 341 (1915). *Am. Annual Phot.*, **30:** 9 (1916).

Photomicrographs in Color. *Am. Phot.*, **11:** 448 (1917).

The Production of Scientific Knowledge. *Science*, **46:** 519 (1917).

The Optical Properties of Light Filters. *J. Opt. Soc. Amer.*, **1:** 22 (1917). *Brit. J. Phot.*, **64:** 462 (1917).

The Photographic Rendering of Tone Values, I-V. *Studio Light*, May-September (1917).

A Simplified Method of Writing Developing Formulae. *Brit. J. Phot.*, **64:** 535 (1917).

A Photographic Research Laboratory. *Sci. Monthly*, **5:** 481 (1917).

Planning a Research Laboratory for an Industry. *J. Ind. Eng. Chem.*, **10:** 476 (1918). *Sci. Monthly*, **7:** 54 (1918).

A New Yellow Dye and Light Filters Made from It. *Brit. J. Phot.*, **66:** 48 (1919). *J. Ind. Eng. Chem.*, **11:** 454 (1919) (with H. T. Clarke).

Report on the Production of Synthetic Organic Chemicals in the Research Laboratory of the Eastman Kodak Company for the Years 1918–1919. *J. Ind. Eng. Chem.*, **11:** 1141 (1919).

The Production and Supply of Synthetic Organic Chemicals in the United States. *J. Soc. Chem. Ind. Rev.*, **39:** 230 (1920) (with H. T. Clarke).

The Structure of the Photographic Image. (John Scott Medal award). *J. Franklin Inst.*, **191:** 631 (1921).

The Measurement of Color. *J. Ind. Eng. Chem.*, **13:** 729 (1921).

Photographic Exposure and the Structure of Light. *Brit. J. Phot.*, **69:** 384 (1922) (with L. Silberstein).

Some New Sensitizers for the Deep Red. *Brit. J. Phot.*, **69:** 474 (1922). *J. Ind. Eng. Chem.*, **14:** 1060 (1922) (with G. O. Gutekunst).

Color Photography. *Trans. Soc. Motion Picture Engrs.*, **14:** 137 (1922).

A New Sub-standard Film for Amateur Cinematography. *Trans. Soc. Motion Picture Engrs.*, **16:** 252 (1923).

Recent Advances in Photographic Theory. *J. Franklin Inst.*, **195:** 1 (1923). *Brit. J. Phot.*, **70:** 139, 160 (1923). *Nature*, **111:** 399 (1923).

Motion Picture Photography for the Amateur. *J. Franklin Inst.*, **196:** 227 (1923).

Photographic Reproduction of Tone. (Fourth Hurter and Driffield Memorial Lecture). *Phot. J.*, **64:** 311 (1924). *Brit. J. Phot.*, **71:** 445, 461 (1924). *Phot. Ind.*, **24:** 131 (1926).

Photography—(all sections, including motion pictures). *Encyclopaedia Britannica* (1929).

American Contemporaries—George Eastman. *Ind. Eng. Chem.*, **17:** 541 (1925).

The Color Sensitivity of Photographic Materials. *J. Franklin Inst.*, **201:** 525 (1926).

Fifty Years of Photography. *Ind. Eng. Chem.*, **18:** 915 (1926).

Research as the Enemy of Stability. *Ind. Eng. Chem.*, **19:** 1217 (1927).

The Processes of Color Photography I-IV. *J. Chem. Ed.*, **5:** 1385, 1577 (1928); **6:** 44, 286 (1929).

Amateur Cinematography and the Kodacolor Process. *J. Franklin Inst.*, **207:** 1 (1929). *Brit. J. Phot.*, **76:** 46, 60, 77 (1929). *Phot. Korr.*, **65:** 21, 54, 87 (1929).

The Physics of Photography. *Brit. J. Phot.*, **76:** 135, 151, 165 (1929).

The Publication of Papers from Research Institutions. *Science*, **70:** 502 (1929).

The Science of Photography (Ninth Annual Sigma Xi Address) *Sigma Xi Quarterly*, **19:** 1 (1931).

Photographic Sensitizers for the Infrared. *Nature*, **126:** 471 (1930).

Color and its Measurement. (Edgar Marburg Lecture). *Proc. Am. Soc. Testing Materials*, **30,** Part II: 9 (1930).

Photographic Plates for Use in Spectroscopy and Astronomy, I. *J. Opt. Soc. Am.*, **21:** 753 (1931). *Brit. J. Phot.*, **79:** 410, 427, 443 (1932).

The Scope of Research Management. *Ind. Eng. Chem.*, **24:** 65 (1932).

Photographic Plates for Use in Spectroscopy and Astronomy, II. *J. Opt. Soc. Am.*, **22:** 204 (1932).

Photographic Plates for Use in Spectroscopy and Astronomy, III. *Brit. J. Phot.*, **80:** 560, 583 (1933). *Phot. Ind.*, **31:** 834 (1933). *J. Opt. Soc. Am.*, **23:** 229 (1933).

Recent Advances in Sensitizers for the Photography of Infrared. *J. Opt. Soc. Am.*, **23:** 216 (1933). *Phot. J.*, **73:** 258 (1933). *Phot. Ind.*, **31:** 1064, 1102 (1933) (with F. M. Hamer and L. G. S. Brooker).

Scientific Thought and Social Reconstruction. *Elec. Eng.*, **53:** 381 (1934). *Sigma Xi Quarterly*, **22:** 13 (1934).

Some Photographic Aspects of Sound Recording. (Trueman Wood Lecture). *J. Roy. Soc. Arts*, **82:** 924 (1934). *Bull. Soc. Franc. Phot.*, **22:** 11, 34 (1935). *J.S.M.P.E.*, **24:** 285 (1935).

Photographic Plates for Use in Spectroscopy and Astronomy, IV. *J. Opt. Soc. Am.*, **25:** 80 (1935).

Sensitizing Dyes and Their Use in Scientific Photography. *Proc. Roy. Inst.*, **29:** 136 (1936). *Nature*, **137:** 726 (1936).

The Development of the Art and Science of Photography in the Twentieth Century. *J.S.M.P.E.*, **28:** 3 (1937).

Photography and the Advance of Pure Science. *J. Franklin Inst.*, **226** 281 (1938).

The Modern Era of Photography. *Phot. J.*, **79:** 225 (1939).

Recent Advances in the Theory of the Photographic Process. *J.S.M.P.E.*, **37:** 10 (1941). *Sci. Monthly*, **55:** 293 (1942).

Direct Processes for Making Photographic Prints in Color. *J. Franklin Inst.*, **233:** 41 (1942).

Modern Colour Photography. *Endeavour*, **7:** 131 (1948).

The Kodak Research Laboratories. *Phot. J.*, **88A:** 50 (1948). *Proc. Roy. Soc.*, **192A:** 465 (1948).

Samuel Edward Sheppard. (Obituary). *Nature*, **162:** 952 (1948). *J. Chem. Soc.*, (1949), 261. *J.S.M.P.E.*, **51:** 667 (1948). *Phot. J.*, **89A:** 18 (1949).

The Growth of Industrial Research. *Bull. Am. Ceramic Soc.*, **29:** 448 (1950).

The View Ahead in Chemistry. (A.C.S. Diamond Jubilee Lecture). *Chem. Eng. News*, **29:** 4062–4064 (1951). *Chemistry*, **25:** 27–43 (October 1951).

Secrecy and Industrial Research. *Nature*, **170:** 972 (1952).

Recent Progress in Astronomical Photography. (Twentieth James Arthur Lecture). *Smithsonian Inst. Report for* **1953**, Publ. 4151, p. 205 (1954).

History of Professional Black-and-White Motion-Picture Film. *J.S.M.P.T.E.*, **63:** 134 (1954).

The Mechanism of Optical Sensitizing (Presidential Address) "Science and Applications of Photography. Proceedings of the R.P.S. Centenary Conference, London, 1953" (Publ. 1955) p. 7.

Fifty Years of Work on the Theory of the Photographic Process. "Science and Applications of Photography. Proceedings of the R.P.S. Centenary Conference, London, 1953" (Publ. 1955) p. 257.

The Structure of the Developed Photographic Image. *J. Franklin Inst.*, **260:** 259 (1955).

Leo Hendrik Baekeland and Photographic Printing Papers. (Baekeland Memorial Lecture). *Chem. and Ind.* (1955), 1134.

The Cyanine Sensitizing Dyes (A Review). *Bull. Research Council Israel*, **5C:** 289 (1957).

Books

Investigations on the Theory of the Photographic Process (with S. E. Sheppard). Longmans, Green and Co., 1907.

Wratten Light Filters. Wratten and Wainwright, 1909.

An Atlas of Absorption Spectra. Wratten and Wainwright, 1909.

The Photography of Coloured Objects. Wratten and Wainwright, 1909.

The Fundamentals of Photography. Eastman Kodak Co., 1920.

The Organization of Industrial Scientific Research. McGraw Hill, 1920. (Second Edition, complete revision, with J. A. Leermakers, 1950.)

Photography. G. Bell and Sons, London, 1936; Macmillan, New York, 1937. (Second Edition, 1942).

The Theory of the Photographic Process. (Edited and written in part by Dr. Mees). Macmillan, 1942. (Revised Edition, 1954).

The Path of Science. John Wiley and Sons, 1946.

PHOTOGRAPHIC SCIENCE AND ENGINEERING
Volume 4, Number 6, November–December 1960

On the Relation between Color Correction and Frequency Response in the Central Part of the Image of a Group of Photographic Systems

TADEUSZ MALINOWSKI AND WALTER MANDLER, *Ernst Leitz Canada Limited, Midland, Ontario*

The image quality of a photographic lens is limited, and in part these limitations are due to the secondary spectrum. The optical materials available for consideration have disadvantages making monochromatic correction difficult. It seems worth while to optimize chromatic correction of achromats. The spectral response of a system (lens and emulsion) can be described by a model curve. The variation of the sine-wave response function of the system with varying color correction of the lens is investigated, and the influence of spherical aberration and spherochromatism are also treated briefly. The findings of this investigation have been used in the design of a telephoto lens. The sine-wave response curve and photographic results for this lens are shown.

The possible concentration of energy in the image formed by a photographic lens is limited by, among other factors, the secondary spectrum. The correction of the secondary spectrum is primarily a question of suitable optical materials. Unfortunately the materials available with the proper refractive characteristics to correct the secondary spectrum generally have three disadvantages: they are expensive, they have poor chemical and mechanical stability, and they have low refractive indices, thus making them poorly suited to use in the correction of monochromatic errors. Considering the "ordinary" glasses only (glasses where the partial dispersion for any two wavelengths is in a linear relationship to the partial dispersion between C and F), we can state that two points of the curve of $\Delta s'(\lambda)$ vs. wavelength λ (where $\Delta s'(\lambda)$ is the deviation of the back focal distance at a certain wavelength from the back focal distance of a standard wavelength, mostly d or e) determine the whole curve, and that there is no focal plane possible in which the image for more than two wavelengths is formed. On any achromatized simplet which is sufficiently well corrected for monochromatic errors, the distribution of energy in the focal plane, based on geometrical optics, is a function of the free lens diameter and of the choice of the wavelength pair, for which achromicy has been obtained. More complex lenses with air spaces may have a secondary spectrum either smaller or larger than the achromatized simplet, usually depending on whether the Petzval sum of the system is smaller or larger than the Petzval sum of the simplet.

Systems which are feasible and practical have a secondary spectrum between 0.5 and 2 times the size of the secondary spectrum of the achromatized simplet. Representative samples show the following values: Petzval lens, 0.7; triplet, 1.2; Gauss-type lens, 1.3; tele system, 1.5.

Typical curves of $\Delta s'(\lambda)$ vs. λ are shown in Fig. 1.

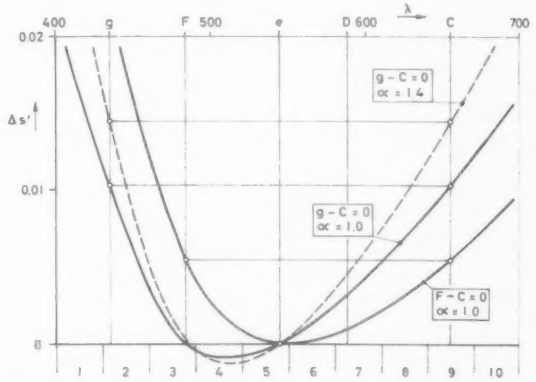

Fig. 1. Longitudinal chromatism for lenses with focal length of 100 mm.

In order to vary the color correction we make use of the fact that lenses made from "ordinary" glasses do not change the secondary color characteristics when slight changes in primary color correction are introduced. Having one curve, $\Delta s'(\lambda)$, as shown in Fig. 1, we can determine, without doing another ray trace, the curve which results when two different wavelengths are combined. This can easily be done by applying a modified version of the formula given by M. Herzberger.[1]

Presented at the Annual Conference, Santa Monica, California, 13 May 1960. Received 9 May 1960.

1. Herzberger, M., *Modern Geometrical Optics*, Interscience Publishers, New York, 1958, p. 145.

$$f_{\lambda'} - f_{\lambda''} = -[A_1(\lambda'') - A_1(\lambda'')]\,\alpha + [A_2(\lambda') - A_2(\lambda'')]\,[f_F - f_C] \quad (1)$$

where f is a symbol of focal length
λ' and λ'' are wavelengths
A_1 and A_2 are functions of wavelengths λ' and λ'' (tabulated by Herzberger)
α is a factor defining the depth of the curve of paraxial chromatic aberration (see Fig. 1)

The different states of color correction can be defined by the value of the factor α and the wavelength which has a common focus with some arbitrarily selected wavelength. For our investigation, we have chosen C (λ = 656 mμ). The question arises as to whether the image quality of the lens can be improved by suitable choice of color correction, deviating from the accepted rule of thumb, to combine C and F for visual and D and g for photographic correction. Since, for the over-all photographic result, the performance of lens and film must be combined, results should be obtained in a form which is convenient for this combination. The most suitable approach seems to be the use of the sine-wave response as originated by Duffieux,[2] which provides a convenient way for cascading several imaging processes.

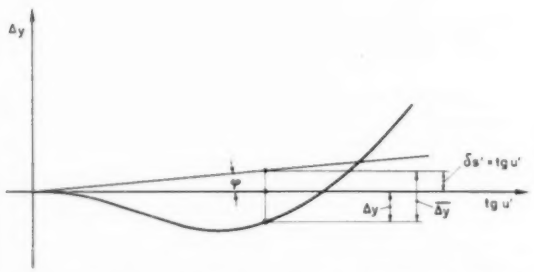

Fig. 2. Lateral aberration curve. Shift of focal plane is introduced by rotation of abscissa around origin "0."

Method of Investigation

The state of geometrical correction of a lens shall be represented by plotting curves $\Delta y'$ vs. tan u' for different wavelengths, for an arbitrary focal plane, usually the Gaussian one. $\Delta y'$ designates the lateral aberration, u' the angle between the emerging ray and the optical axis of the lens. Figure 2 shows the state of correction of a lens for one wavelength plotted as described. This representation has the advantage that the curves plotted for one focal plane may also be used to represent the correction in focal planes slightly in front of and behind it, without requiring further ray tracing or calculation. Introducing a shift of focal plane $\delta s'$, we obtain the lateral aberration

$$\overline{\Delta y} = \Delta y - \delta s' \tan u' \quad (2)$$

2. Duffieux, P. M., *L'Intégrale de Fourier et ses applications a l'optique*, Rheims, 1946 (privately published).

showing that all Δy's in the new focal plane can be read from the same plot by using an inclined system of coordinates. The angle of inclination φ is given by

$$\tan \varphi = c\,\delta\,s', \text{ where} \quad (3)$$

c is an arbitrary scale factor, depending on ordinate and abscissa scale. If the choice of scales is made so as to give values of $\varphi \leqq 0.2$ with the shifts $\delta s'$ involved, the values of Δy may be read directly in a grid, as shown in Fig. 3, which is rotated around the

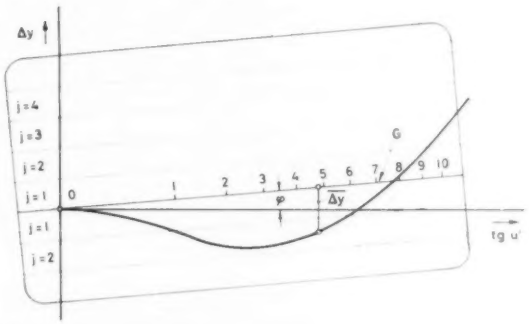

Fig. 3. Transparent grid with scale G to facilitate reading of lateral aberration in different focal planes.

origin 0. By dividing the absissa of this grid into intervals corresponding to the radii of ring-shaped zones of equal area in the entrance pupil, it is a simple matter of counting to determine the fraction of the total radiation passing through a given ring-shaped area $j = 1, 2 \ldots k$ in the chosen focal plane.

These results may be used to obtain the point-spread-function. This, in turn, may be converted to the square or sine-wave response as indicated by Cox[3] and Shack.[4] By multiplying the respective values of lens and film response, a reliable prediction of the performance of the combination, which in the following discussion will be called the "photographic system," is possible.

The problem becomes more complex if white light is used. The distribution of energy in the focal plane now depends on the following parameters:

- Choice of focal plane
- Color correction
- Spherical correction
- Spectral transmission of lens
- Sine-wave response of emulsion
- Spectral quality of "white light"
- Spectral response of emulsion

In order to simplify the investigations of the influence of color correction on the sine-wave response of the system, it may be assumed that certain parameters can be neglected. For the first part of our

3. Cox, A., *Image Evaluation by Edge Gradients*, Nat. Bur. Standards (U.S.) Circ. 526 (1954), pp. 267–273.

4. Shack, R. V., *A Proposed Approach to Image Evaluation*, *ibid.*, pp. 275–286.

investigation, we will assume that no spherical aberration exists in the lens. It will be shown later that lenses with negligible spherical aberration are feasible. The illuminating light for our test target is supposed to have an equal energy spectrum. The spectral sensitivity of the emulsion and the spectral transmission of the lens shall be combined in a weighting function $W(\lambda)$, which is to be used for the superposition of images formed by the different parts of the spectrum. Figure 4 shows this weighting function, which was obtained as a rough average of

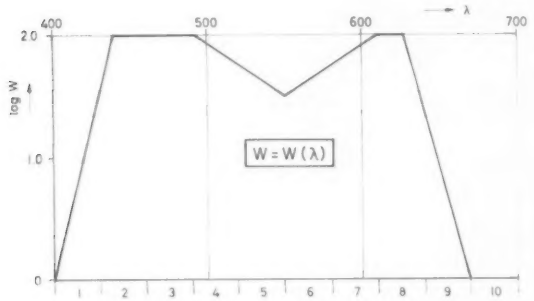

Fig. 4. Weighting function W(λ) giving the relative spectral response of the photographic system.

manufacturers' data on panchromatic films and from our own transmission curves for lenses. The choice of this weighting function is not too important, because it will not change the nature of our findings but merely slightly vary some numerical results.

For the required superposition of different wavelengths, the method of Cox and Shack is very time consuming, although it gives the edge gradient and line-spread-function as intermediate results which can be very valuable. Lukosz[5] gives a more direct method for obtaining the sine-wave response.

For our investigations, we have to rearrange the formulas given by Lukosz in accordance with the following considerations. The energy in ten color sectors, numbered $i = 1, 2 \ldots 10$ (see Fig. 1), passes through a certain number of concentric ring-shaped zones of equal area in the entrance pupil, and is distributed over several concentric ring-shaped zones in the aberrated image of a point. These zones in the point image can be represented in a graph of the lateral aberration similar to Fig. 3 by parallel strips $j = 1, 2 \ldots k$.

Substituting ϵ for Δy, and following Lukosz, the sine-wave response (SWR) for color sector 1 and line frequency n, is

$$SWR_{1,n} = \frac{\sum_{j=1}^{k} E_{1,j} J_0 (2\pi n \epsilon_{1,j})}{\sum_{j=1}^{k} E_{1,j}}$$

where J_0 is the Bessel function of 0 order.

5. Lukosz, W., *Die geometrisch-optische Berechnung des Übertragungsfaktors*, Hausmitteilungen Jos. Schneider & Co., **11** (1958–59), pp. 15–24.

We now superimpose the sine-wave response of the different color sectors and obtain

$$SWR_n = \frac{\sum_{i=1}^{10} \sum_{j=1}^{k} E_{ij} J_0 (2\pi n \epsilon_{ij})}{\sum_{i=1}^{10} \sum_{j=1}^{k} E_{ij}}$$

By carrying out the summation in the numerator first over i and then over j, as $\sum_{j=1}^{k} \sum_{i=1}^{10}$, we only need one value of J_0 for each strip $j = 1, 2 \ldots k$, and this value is obtained from a table of Bessel functions.

Graphical computation of sine-wave response according to these formulas can be done very quickly. Since we assume the absence of spherical aberration, all curves $\Delta y'$ vs. tan u' (see Fig. 2) will be straight lines, the slopes depending on the respective longitudinal chromatic aberration. This can be obtained from a graph similar to Fig. 1.

The values of E_{ij} are proportional to the weighting function $W(\lambda)$ in color sector i, and to the length of the aberration curve corresponding to color sector i in strip j, when measured in terms of scale G (see Fig. 3).

The computation of SWR_n for several line frequencies n gives a sufficient approximation for the sine-wave response curve of the lens. For the sine-wave response of the emulsion of our photographic system, we will use the highest values published for panchromatic emulsions.[6] It should be noted that all publications on the sine-wave response of the photographic emulsion either do not specify the spectral quality of light used, or refer only to monochromatic light. For the purpose of our investigation equal sine-wave response for the light admitted by weighting function $W(\lambda)$ shall be assumed.

The sine-wave response curve of our photographic system is sufficiently described by computing five points, at 10, 25, 50, 75 and 100 lines/mm. Values beyond 100 lines/mm are of very little interest, since with the emulsion chosen no useful contrast can be obtained for higher line frequencies. For the same reason we can treat the whole problem without considering the effects of diffraction. The sine-wave response curve for diffraction-limited lenses as given by O. Schade[7] shows that for line frequencies below 100 lines/mm and apertures of $f/5$ and faster, diffraction can be neglected.

Results

To obtain a full picture of the relationship between paraxial chromatic correction of the photographic system and its sine-wave response in the vicinity of the axis, three series of systems have been selected, having depth factors of $\alpha = 1.0$, $\alpha = 1.4$, $\alpha = 1.8$,

6. Schrader, W., *Der Einfluss der photographischen Schicht auf den Übertragungsfaktor*, *ibid.*, pp. 37–45.

7. Schade, O., *A New System of Measuring and Specifying Image Definition*, Nat. Bur. Standards (U.S.) Circ. 526 (1954), pp. 231–249.

for the curve of chromatic aberration. These are the curves of Fig. 1.

In each series, five different states of color correction have been considered:

$$\Delta(420 - C) = 0;\ \Delta(g - C) = 0;\ \Delta(460 - C) = 0;$$
$$\Delta(F - C) = 0;\ \Delta(e - C) = 0.$$

All systems have a focal length of 100 mm and a relative aperture of $f/5$. As indicated above, no spherical aberration is considered.

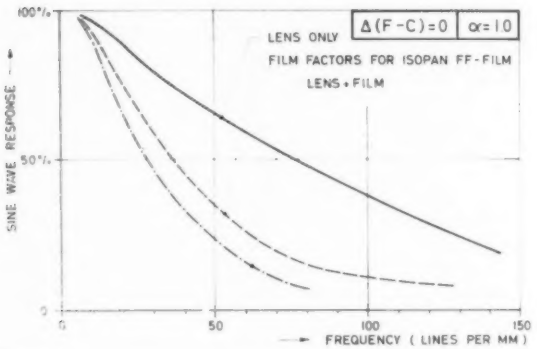

Fig. 5. Sine-wave response for "white light." Lens $f = 100$ mm, $f/5$.

Figure 5 shows a sine-wave response curve (labelled "Lens Only") which was computed according to the method described above, for the curve of chromatic aberration defined as $\alpha = 1.0$ and for $\Delta(F - C) = 0$. By multiplying the abscissas of this curve and of the sine-wave response of the emulsion,[6] we obtain the curve labelled "Lens + Film," which gives the sine-wave response of this photographic system.

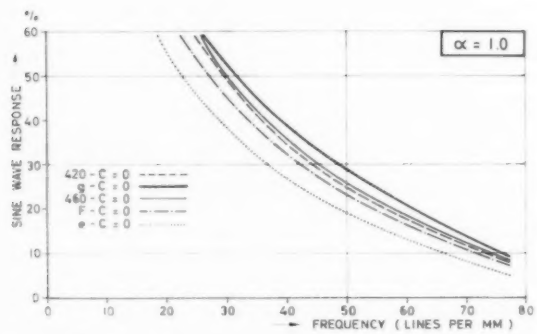

Fig. 6. Sine-wave response for "white light" for different states of color correction. Lenses $f = 100$ mm, $f/5$.

Similar curves have been determined for all other cases under consideration. Figure 6 shows these curves for $\alpha = 1.0$ and the five chromatic corrections mentioned above. Making a section through these curves at the 10%, 30%, and 50% response levels, we can trace the lines shown in Fig. 7. All these curves have a very distinct maximum, which in this case is located between g and 460 mμ.

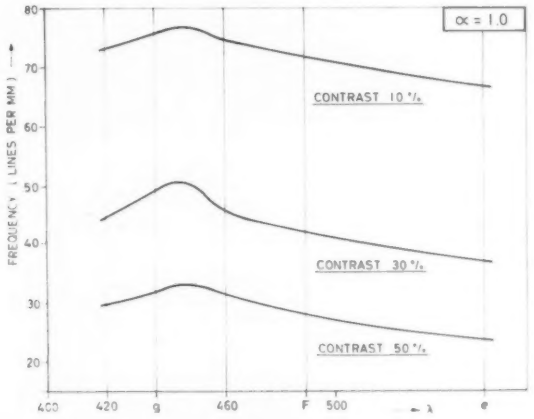

Fig. 7. Resolution in the image of a high-contrast target for different contrast transmission levels and varying color correction.

Figure 8 contains the same curves as Fig. 7 for all three series: $\alpha = 1$, $\alpha = 1.4$, $\alpha = 1.8$.

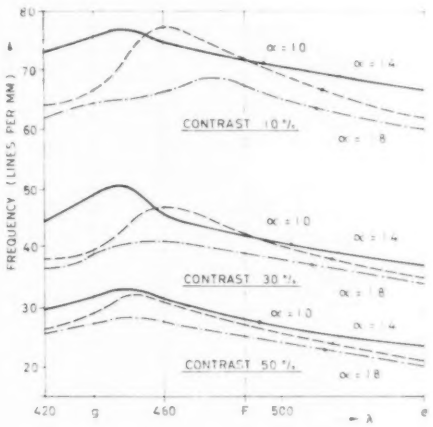

Fig. 8. Resolution in the image of a high-contrast target for different amounts of secondary spectrum.

The results shown so far have all been obtained for achromatic lenses, e.g., lenses which have $ds'/d\lambda = 0$ for only one wavelength. For an apochromatic lens, $ds'/d\lambda = 0$ is obtained for two wavelengths. It seems to be worth while to study the possible improvement of the sine-wave response curve of our systems which can be obtained through apochromatic correction.

As a typical example of an apochromat, we will use a well-known objective lens computed by A.

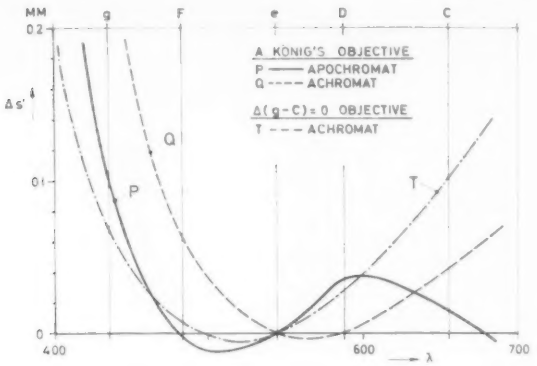

Fig. 9. Comparison between achromatic and apochromatic correction.

Koenig.[8] The chromatic aberration curves P and Q in Fig. 9 are taken from Ref. 8. Curve T, which we have already studied ($\Delta(g - C) = 0$; $\alpha = 1.0$), has been added for comparison. The respective curves

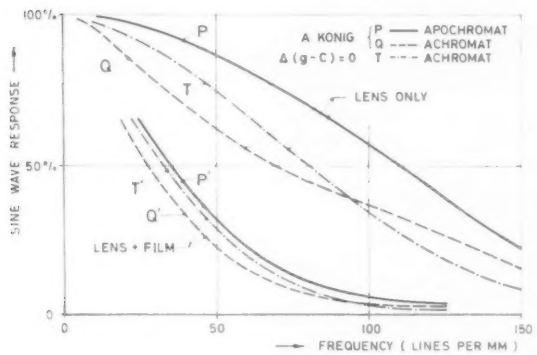

Fig. 10. Comparison between achromatic and apochromatic correction.

of sine-wave response are shown in Fig. 10 for the lenses only, as well as for the complete photographic system. Curves P', Q', and T' show that the effect of the apochromatic correction is greatly diminished by the response of the emulsion. Furthermore, it should be noted that the monochromatic correction of this apochromat for aperture $f/5$ should present difficulties because of the steep curvatures involved.

All lenses so far considered have had a focal length of 100 mm and an aperture of $f/5$, leaving an entrance pupil of 20-mm diameter. Since, in the absence of spherical aberration, the lateral chromatic aberration is proportional to the diameter of the entrance pupil, the frequency response curves obtained for these lenses may be used for other diameters as well.

8. Sonnefeld, A., "Der Koenigsche Apochromat B," *Z. Instrumentenk.*, **61**: 261 (1941).

We only have to change the frequency scale accordingly; i.e., for a lens with a diameter of 40 mm, the frequency scale should show 50 lines/mm instead of 100 lines/mm. The response values of these new curves must then be multiplied by the respective emulsion response values for the new corresponding frequencies to obtain the system response.

All statements so far apply to lenses without spherical aberration. We will now have a short look at the effects of spherical aberration and sphero-chromatism. Two intermediate stages in the correction of a 90mm $f/2$ lens have been used to determine the sine-wave response curves R and S in Figs.

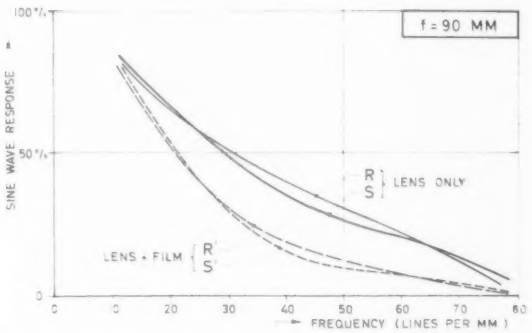

Fig. 11. Sine-wave response considering only chromatic aberration.

11 and 12. In Fig. 11, the problem was treated as in the foregoing cases; that is, only chromatic aberration was considered. Figure 12 shows the evaluation of the actual caustic. Since there is no significant difference between the corresponding

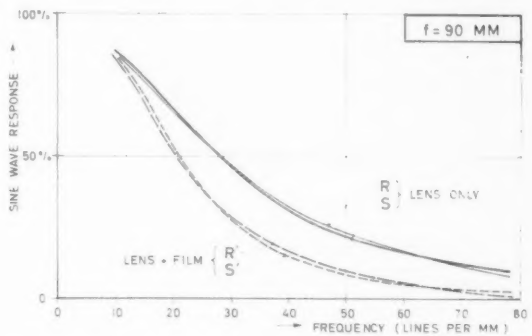

Fig. 12. Sine-wave response for the actual caustics.

curves in Figs. 11 and 12, we can conclude that spherical aberration and sphero-chromatism are corrected to a state where they are no longer important. Figure 13 shows the actual curves of spherical aberration for four different wavelengths of the lenses R and S. The correction of paraxial chromatism is different for both cases in order to take care of the

different sphero-chromatism. As Fig. 12 shows, both lenses should perform equally at full aperture. However, lens *S* should perform better when stopped down and should therefore have preference.

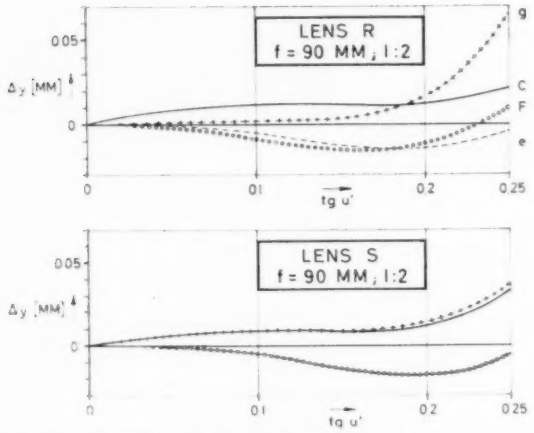

Fig. 13. Curves of lateral aberration for lenses *R* and *S*.

Conclusion

In order to optimize the sine-wave response of photographic systems, the following points should be considered:

1. The type of lens selected should have a value, α (depth of secondary spectrum), as small as possible without interfering with the requirements of field correction and mechanical dimensions.
2. Spherical aberration should be corrected to an extent where it ceases to affect sine-wave response.
3. The most suitable type of achromatization should be selected for the spectral response of the system. For panchromatic emulsions, $\Delta (460 - C) = 0$ seems to be the best choice in the absence of sphero-chromatism.

Application

A telephoto lens, 1:4.8/280 mm, was designed in order to make use of the findings of this investigation. The layout of this lens is shown in Fig. 14.

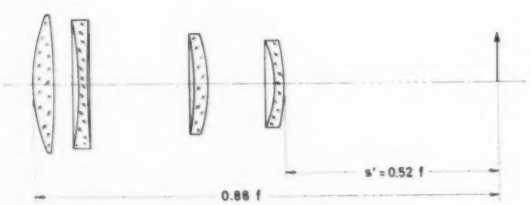

Fig. 14. Telephoto lens, f = 280 mm, f/4.8.

Despite the short mechanical length of 0.88 *f*, as compared to 1.2 *f* for a triplet lens, the Petzval sum is 0.2, and α is only 1.24. The spherical aberration is corrected within the Rayleigh-limits, and *C* and 470 mμ are combined, as shown by Curve *M* in Fig. 15.

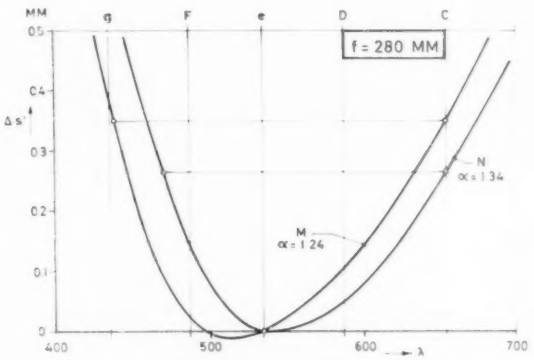

Fig. 15. Longitudinal chromatism for telephoto lens f = 280 mm, f/4.8.

Curve *N* in the same figure shows a slightly varied color correction, obtained by introducing a glass with different dispersion but equal mean refractive index in one element. The sine-wave response curves obtained for both lenses and also for the lens-film combinations are shown in Fig. 16.

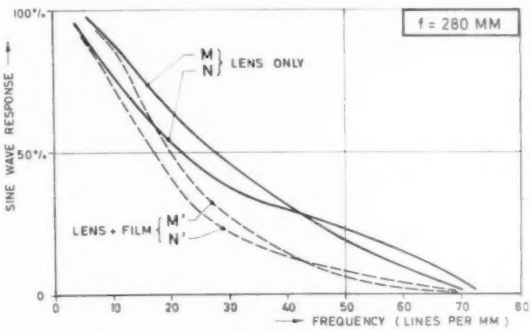

Fig. 16. Sine-wave response curve for actual photographic system.

In practical use, the lens performed quite well. On the same photographic material as was used in this investigation (Agfa IFF), the lens gave optimum performance at *f*/5.6. This is quite unusual for a lens of this focal length in combination with a high-resolution film. Figure 17 shows the whole frame enlarged 2 ×, and sections of the frame enlarged 4, 8, 16 and 32 ×. Only on the 32 × enlargement does the 100-line screen used for the printing fail to conceal the deficiencies of the image.

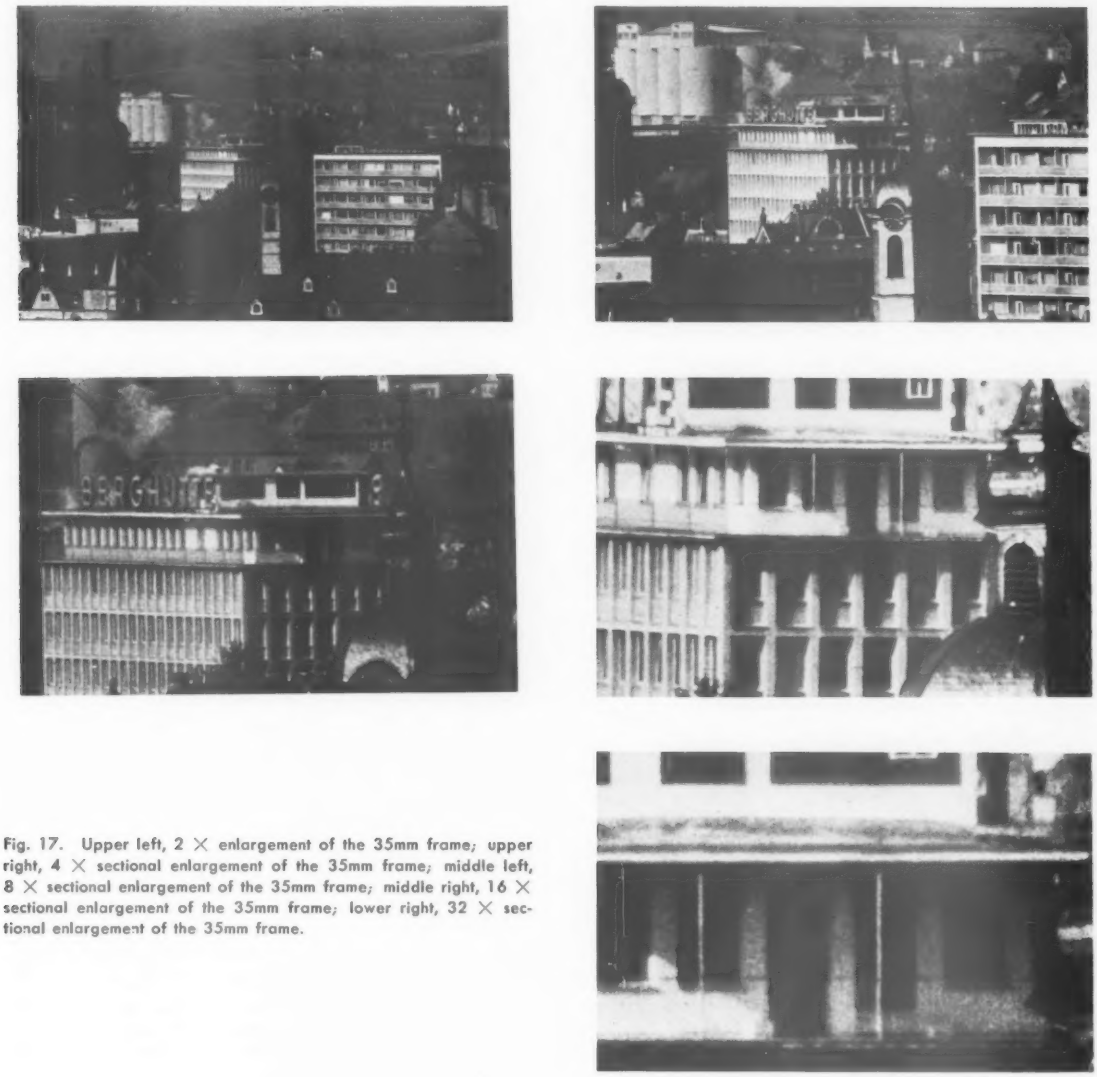

Fig. 17. Upper left, 2 × enlargement of the 35mm frame; upper right, 4 × sectional enlargement of the 35mm frame; middle left, 8 × sectional enlargement of the 35mm frame; middle right, 16 × sectional enlargement of the 35mm frame; lower right, 32 × sectional enlargement of the 35mm frame.

PHOTOGRAPHIC SCIENCE AND ENGINEERING
Volume 4, Number 6, November–December 1960

Spread Function and Contrast Transfer Function of Photographic Layers

H. FRIESER, *Institut für wissenschaftliche Photographie der Technischen Hochschule, Munich, West Germany*

The reproduction of small details by photographic layers is characterized by the spread function (SF) or the contrast transfer function (CTF). These functions are connected with each other by Fourier transformation. An equation which has been confirmed by experiments is given for SF. An attempt is made to derive this equation from the properties of the layer. CTF is calculated from the equation for SF. With the aid of this equation, it is possible to represent satisfactorily the results of various authors, whereby the one-parameter form is sufficient up to a frequency $\nu < \nu_{1/2}$, while one or two more parameters have to be added for larger frequencies.

The theory of image transfer in photographic reproduction differs from that of optical image transfer in two respects: First, the spread function is symmetrical except in exposures where the incidence is particularly oblique. This indicates that the spread is independent of the direction. Thus it is possible to characterize the spread by a one-dimensional function, and no phase shifts occur in the reproduction of periodical gratings. Second, the nonlinear transfer in the photographic process results in more complicated conditions than in the case of optical transfer. Since the theory of transfer is usually based on linear relations, it appears appropriate to extend this examination not to the densities of the photographic image but to "effective intensities." These result from the intensities which expose the layer from the outside ("printed-on intensity") by the spread of light within the emulsion layer. The effective intensity is related by means of the characteristic curve to the density obtained after development; i.e., it is possible to determine the distribution of the effective intensity with the aid of the characteristic curve and vice versa (Fig. 1).

Presented at the Annual Conference, Santa Monica, California, 13 May 1960. Received 29 April 1960.

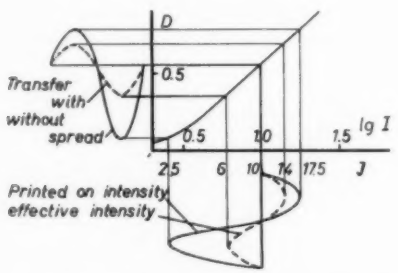

Fig. 1. The printed-on intensity and the effective intensity related to the corresponding density by means of the characteristic curve.

It is assumed that, for small details, the same characteristic curve that is measured on large areas is valid. This was experimentally confirmed for normal rapid developers with strong agitation. For certain developers (for example, strongly diluted developer) and for insufficient agitation during development, this is not valid due to the adjacency effect. The linearity of the transfer is disturbed,[1,2] and the reproduction of small details is usually improved. As long as the adjacency effect is not pronounced, it is nevertheless possible to obtain a good approximation by applying the linear calculation with some restrictions. A pronounced adjacency effect is usually avoided in practice because of its undesirable distortions.

In the reproduction of relatively large-sized details, the printed-on and the effective exposure are identical. They will, however, differ in the reproduction of small details, i.e., the quality of reproduction decreases with decreasing detail size.

It is advantageous to describe the quality of the transfer by the *spread function* (SF) or by the *contrast transfer function* (CTF). The SF indicates the distribution of the effective intensity in the vicinity of an exposed very small slit. The CTF indicates the decrease of the amplitude or modulation of a sine-wave grating, due to spread, as a function of the space frequency. The two functions are related to each other by a Fourier transformation.

Both functions are of practical significance. Each can be employed for the calculation of the effective exposure and, with the aid of the characteristic curve, for the computation of the density distribution. On the other hand, it is possible to determine the effective exposure from the density distribution by means of the characteristic curve and to establish the SF with a slit and the CTF with a grating. Subsequently, CTF can be ob-

1. H. Frieser, *Phot. Korr.*, **91**: 69 (1955).
2. L. O. Hendeberg, *Arkiv Fysik*, **16**: 457 (1960).

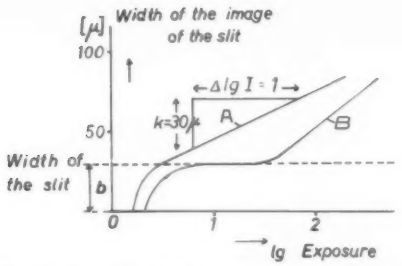

Fig. 2. The width of the image of a printed-on slit width (b) as a function of the logarithm of the exposure. A = strongly diffusing layer; B = slightly diffusing layer.

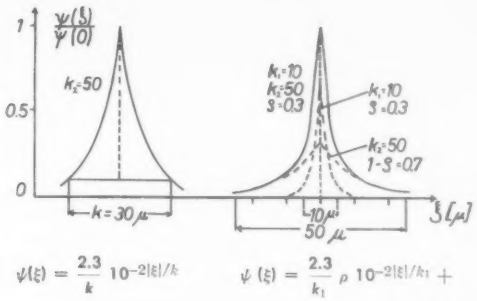

Fig. 3. Spread functions calculated according to Eq. (1) ($k = 30\mu$) and Eq. (3) ($k_1 = 10\mu, k_2 = 50\mu, \rho = 0.3$). Dotted lines = the two terms of Eq. (3).

tained from SF, and SF from CTF, by Fourier transformation. The CTF for adjacency effects was indicated by Sayanagi.[3]

In addition, other functions of practical significance can be derived, as, for example, the function indicating the degree of the effective exposure on an edge, as well as the two-dimensional SF showing the light distribution around a printed-on dot.[4–6]

With each of these functions, it is possible to convert the printed-on intensity to the effective intensity with the help of the transfer theory. According to the type of problem involved, one or the other of these functions will be selected. The CTF is particularly useful when the reproduction of periodical structures is observed. It is equally suitable for the characterization of a photographic layer with regard to its ability to reproduce small-sized details. The SF, however, is only expediently applied to the calculation of nonperiodic objects as slits and lines. Above all, it will be necessary to use SF as a base for all investigations concerning the theory and origin of spreading, because SF can be related to the optical properties of the layer in a far easier manner than CTF. For that reason, SF will be discussed first.

Spread Function

The fact that the width of the image of a printed-on slit increases linearly with the logarithm of the exposure (Fig. 2, Curve A), as stated by several authors,[4,7–9] permits the deduction of an exponential decrease of the scattered light in the vicinity of the slit already mentioned by Ross.[7]

Frieser[1,4,9,10] stated that for SF:

$$\psi(\xi) = \frac{2.3}{k} 10^{-2|\xi|/k} \tag{1}$$

where ξ is the distance from the printed-on slit.

For the effective intensity $I(x)$ when the distribution of the printed-on intensity is equal to $I_0(x)$, we obtain:

$$I(x) = \frac{2.3}{k} \int_{-\infty}^{+\infty} I_0(x + \xi)\psi(\xi)d\xi \tag{2}$$

where x is the longitudinal coordinate and k is a constant designating the magnitude of the spread and characteristic for the layer concerned. k corresponds to the "$^1/_{10}$ width" of the SF (Fig. 3). k can be determined by direct measurement of slit images obtained by exposures with different intensity. It is also possible to measure the slit images in the microphotometer and to define the width by the distance between two points indicating a certain density, as, e.g., 0.1 (Ref. 11).

Equation (2) proved exceptionally valuable for the calculation of the effective intensity in the case of various objects including those of two dimensions (slit, line, edge, grid, circle, annuli, and others).[1]

Recent examinations[12] show, however, that most commercial photographic layers do not correspond to Curve A but to Curve B of Fig. 2. Although a linear increase of the image width can also be observed for higher exposures, the width of the image is constant over a certain exposure range and equals the width of the slit for smaller exposures. This obviously means that the diffusion halo is composed of two parts. One part consists of the nondiffused light, or light only slightly diffused in a small angle (see below), and offers a sharp image. The other part consists of diffused light and causes the diffusion halo. This fact can be expressed by the following formula[12] (Fig. 3):

$$\psi(\xi) = \frac{2.3}{k_1} \rho\, 10^{-2|\xi|/k_1} + \frac{2.3}{k_2} (1 - \rho)\, 10^{-2|\xi|/k_2} \tag{3}$$

where k_1 and k_2 are again the "$^1/_{10}$ widths" of the two distributions, and ρ indicates the share of the expo-

3. K. Sayanagi, *J. Opt. Soc. Am.*, **50:** 185 (1960).
4. H. Frieser, "Körnigkeit und Auflösungsvermögen" in *Fortschritte der Photographie*, Akadem. Verlagsges, Leipzig, **II:** 276 (1940); **III:** 73 (1944).
5. H. Frieser, Interntl. Confer. Phot., London, 1953, p. 203.
6. H. Molitz, *Phot. Korr.*, **95:** 3, 19 (1959).
7. F. E. Ross, *The Physics of the Developed Image*, Van Nostrand, New York, 1924.
8. R. Wildt, *Z. wiss. Phot.*, **25:** 153 (1928).
9. H. Frieser, C. R. Congrès Interntl. Phot., Paris, 1935, p. 207: Ref. 4, Vol. III, p. 318 ff.
10. H. Frieser, *Kino-Technik*, **17:** 167 (1935).
11. A. Küster, *Veröffentl. wiss. Zentral-Labs. phot. Agfa*, **3:** 93 (1938).
12. H. Frieser *Phot. Korr.* **92:** 51; 183 (1956).

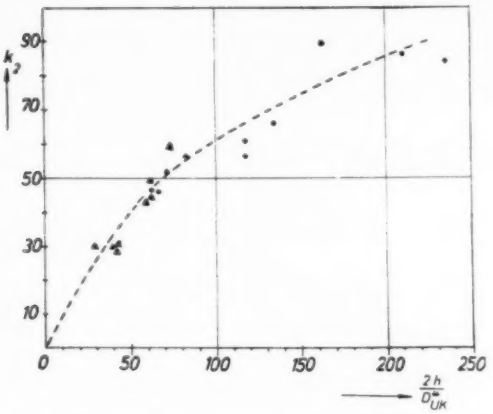

Fig. 4. The value of k_2 as function of $2h/D^{\ddagger}$. ▲ and ● = two different emulsions of different layer thicknesses and different silver halide concentrations.

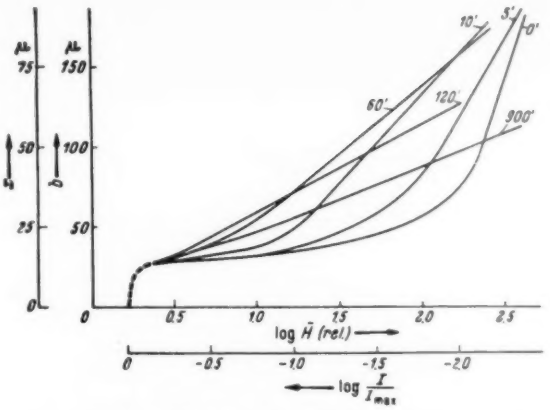

Fig. 5. Slit image width b as function of the logarithm of exposure (log H) and of the effective intensity I/I_{max} in the vicinity of the slit (width of the original slit 30 µ; x = distance from the slit center) for various ripening times (different crystal sizes). The curves are shifted parallel to the abscissa so that all have the same initial point.

sure of the first distribution. In layers examined, k_1 was found to be approximately 10 µ. Whether k_1 is a property of the emulsion or a result of experimental conditions remains undetermined. The spread is caused by the objective aperture value of 2 in the exposure and the measurement. Together with objective and adjustment errors, a spread approaching a k_1 value of 10 µ is possible. The determination of the constants is described in Ref. 12.

Because of its three constants, Eq. (3) is inconvenient for practical application. In numerous applications, however, it can be approximated by the far simpler Eq. (1), where an average k value, k', depending on the type and size of the object, is introduced; k' can be determined with a line of 15 µ width.[12]

The intensity in the middle of a line having the width b, formed by scattered light, can be calculated with the aid of Eq. (1) (Ref. 4, Vol. II; Ref. 5):

$$I_M/I_0 = 10^{-b/k'}$$

where I_M = effective intensity in the center of a line
I_0 = printed-on intensity
b = width of the line
k' = average k value

If we use Eq. (3):

$$I_M/I_0 = \rho\, 10^{-b/k_1} + (1 - \rho)\, 10^{-b/k_2} = 10^{-b/k'} \qquad (4)$$

from which we obtain:

$$k' = b/\log\, [\rho\, 10^{-b/k_1} + (1 - \rho)\, 10^{-b/k_2} \qquad (5)$$

It is also possible to define k' for gratings of certain space frequency.

Light Scattering and Absorption

Equation (3) can be interpreted as follows: The first term indicates the exposure by nonscattered light. The second term describes the exposure by scattered light, and the decrease of the scattered light with an increasing distance from the exposed part. The decrease of the scattered light is caused by absorption of the light in the emulsion as well as by losses in the boundary areas. With a diffusing layer and a printed-on narrow slit, this decrease will essentially proceed in an exponential manner, since the decrease of intensity through a layer element dx at a distance of x from the slit drops in proportion to the prevailing radiation and the magnitude dx. The exponential decrease corresponds to the straight-line portion of the image width curves in Fig. 2 (Curve B). A steeper decrease must be expected with a point-shaped source since the exponential decrease is supplemented by the weakening caused by radial expansion, contrary to the assumption of Sayanagi.[13]

The spread of scattered light within the emulsion plane is measured by the constant k_2. This spread is limited, due to the gradual intensity loss of the scattered light intensity. According to the definition, k_2 is equal to the "$^1/_{10}$ width" of the distribution of scattered light around a narrow slit. Thus, at a distance $k/2$ from the slit center, the intensity drops to the tenth part of that in the center of the slit. This corresponds to an exposure module of $2/k$ to the base 10. One can now attempt to relate the extinction module in the layer plane to the extinction module normal to the layer. This is equal to D/h, where D is the diffuse density of the undeveloped emulsion, and h is the thickness of the layer. If this consideration is valid, $2h/D$ would equal k_2. Figure 4 shows this to be approximately the case for small values of k_2, while $k_2 < 2h/D$ applies to large values. In any case, the values established for two layers

13. K. Sayanagi, *J. Opt. Soc. Am.*, **47**: 566 (1957).

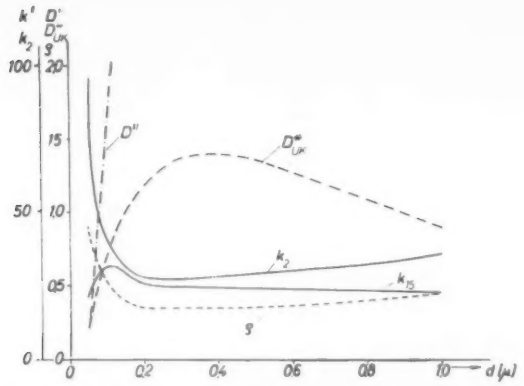

Fig. 6. Diffuse density, $D^{\perp\!\!\!\perp}$, density in specular light, $D^{\shortparallel}$, and constants of the diffusion halo, k_2, ρ, and k', as function of the average grain diameter, d.

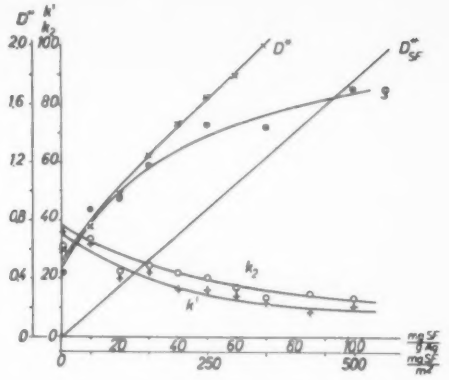

Fig. 7. Effect of dyeing the emulsion with acid fuchsin (SF) on the diffusion halo. Values D, ρ, k_2, and k', as function of the dye concentration. D_{SF} corresponds to the density values obtained by dyeing a gelatin without silver bromide (5 grams Ag per sq m; thickness of layer, 15 μ).

with strongly varying grain size, coating weight, and layer thickness, are close to the entered line.

It is of special interest to study the SF as a function of the grain size of the emulsions examined. Figure 5 presents the width of the slit image as a function of the logarithm of the exposure for emulsions with various silver halide crystal sizes obtained at various ripening times.

On the basis of these and similar experiments, it was possible to determine the various constants of the SF, as shown in Fig. 6 by the densities of the undeveloped layer in specular ($D^{\shortparallel}$) and diffused light ($D^{\perp\!\!\!\perp}$). Figure 7 gives data on an experiment in which the effect of dyeing the layer with an inert dye was examined.

The results can easily be interpreted by use of the previous concept (see Fig. 8).

Very fine grain layers (Grain size $d \sim 0.04$ μ). Ripening time 0 min. Spread and absorption are very limited, while k_2 is correspondingly large. The portion of the light that causes the diffusion halo is quite limited. As a result of limited absorption, however, the radiation shows a considerable spread resulting in the steeply ascending image width curve (Figs. 5 and 6).

Fine-grain layers ($d \approx 0.06$ μ). Spread and absorption are still limited, although both values are distinctly larger than with layers possessing a still finer grain. $\rho = 0.65$; $k_2 = 70$ μ. k' is relatively large.

Medium-grain layers. Spread and absorption are quite extensive. Accordingly, $\rho = 0.35$ and $k_2 = 30$ μ. As a result of the extensive absorption k' is smaller. Although the intensity of the scattered light is considerable, it decreases noticeably at a small distance from the slit.

Coarse-grain layers. The spread is more limited. ρ and k_2 are correspondingly larger.

Dyed layer. The absorption increases, and k_2 drops accordingly. ρ is increased and k' is reduced correspondingly (Fig. 7).

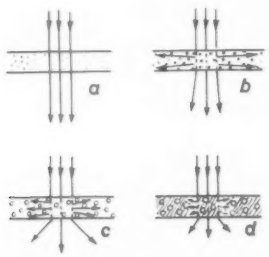

Fig. 8. Schematic drawing of the origin of the diffusion halo in various types of layers. (a) Very fine grain layer, $d \sim 0.04$ μ; absorption very slight, k_2 very large; spread very slight ($\rho \sim 1$). (b) Fine grain layer, $d \sim 0.06$ μ; absorption slight, k_2 large ($k_2 = 70\mu$); spread slight, ρ large ($\rho \sim 0.65$). The diffusion halo is not very intensive but shows considerable expansion. (c) Medium grain layer, $d \sim 0.4$ μ; strong absorption, $k_2 = 30$ μ; strong diffusion halo, but restricted spread. (d) Same layer as in (c), but dyed; absorption, particularly of scattered light, intensified; therefore, k_2 is reduced, ρ enlarged.

Contrast Transfer Function

The CTF is obtained from the SF by Fourier transformation. For the SF according to Eq. (1) we obtain:

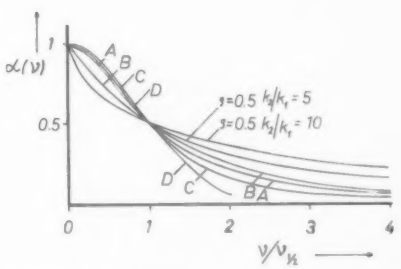

Fig. 9. Comparison of different CTF proposed in the literature (see Table I). A = function according to Eqs. (6) and (7) (SF is an exponential function); B = exponential function; C = the two-dimensional SF (point-SF), an exponential function (Sayanagi); D = Gaussian function.

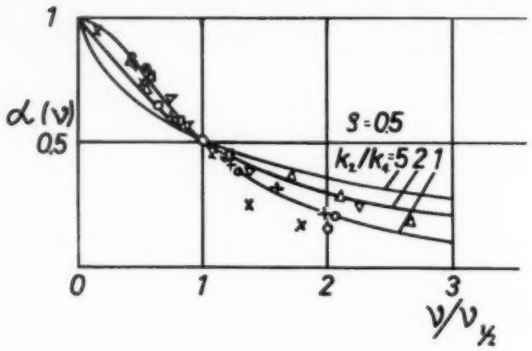

KEY TO SYMBOLS IN FIGURE 10

According to	Symbol	Film	Developer	$\nu_{1/2}$ in mm^{-1}
Hendeberg[16]	×	Agfa IFF (A)	Final	66
	+	Agfa IFF (B)	Final	73
	○	Agfa IF	Final	57
	△	Agfa ISS	Final	44
	▽	Agfa IU	Final	34
Lamberts[17]	○	Tri-X	DK-50,	28
		* Panatomic-X	5 min	60
		* Microfile		65
Our own experiment[18]	□	Agfa ISS	Final	30

* The shape of the curves for Panatomic-X and Microfile is similar to that for Tri-X Film.

Fig. 10. Comparison of CTF according to Eqs. (6) and (7), with experimental values (A_1 and A_2 in Table I, below).

$$\alpha(\nu) = \frac{1}{1 + (\pi k\nu/2.3)^2} = \frac{0.54}{0.54 + (k\nu)^2} \qquad (6)$$

where ν = frequency in mm^{-1}, and according to Eq. (3):

$$\alpha(\nu) = \frac{\rho}{1 + (\pi k_1\nu/2.3)^2} + \frac{1 - \rho}{1 + (\pi k_2\nu/2.3)^2} = \rho\alpha_1(\nu) + (1 - \rho)\alpha_2(\nu) \ldots . \qquad (7)$$

Equation (6) was established by Frieser[9,10] in 1935. According to Frieser and Linke,[14] CTF can be determined with sufficient accuracy by a k-value established from the slit image width, although obviously only for the relatively thick layers with a limited ρ value used at that time. In the case of larger values of ρ, Eq. (3) must be applied and the spread function calculated by Eq. (7).

These and a few additional formulas listed in Table I and presented in Fig. 9 are offered for the CTF.

In Fig. 10, Eqs. (6) and (7) (i.e., A_1 and A_2 of Table I) are compared with results reported by several authors. The majority of the values given are taken from Hendeberg's paper[16] composed at the

14. H. Frieser, and H. Linke, *Z. wiss. Phot.*, **37:** 19 (1938).

15. R. C. Jones, *Phot. Sci. & Eng.*, **2:** 198 (1958).
16. L. O. Hendeberg, *Arkiv Fysik*, **16:** 417 (1960).
17. R. L. Lamberts, *J. Opt. Soc. Am.*, **49:** 425 (1959).
18. H. Frieser, *Phot. Korr.*, **94:** 115, 131, 147 (1958).
A. Narath, *Kino-Technik*, **20:** 93 (1938).
H. Frieser, *Phot. Korr.*, **92:** 183 (1956).

TABLE I—Various Spread Functions (SF) and Contrast Transfer Functions (CTF) Proposed in the Literature

Source (see footnote)	1-dimensional (Slit-SF)	2-dimensional (Point-SF) $r^2 = x^2 + y^2$	CTF
A_1	$\frac{2.3}{k}\,10^{-2\lvert x\rvert/k}$	$\frac{2}{\pi}\left(\frac{2.3}{k}\right)K_0\left(\frac{2\cdot 2.3}{k}\right)$	$\frac{1}{1 + (\pi k\nu/2.3)^2}$
A_2	$\frac{2.3\rho}{k_1}\,10^{-2\lvert x\rvert/k_1} + \frac{2.3(1-\rho)}{k_2}\,10^{-2\lvert x\rvert/k_2}$		$\frac{\rho}{1 + (\pi k_1\nu/2.3)^2} + \frac{1-\rho}{1 + (\pi k_2\nu/2.3)^2}$
B	$\frac{a}{\pi(a^2 + x^2)}$	$\frac{a}{\pi(a^2 + r^2)^{3/2}}$	$e^{-a\nu}$
C	$\frac{1}{\pi s}\left(\frac{\lvert x\rvert}{s}\right)K_1\left(\frac{\lvert x\rvert}{s}\right)$	$\frac{1}{2\pi s^2}\,e^{-r/2}$	$[1 + (2\pi s\nu)^2]^{-3/2}$
D	$\frac{1}{\sqrt{2\pi}\sigma}\,e^{-x^2/2\sigma^2}$	$\frac{1}{2\pi\sigma^2}\,e^{-r^2/2\sigma^2}$	$e^{-\sigma^2(2\pi)\nu^2/2}$

A_1 and A_2—H. Frieser[1,9,10,12]; B—R. C. Jones[15]; C—Sayanagi[13]; D—Gaussian function[6,16]; K is the Bessel function, second order.

Institute for Optical Research in Stockholm (Prof. Ingelstam), which contains particularly careful measurements. In addition, measurements from the Kodak Laboratories as well as our own results are mentioned. It is shown that the points corresponding to the experimental values with low space frequencies ($\nu < \nu_{1/2}$) are well presented by a curve but deviate strongly in the lower part of the curve.

In the discussion of his results, Hendeberg states that the Gauss function generally presents the results in a satisfactory manner only for values $\nu < \nu_{1/2}$. The exponential function particularly fails in the case of smaller frequencies because $(d\alpha/d\nu)_\nu = 0$, which does not agree with experience. The measured values can best be shown by functions A and B, although there are some deviations here. Thus, Hendeberg reaches the correct conclusion that a one-parameter function definitely prevents the possibility of an exact representation. As shown in Fig. 10, the graphic representation of the points is possible through a CTF corresponding to Eq. (7). In our diagram, the measured values are compared with curves calculated on the basis of Eq. (7) and using the values: $\rho = 0.5$, and $k_2/k_1 = 1$, 2, and 5.

By suitable selection of the parameters, it is easy to obtain a curve which agrees quite well with the function of Sayanagi (Eq. C in Table I). Thus, it is shown that the theory according to which the SF consists of two exponential functions results in a CTF which agrees well with experience. In the case of frequencies $\nu < \nu_{1/2}$, it is obviously possible to use the simple Eqs. (1) and (6) respectively, whereby an average k-value (k') is applied. The extended formula (Eq. (3), Eq. (7)) is required for large frequencies. For practical applications, however, two parameters proved sufficient. It is, of course, also possible to derive other two-parameter formulas which are quite simple in their application. However, they lack any theoretical foundation.

1961 Annual Conference

May 22–26

Arlington Hotel, Binghamton, New York

The 1961 Annual Conference of the Society will be held the week of May 22 in Binghamton, New York. A special group of papers on color photography and papers pertaining to other scientific and engineering aspects of photography and photosensitive materials, photographic equipment, and instrumentation are being planned.

Inquiries about papers should be directed to:

Dr. F. H. Gerhardt
771 River Road
M.R. 97
Binghamton, New York

Other conference committee chairmen are:

Conference Chairman:
M. G. Anderson
Ansco Division
Vestal Parkway East
Binghamton, New York

Exhibits Chairman:
C. W. Seager
Ansco Division
Vestal Parkway East
Binghamton, New York

PHOTOGRAPHIC SCIENCE AND ENGINEERING
Volume 4, Number 6, November–December 1960

The Effect of the Variables of a Photographic System on Detail Rendition, with Special Reference to Camera Motion

ROBERT N. WOLFE AND SAM A. TUCCIO, *Research Laboratories, Eastman Kodak Company, Rochester, N.Y.*

A theoretical discussion is given to show the way in which the various photographic parameters, such as lens focal length, aperture diameter, scene luminance, granularity, and emulsion sensitivity can be varied so that, for a given speed of linear image motion, detail rendition can be optimized. The conclusions are confirmed experimentally and their application to aerial photography is indicated. The same principles can be applied when the camera is stationary and other characteristics of the system are varied.

Numerous studies have been made on resolving power as a function of the characteristics of a photographic system. Mees[1] discusses them in detail and an extensive review of the literature is contained in a paper by Perrin and Altman.[2] In the case of aerial photography, camera motion is an additional significant factor. The earliest study of the effect of camera motion on aerial photographs seems to have been that reported by Antilli,[3] and later Tearle[4] discussed the work done by Gregory on this subject. Cruset,[5] Wolfe and Lamberts,[6] and Ryabushkin[7] made critical experimental studies of it for shutters of various efficiencies. In so far as the work of these experimenters overlapped, their results agree.

But resolving power is only one factor, albeit an important one, governing the rendition of detail in an aerial photograph. In the work reported in the present paper, the interrelationships between camera motion and the other important characteristics of a photographic system, such as the focal length and diameter of the lens, the luminance of the scene, and the sensitivity, spread function, and granularity of the emulsion, are studied so that the requirements for obtaining the maximum amount of detail in the presence of a given amount of camera motion can be determined. The results, of course, are also applicable when the camera is stationary.

In this paper, a theoretical discussion which is an extension of a theory of informational sensitivity developed by Zweig, Higgins, and MacAdam[8] will be given and then an experimental confirmation will be presented. This theory of informational sensitivity was developed concurrently with the experimental work described in the present paper, but the experimental data were arrived at empirically and independently of the theory. The extension of the theory was especially tailored to fit the conditions of aerial photography.

Theory

The negative section of the photographic system used for aerial photography is shown in Fig. 1. The aerial camera lens L has an entrance pupil of diameter A and, for the purpose of this discussion, its performance is considered to be limited by diffraction alone. The camera is at a height H above the ground and is pointed vertically downward. The lens forms an image of the terrain on the photographic film E. The lens-to-film distance is f and the camera is moving with the ground speed V.

The distribution of illuminance I in the image of a long line source of light, i.e., the line integral of the Airy disk or the line spread-function, is given by the relation,[9]

$$I(z) = 1 - \frac{4z^2}{3\cdot 5} + \frac{4^2z^4}{3\cdot 5^2\cdot 7} - \frac{4^3z^6}{3\cdot 5^2 2\cdot 7^2\cdot 9} + \cdots$$

In this equation,

$$z = \pi A x'/\lambda f,$$

where x' is the distance of the point for which the

Communication No. 2108 from the Kodak Research Laboratories. Presented at the National Conference, Chicago, 28 October 1959, under the title "The Effect of Image Motion on the Detail Rendition of Photographic Systems." Received 14 July 1960.

1. C. E. K. Mees, *The Theory of the Photographic Process*, rev. ed. Macmillan, New York, 1954, pp. 1010–1024.
2. F. H. Perrin and J. H. Altman, *J. Opt. Soc. Amer.*, **43:** 780 (1953).
3. C. Antilli, *Riv. aeronaut.*, **3:** 15 (1927).
4. J. L. Tearle, "Definition in Air Photographs," in *La Théorie des Images Optiques*, Revue d'Optique, Paris, 1949, p. 304. Summary of the International Colloquium on the Theory of Optical Images held at Paris in 1947.
5. J. Cruset, *Archives Internationales de Photogrammétrie. Proceedings of the 7th International Congress of Photogrammetry*, 1952, Vol. 11, Part I, American Society of Photogrammetry, 1954, pp. 49–69 (or p. 280).
6. R. N. Wolfe and R. L. Lamberts, *Phot. Eng.*, **6:** 270 (1955).
7. Yu. V. Ryabushkin, *Zhur. Nauch. i Priklad. Fotografii i Kinematografii*, **3:** 197 (1958).
8. H. J. Zweig, G. C. Higgins, and D. L. MacAdam, *J. Opt. Soc. Amer.*, **48:** 926 (1958).
9. Lord Rayleigh, *Scientific Papers*, Vol. III, Cambridge University Press, 1902, p. 95.

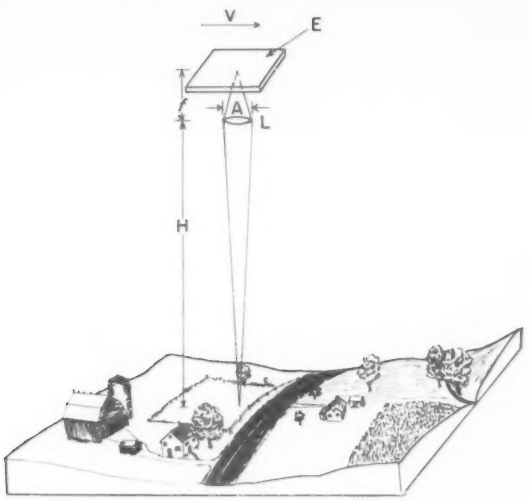

Fig. 1. Sketch of photographic system used for aerial photography to illustrate the symbols used in the text.

intensity is evaluated from the center line of the image and λ is the wavelength of the light.

This line spread-function and the line spread-function for other elements of the system to be discussed later can be closely approximated by the Gaussian curve,

$$y = e^{-x^2/2\sigma^2},$$

where σ is determined so that the area under the normalized Gaussian curve, i.e.,

$$2\int_0^\infty e^{-x^2/2\sigma^2}\,dx = (2\pi)^{1/2}\,\sigma,$$

is equal to the area under the actual normalized line spread-function curve. This quantity σ is a single parameter which can be used to characterize each of the distribution curves. It is equal to the area under the curve divided by $(2\pi)^{1/2}$ and also to the half-width of the Gaussian curve at $y = 0.606y_{max}$. It has the units in which x is expressed and the dimensions of length when x represents a length.

In the case of the diffraction curve, the area under it is approximately equal to $3.54\lambda f/\pi A$. When this is equated to $(2\pi)^{1/2}\,\sigma_{L'}$, where $\sigma_{L'}$ determines the Gaussian approximation to the diffraction curve, we have

$$\sigma_{L'} = 0.45\,\lambda f/A.$$

In the case of the spread functions, primed symbols will refer to distances along the film, and plain symbols will refer to distances along the ground.

A comparison between the diffraction spread-function of a line source for a diffraction-limited $f/8$ lens and the Gaussian approximation is shown in Fig. 2. Over the important central maximum, the broken curve representing the Gaussian distribution closely matches the solid curve representing the lens spread-function. In this case, where λ was taken as 0.58μ, $\sigma_{L'}$ is 2.1μ.

As an aid to understanding this problem and to interpreting the data later, all spread functions will be "projected onto the ground," i.e., they will be multiplied by the scale factor H/f. Thus

$$\sigma_L = 0.45\,\lambda H/A.$$

It should be noted that σ_L is independent of f.

The parameter $\sigma_{F'}$ for the line spread-function of the emulsion is obtained by integrating the spread function graphically and then dividing this integral by $(2\pi)^{1/2}$. Figure 3 shows a comparison between the emulsion spread-function for Kodak Plus-X Aerecon Film and its Gaussian approximation. In this case, the value of $\sigma_{F'}$ is 4 μ and

$$\sigma_F = \sigma_{F'}\,H/f.$$

A line spread-function analogous to the spread function just mentioned is introduced into the system by the motion of the camera relative to the ground during the time the exposure is made. It will help in understanding this spread function if we imagine a line source of light at the film plane of the camera to be imaged on the ground with an impossibly perfect lens, i.e., one that images a point as a point

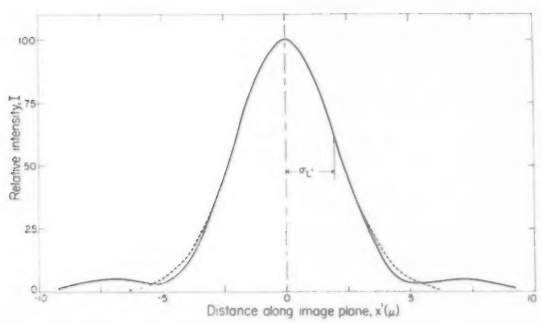

Fig. 2. Diffraction spread-function of a line source for an f/8 lens and $\lambda = 0.58\ \mu$ (solid curve) compared with Gaussian approximation having $\sigma_{L'} = 2.1\ \mu$.

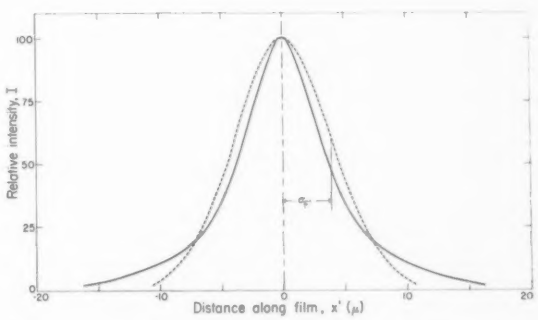

Fig. 3. Line spread-function of Kodak Plus-X Aerecon Film (solid curve) compared with Gaussian approximation having $\sigma_{F'} = 4\ \mu$.

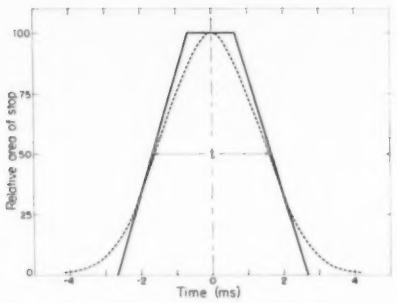

Fig. 4. Area–time curve of typical shutter of 62.5% efficiency (solid curve). Nominal exposure time t is for 50% opening.

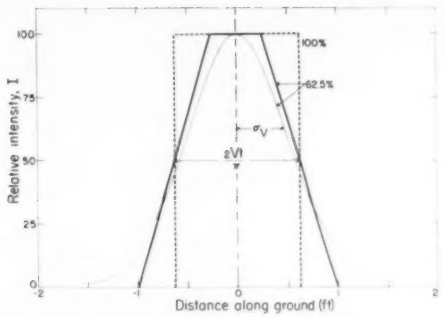

Fig. 5. Relative intensity in image of a line as a function of distance along ground for shutter of 100% efficiency (rectangular curve) and 62.5% efficiency (trapezoidal curve) for ground speed of 360 mph and shutters of nominal speed (at 50% opening) of $1/300$ sec. Line orientation is averaged between directions parallel and perpendicular to line of flight. Dotted curve, Gaussian approximation having $\sigma_V = 0.34$ ft.

(free from both diffraction and aberrations). Now consider the intensity distribution or spread function of this image on the ground during the time that an exposure is made. This spread function is determined by the relative area–time curve of the shutter. Such a curve is shown solid in Fig. 4. The nominal[10] exposure time t is the time interval between the two positions that make the area of the shutter 50% of the total, and this quantity is represented by the width of the spread function at this 50% ordinate. The integral of the resulting trapezoidal figure is equal to t. As before, a Gaussian curve (broken) can be fitted to this figure. Thus

$$\sigma_t = t/(2\pi)^{1/2}.$$

The values along the time axis, multiplied by the ground speed V of the camera, obviously give the abscissa values for the image-motion spread-function projected onto the ground. This spread function is for lines on the ground perpendicular to the line of flight, and thus it has the maximum width (i.e., its width is greater than for lines of any other orientation). At the other extreme, lines parallel to the line of flight have an image-motion spread-function of zero width. In general, if θ is the angle made between a line on the ground and the line of flight, the width of the spread function is

$$\sigma = Vt/(2\pi)^{1/2} \sin\theta,$$

where

$$0 \leqq \theta \leqq \pi/2.$$

Then it follows that the average value of σ is

$$\sigma_V = \frac{Vt}{(2\pi)^{1/2}} \cdot \frac{\int_0^{\pi/2} \sin\theta \, d\theta}{\pi/2} = \frac{2Vt}{\pi(2\pi)^{1/2}} = 0.254Vt.$$

The broken curve in Fig. 5 is the normalized image-motion spread-function for a shutter with an efficiency of 100% when the effective component of velocity is $(2/\pi)V$. The solid curve is the spread function for a typical shutter operating at an efficiency of 62.5% and giving the same exposure. The values of the abscissas, instead of being in terms of exposure time as in Fig. 4, are in terms of distance on the ground in feet on the assumption that the exposure time is 1/300 sec and that the camera has a ground speed of 360 mph. The dotted curve is the Gaussian curve representing the same exposure.

Now we must note the photographic factors which determine the time of exposure. For any photographic system, the exposure time is directly proportional to the square of the f-number, which is defined as f/A, and is inversely proportional to both the luminance of the scene I and the sensitivity of the emulsion S:

$$t = (f^2/A^2)\,(IS)^{-1}.$$

The constant of proportionality is here considered as being included in S. Making use of this relationship, we can say that

$$\sigma_V = \frac{2Vf^2}{\pi(2\pi)^{1/2}ISA^2} = \frac{0.254Vf^2}{ISA^2}.$$

Finally, the composite spread-function, projected onto the ground, is found by the convolution of the lens, emulsion, and image-motion spread-functions. Since these spread functions have been approximated by Gaussian curves, this spread function is also of the form

$$y = e^{-1/2(x/\sigma_B)^2},$$

where

$$\sigma_B = (\sigma_L^2 + \sigma_F^2 + \sigma_V^2)^{1/2}.$$

From this it follows that

$$\sigma_B^2 = \left(\frac{0.45\lambda H}{A}\right)^2 + \left(\frac{\sigma_{F'}H}{f}\right)^2 + \left(\frac{0.254Vf^2}{ISA^2}\right)^2. \quad (1)$$

Figure 6 shows an example in which the lens and film spread-functions of Figs. 2 and 3 are projected onto the ground (solid curves) and then convoluted with

10. W. F. Berg, *The Fundamentals of Camera Technique*, 2nd ed., Focal Press, London, 1955, p. 86.

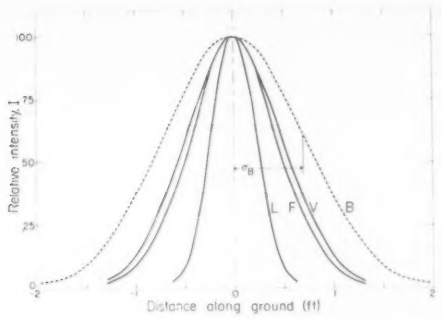

Fig. 6. Gaussian approximations to lens (L), film (F), and ground-motion spread-functions (V), shown in preceding figure, and (B) their combination by Eq. (1).

the image-motion spread-function from Fig. 5 to give the broken composite curve.

It can be shown, on the basis of the theory developed by Zweig, Higgins, and MacAdam,[8] that

$$I \cdot E = \frac{\gamma}{[a_s^{1/2}\sigma_s(D)]a_s^{1/2}}, \tag{2}$$

where I is informational sensitivity, E is photographic exposure, γ is the slope of the straight portion of the D-log E curve, a_s is the area of the emulsion spread-function, and $\sigma_s(D)$ is the rms fluctuation in density as the emulsion is scanned with an aperture having a diameter $(4/\pi)^{1/2}a_s^{1/2}$. It seems reasonable to interpret the product $I \cdot E$ as a measure of the information* or the detail reproduced in a picture.

Detail reproduction in this sense can only be determined by making a subjective appraisal of a picture. Let us define ρ as being proportional to this appraisal. Then, if we hold γ constant, we can write the psychophysical relationship as

$$\rho \propto \{[(a_s^{1/2}\sigma_s(D)]a_s^{1/2}\}^{-1}.$$

Now $a_s^{1/2}\sigma_s(D)$ is the Selwyn[11] granularity of the material. We can thus say that the detail reproduction which a photographic material will give should be inversely proportional to the Selwyn granularity multiplied by the square root of the spread-function area. This rule, of course, assumes that there are no other elements of the photographic system contributing to any loss of detail reproduction.

It seems reasonable to extend this concept to the entire photographic system by substituting σ_B for $a_s^{1/2}$. If we make all the photographic reproductions to be intercompared so that the scale relative to the original scene is constant and if the pictures are all viewed from the same distance, the size of the scanning aperture, i.e., the effective retinal element projected onto the picture, is also constant. Designating the diameter of this scanning aperture by ϕ', we can write

$$\rho \propto [\phi' \cdot \sigma(D) \cdot \sigma_B]^{-1}.$$

Since ϕ' is constant for fixed viewing conditions, we can simplify this equation and write

$$\rho \propto (\sigma_G \cdot \sigma_B)^{-1}. \tag{3}$$

Here $\sigma(D)$ is written σ_G for consistency of symbolism. It must be emphasized again that the quantity ρ, representing detail reproduction, can be determined only by the visual examination of pictures.

The value of σ_G can be computed from the value of $\sigma(D)$ as measured for an aperture 24 μ in diameter. Stultz and Zweig[12] have shown that, when a group of observers arrange a set of negatives at a magnification M_1 of 24 $\times$ in the order of their objectionability from the standpoint of graininess, the order comes out to be the same as it is when the negatives are arranged in their order of $(\sigma_G)_1$ for a scanning aperture ϕ_1 of 24 μ. On the basis of Selwyn's relation, we may therefore set

$$\sigma_G = (\sigma_G)_1 (M/M_1), \tag{4}$$

where σ_G is the rms density variation corresponding to any degree of enlargement M.

In order to make a subjective comparison of the amount of detail recorded by lenses differing in focal length, it is necessary[13] to enlarge the resulting camera negatives so that the various enlargements all have the same scale P_E relative to the sizes of objects on the ground, as was mentioned earlier. The viewing or enlarging magnification necessary to achieve this is given by the relation

$$M = (H/P_E)(1/f). \tag{5}$$

Substituting this value of M in Eq. (4) gives

$$\sigma_G = \frac{(\sigma_G)_1 H}{M_1 P_E f}. \tag{6}$$

Substituting the expression for σ_B from Eq. (1) and that for σ_G from Eq. (6) into Eq. (3), we have

$$\rho^{-1} = \frac{(\sigma_G)_1 H}{M_1 P_E f}\left[\left(\frac{0.45\lambda H}{A}\right)^2 + \left(\frac{\sigma_{F'} H}{f}\right)^2 + \left(\frac{0.254 V f^2}{ISA^2}\right)^2\right]^{1/2}. \tag{7}$$

If P_E is taken as unity, i.e., if objects on the ground are reproduced in their natural sizes, the σ_G-values will also be "projected onto the ground," but this is not necessary in the argument to follow. All that is necessary is that P_E be constant.

It can be seen by inspecting Eq. (7) that there is some value of f which will optimize the detail rendition because of the way f and f^2 enter the equation. Differentiating the equation with respect to f, setting the derivative equal to zero, and solving the re-

* The term "information" as used in this paper should not be construed to relate in any manner to the specialized meaning that the word has acquired in "information theory." Instead it is used in its common nonspecialized sense, as was done in Ref. 8 by Zweig, Higgins, and MacAdam.

11. E. W. H. Selwyn, *Phot. J.*, **75**: 571 (1935); **79**: 513 (1939).

12. K. F. Stultz and H. J. Zweig, *J. Opt. Soc. Amer.*, **49**: 693 (1959).

13. R. N. Wolfe, *J. Opt. Soc. Amer.*, **49**: 172 (1959).

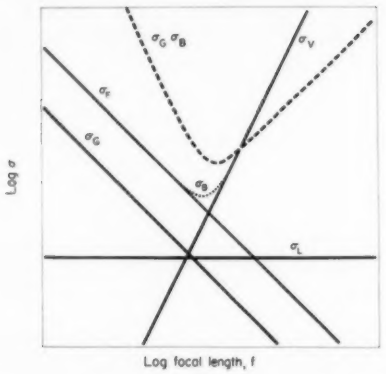

Fig. 7. Variation of the spread-function parameters of lens (σ_L), film (σ_F), ground motion (σ_V), and granularity (σ_G) with focal length of camera lens. Dotted curve, parameter σ_B of combination of σ_L, σ_F, and σ_V; broken curve, parameter $\sigma_G\sigma_B$ representing detail rendition.

sulting cubic equation, we find the focal length giving the maximum detail rendition to be

$$f_0 = (1/0.254)^{1/3}\,(\sigma_{F'}ISA^2/\omega)^{1/3} \times$$
$$[(1 + <1 - R>^{1/2})^{1/3} + (1 - <1 - R>^{1/2})^{1/3}]^{1/2}, \quad (8)$$

where

$$R = \frac{(0.45)^6\pi^3\lambda^6 I^2 S^2}{54\omega^2 A^2 \sigma_{F'}^4} \quad (9)$$

and $\omega = V/H$, the angular velocity of the camera relative to the ground.

As ω increases greatly with respect to the other factors, the fraction R approaches zero and $1-R$ approaches unity. For high velocities, therefore,

$$(f_0) = \pi^{1/2}(\sigma_{F'}ISA^2/\omega)^{1/3}. \quad (10)$$

(The trigonometric solution for the case when $R > 1$ will not be discussed here.)

The value of the optimum focal length f_0 can be obtained from Eq. (8). By substituting this value for f in Eq. (7), the optimum value of the product $(\sigma_G \cdot \sigma_B)_0$ can also be obtained for the given set of photographic-system parameters. This is illustrated in Fig. 7. The logarithms of the various quantities are shown plotted against the logarithm of the focal length. As previously pointed out, σ_L is independent of focal length. However, σ_F and σ_G, which are inversely proportional to focal length, have graphs with a slope of -1. Also, σ_V, which is directly proportional to the square of the focal length, has a graph with a slope of $+2$. Since

$$\sigma_B = (\sigma^2_L + \sigma^2_F + \sigma^2_V)^{1/2}, \quad (11)$$

the curve of σ_B follows the curves for σ_F and σ_V closely and shows a sharp minimum in the region of their crossing. The application of the factor σ_G to σ_B tends to raise the curve of $\sigma_G\sigma_B$ above the curve of σ_B on the left in the region of shorter focal lengths and lowers it on the right in the region of longer focal lengths, thus shifting the minimum slightly to the right from that for the curve of σ_B.

The conditions for a stationary camera are easily seen because then $\sigma_V = 0$ and σ_B is determined only by σ_F and σ_L. This means that σ_B, like σ_G, continually decreases as the focal length f increases. Since $\sigma_G\sigma_B$ thus continually decreases with increasing focal length, the quantity ρ in Eq. (3) representing the ability of the system to record detail continually increases. There is thus some justification for the statement sometimes made that the longer the focal length of the camera, the finer the detail that can be recorded.

Experimental Procedure

The theoretical predictions that the subjective quantity "detail rendition" can be evaluated and that, when the camera moves, there is a focal length for a camera lens of given linear aperture which will give an optimum value of detail rendition were tested experimentally. The procedure was to make photographs of a scene under controlled conditions and then have the photographs judged so that the pertinent physical and psychometric data could be obtained.*

The scene used as the "test object" is shown in Fig. 8. The numbers on the panels indicate their widths in inches. An attempt was first made to photograph this scene itself from a distance of approximately 6 miles—30,000 ft. In this way the various objects in the scene would be reproduced on the negative as images having the same sizes as they would have in typical aerial photography. Such photographs were made, but the first attempt showed that the experiment could not be carried out in this way because of the adverse effects of atmospheric haze and turbulence. These atmospheric effects covered up many of the differences we expected to find between the various lens–film combinations.

It was therefore necessary to obtain negative images of the proper sizes indirectly in the laboratory. A close-up photograph of the scene was made and a positive transparency was prepared from it of such a

* Some of the experimental data presented in this paper are the same as were presented in a previous paper (Ref. 13), which was concerned only with the case where the camera was stationary.

TABLE I. Data on Materials Studied

Kodak film	IS* sec^{-1}	$\sigma_{F'/\mu}$	$(\sigma_G)_1$†
Tri-X Aerial Recon	180	7.32	0.0952
Plus-X Aerecon	40	4.03	0.0584
Panatomic-X	20	2.87	0.0432
Micro-File	0.40	1.63	0.0128
Experimental document-recording	0.008	0.62	0.004

* Laboratory conditions. Exposure time is approximately 1000 times greater than would be used in practice because the lower value of I was used.

† For circular aperture of diameter $\phi = 24\ \mu$.

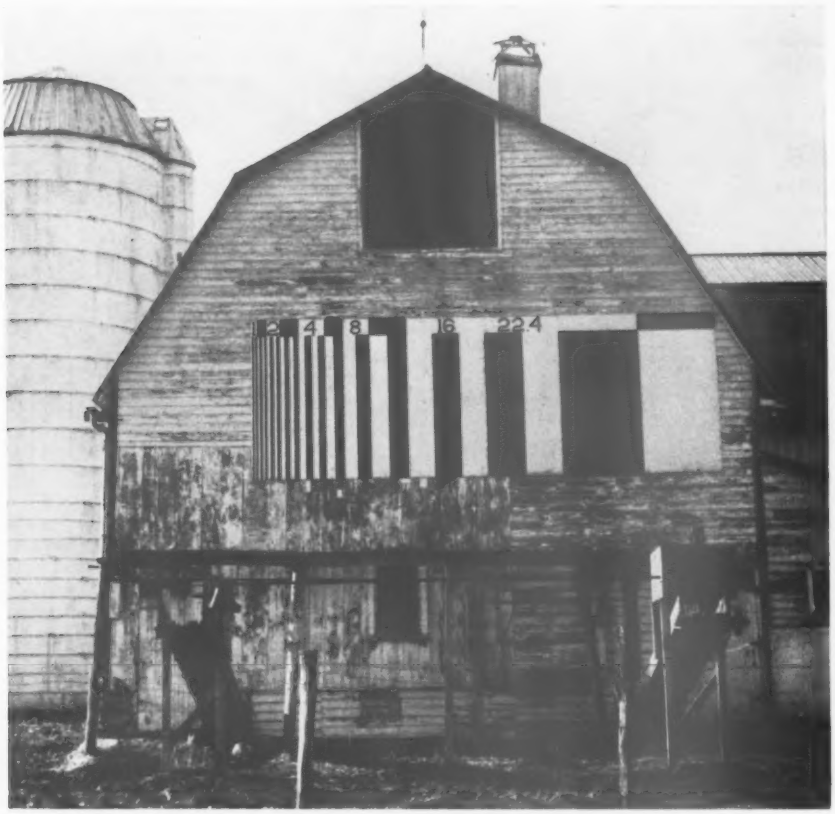

Fig. 8. Scene used for making pictures for judging detail rendition.

size that when it was, in turn, photographed in the laboratory from a distance of approximately 80 ft with the lenses used for the experiment, the negative images were the sizes that they would have been if the original scene had been photographed from 30,000 ft. This distance varied only from 83 ft for the shortest focal length to 86 ft for the longest. In the calculations shown in this paper, the distance to the original scene is taken as 9.53 km (31,266 ft).

A list of the films which were used in this experiment is shown in Table I. This table also shows IS, $\sigma_{F'}$, and $(\sigma_G)_i$ for the films. Under the conditions of illumination used in the laboratory, the exposure times were approximately one thousand times greater than would have been needed for actual outdoor exposures. The values of $\sigma_{F'}$ were derived from the emulsion spread-function curves shown in Fig. 9. These curves were obtained from the Fourier transforms of the sine-wave response curves that were, in turn, measured experimentally with the technique described by Lamberts.[14] The values of $(\sigma_G)_i$ were obtained with a circular scanning aperture having a diameter of 24 μ.

The Kodak Tri-X emulsion was one of the fastest aerial materials available when the experiment was made. The Kodak Plus-X emulsion was comparable with the aerial materials then in current use, while the Kodak Panatomic-X emulsion was somewhat slower than the first two and was finer-grained. The Kodak Micro-File emulsion was a slow, fine-grained material for copying documents, and the experimental document-recording emulsion was a still

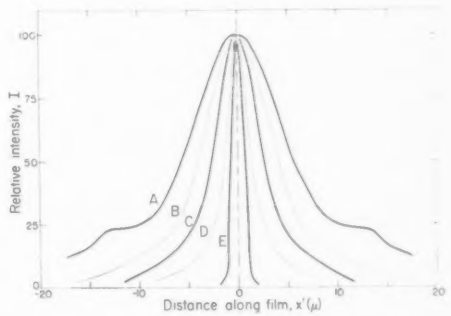

Fig. 9. Spread functions of Kodak films studied. *A*, Tri-X; *B*, Plus-X; *C*, Panatomic-X; *D*, Micro-File; *E*, Experimental document-recording films.

14. R. L. Lamberts, *J. Opt. Soc. Amer.*, **49:** 425 (1959).

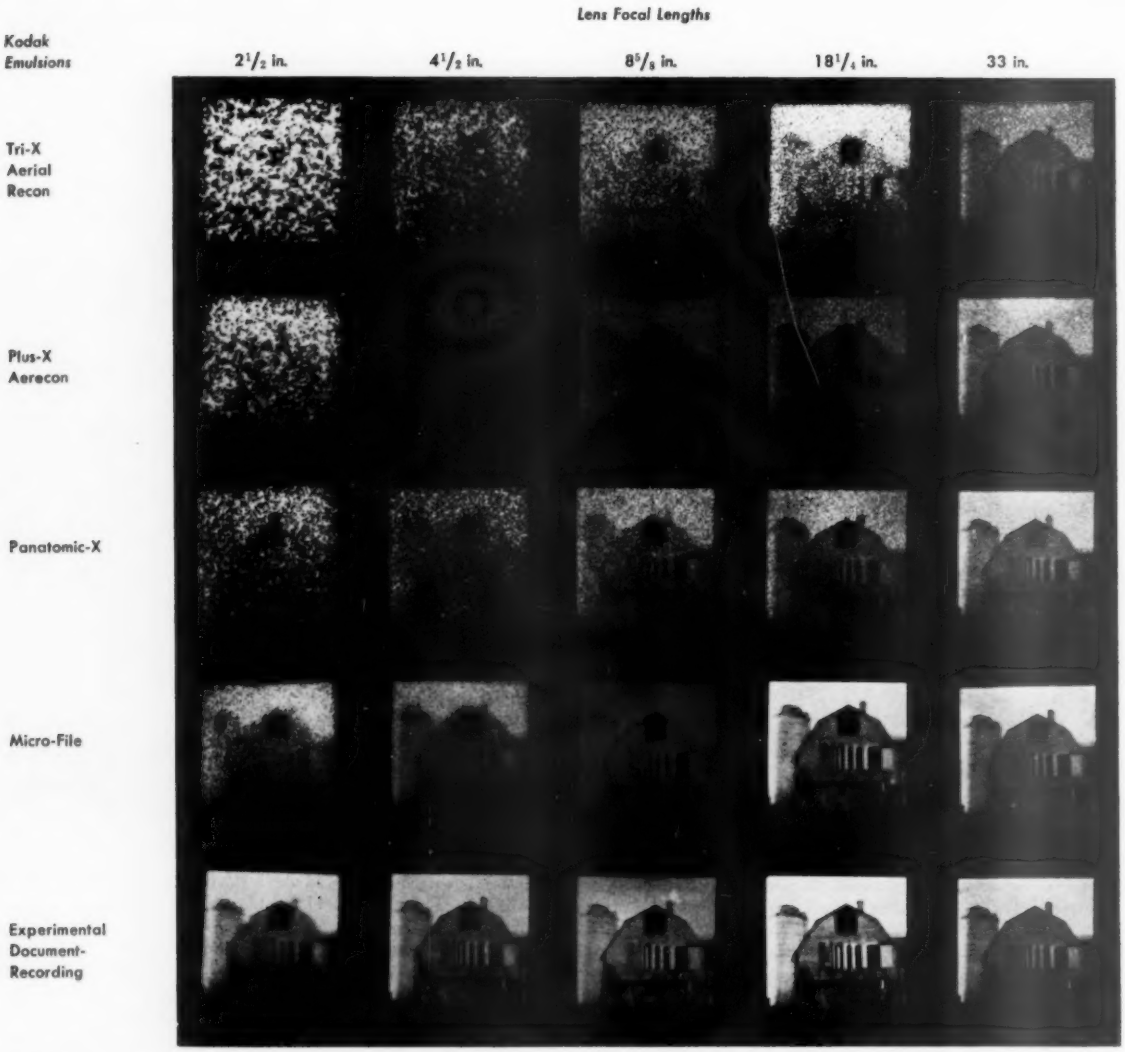

Fig. 10. Reproduction of transparencies used for judging the rendition of detail. The print scale P_E in every case was 372× but the camera scale varied as given in Table II. No motion.

finer-grained material designed to give the best possible reproduction of fine detail.*

In this experiment, all the emulsions were developed to a gamma of approximately 1.5. In general, the emulsions were developed in different developers and under different conditions than are normally recommended for them. This was necessary in order to keep the tone-reproduction characteristics constant so that valid subjective comparisons of the resulting pictures could be made. Consequently, the comparisons of the various photographic materials given in this paper do not represent exactly their relative behavior in practice.

All these films were used with each of the lenses listed in Table II. In this table, the lens apertures, $\sigma_{L'}$-values, camera scales, and enlarging magnifications are also shown. The longest focal length of any camera lens was 13 times that of the shortest, but the diameter of the entrance pupil A was $1^1/_4$ in. (32.1 mm) for every lens. The $2^1/_2$-in. and $4^1/_2$-in. lenses probably gave as good imagery as can be obtained with the required relative apertures. Their values of $\sigma_{L'}$ were measured with the sine-wave re-

* The data presented in this paper are representative of the emulsions manufactured at the time the experiments were made. However, it must be recognized that the characteristics of products of the same name may vary within manufacturing tolerances and may change significantly as improvements are effected.

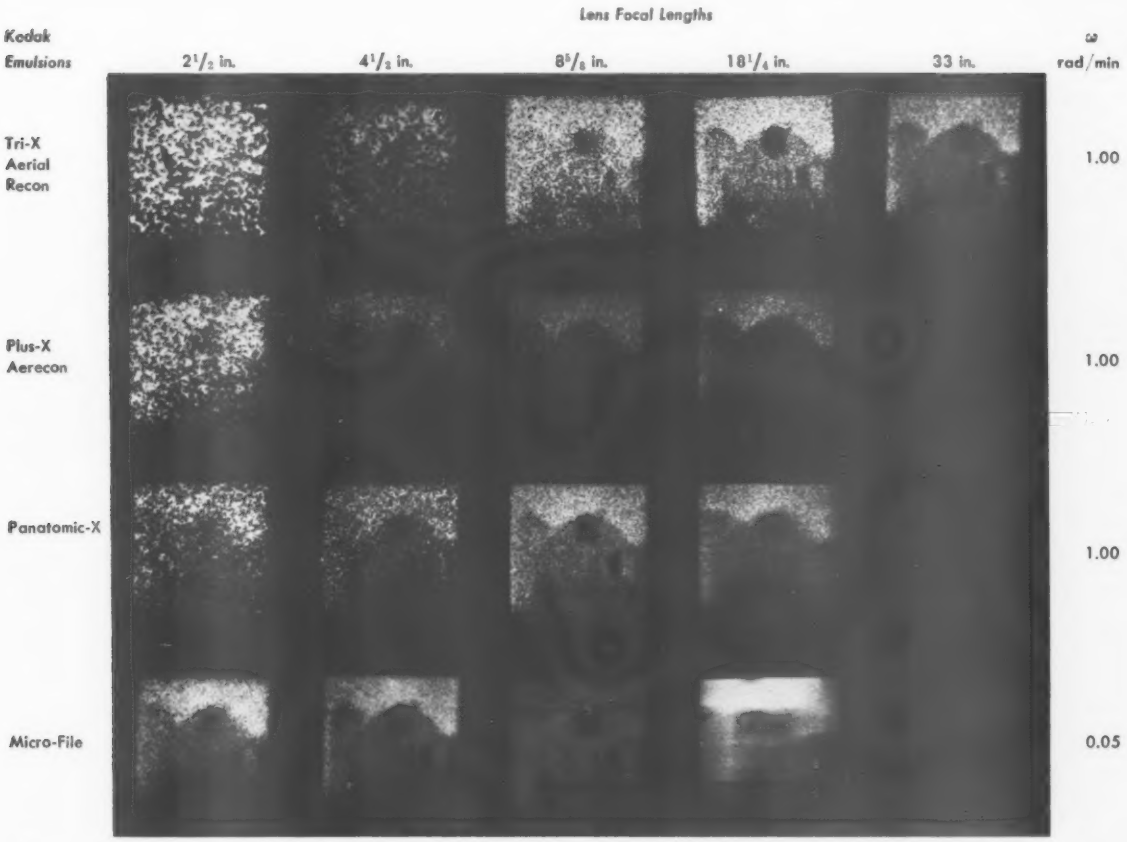

Fig. 11. Reproduction of transparencies used for judging the rendition of detail. The print scale in every case was 372× but the camera scale varied as given in Table II. The motion was at the speeds indicated.

sponse technique.[15] The 8⅝-in., 18¼-in., and 33-in. lenses were telescope lenses and were essentially diffraction-limited over the small field they were required to cover, which was approximately 7′ of arc. Their values of $\sigma_{L'}$ were measured by means of this same technique and were checked against diffraction theory. For the 33-in. lens, this 7′ covered 1.7 mm on the negative.

Enlargements in the form of positive transparencies were made from all the negatives onto Kodak Commercial Film with an excellent photomicrographic camera. The graininess of this film and the spread function of the photomicrographic camera are not significant under the viewing conditions used, and even if they were, they would be very small constant factors which should not affect the conclusions drawn from the experiment. The ratio of the size of an object to its size in the enlargement, P_E, was 372×. This value of P_E was obtained by using the magnification values M shown in Table II.

Image motion was introduced by moving the transparency laterally at a constant velocity throughout the duration of the exposures. Under the conditions of the experiment, this rate was 40 mm/min. With the test object at a distance of 84 ft from the camera lens, this corresponds to an angular velocity of 1.56×10^{-3} rad/min or 2.60×10^{-5} rad/sec. The exposure times used for the three camera negative materials were such that the amount of motion occurring during the exposure was the same as it would have been if the photograph had been ob-

TABLE II. Lens and Enlargement Data

Focal length, f		Aperture*	σ_L,† microns	Camera scale, H/f	Enlarging magnification, M
in.	mm				
2½	64.2	$f/2.0$	1.78	146,700	393
4½	114	$f/3.6$	1.75	82,600	221
8⅝	220	$f/6.9$	2.04	42,800	115
18¼	463	$f/14.5$	3.98	20,300	54
33	841	$f/26.3$	7.94	11,200	30

* Diameter of entrance pupil, A = 32.1 mm in all cases.
† λ = 0.58 μ.

15. R. L. Lamberts, *J. Opt. Soc. Amer.*, **48**: 490 (1958).

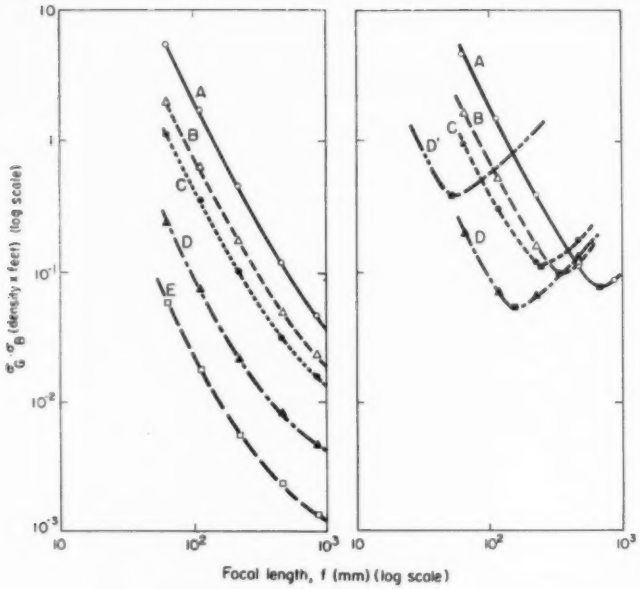

Fig. 12A (Left). Plot of $\sigma_G\sigma_B$ against focal length of camera lens for each film, for stationary camera. Each point represents a picture in Fig. 10.

Fig. 12B (Right). Plot of $\sigma_G\sigma_B$ against focal length of camera lens for each film and for ground speeds shown in the first column of Table III. Solid squares represent theoretical minima computed from Eq. (8); each of the other points represents a picture in Fig. 11.

Kodak films used were (A) Tri-X; (B) Plus-X; (C) Panatomic-X; (D) Micro-File; and (E) Experimental document-recording. D′ is the computed curve for Micro-File Film and a velocity of 1.0 rad/min.

tained from a camera at an altitude of 6 miles moving with a ground speed of 360 mph, as was mentioned earlier. This corresponds to an angular velocity of 1 rad/min. In the case of Micro-File Film, the effective velocity had to be reduced to 5% of this amount (corresponding to 0.05 rad/min). It was not possible to obtain photographs on the document-recording material with camera motion because of the limitations of the experimental equipment.

The photographs obtained with these various lens–film combinations are shown in Figs. 10 and 11. In Fig. 10 the camera was stationary. In Fig. 11 it was effectively moving with respect to the test object at the angular velocities indicated. In Fig. 10 it can be seen that the detail rendition increases continually towards the right as focal length increases and also downwards as the emulsion spread-function decreases in width, which is predicted from Eq. (7). Moreover, in accordance with this equation, the graininess decreases as the focal length increases. In Fig. 11 the improvement is not continual and the prediction from Eq. (8) that there is a focal length giving optimum detail rendition when there is uniform image motion is seen to be fulfilled.

TABLE III. Values of σ_G

Kodak film	Focal length of lens, in.				
	$2^1/_2$	$4^1/_2$	$8^5/_8$	$18^1/_4$	33
Tri-X Aerial Recon	1.559	0.877	0.456	0.216	0.119
Plus-X Aerecon	0.956	0.538	0.280	0.133	0.073
Panatomic-X	0.708	0.398	0.207	0.098	0.054
Micro-File	0.210	0.118	0.061	0.029	0.016
Experimental document-recording	0.066	0.037	0.019	0.009	0.005

We can now make some predictions that are more quantitative than these by calculating values of $\sigma_G\sigma_B$ for the pictures in the two figures. Here σ_G is the density variation corresponding to the enlargement M of the negative and σ_B is the σ-value in feet that the composite spread-function would have had if it had been projected on an object at a distance of 9.53 km (approximately 30,000 ft).

For each of the pictures, the values of σ_G, σ_B, and $\sigma_G\sigma_B$ are shown in Tables III, IV, and V, respectively. The quantity $\sigma_G\sigma_B$ should, of course, be inversely proportional to detail rendition. It is shown plotted against focal length in Fig. 12A for no image motion and Fig. 12B for image motion at the indicated velocities. In the latter figure, the values of f_0 as calculated from Eq. (8) and the corresponding values of $(\sigma_G\sigma_B)_0$ are also shown by the squares on the curves. They obviously fall very close to the minima.

It can be seen that the qualitative predictions made by viewing the pictures can now be made in a quantitative manner and the values of f_0 and $(\sigma_G\sigma_B)_0$ can be determined. These values, which are listed in Table VI, can be seen to be consistent with the photographs in Fig. 11. In this table, values of $(\sigma_G)_0$ and $(\sigma_B)_0$ are also shown.

Curve D′ in Fig. 12B is for Micro-File Film when used in a camera moving at the same velocity as that used for the other materials (1.0 rad/min). The corresponding values of f_0, $(\sigma_G)_0$, $(\sigma_B)_0$, and $(\sigma_G\sigma_B)_0$ are listed in Table VI. In order to obtain an optimum picture with Micro-File Film for a given lens aperture and ground speed, one needs to use a lens of much shorter focal length (i.e., a smaller *f*-

TABLE IV. Values of σ_B in Feet in Original Scene

Kodak film	ω, rad/min	Focal length of lens, in.				
		2 1/2	4 1/2	8 5/8	18 1/4	33
Tri-X Aerial Recon	0	3.615	2.031	1.117	0.554	0.396
Plus-X Aerecon	0	2.111	1.184	0.633	0.377	0.326
Panatomic-X	0	1.621	0.907	0.494	0.326	0.309
Micro-File	0	1.160	0.646	0.367	0.286	0.297
Experimental document-recording	0	0.905	0.501	0.299	0.268	0.282
Tri-X Aerial Recon	1	3.615	2.031	1.297	0.602	0.859
Plus-X Aerecon	1	2.113	1.186	0.678	1.121	
Panatomic-X	1	1.622	0.917	0.691	2.137	
Micro-File	0.05	1.165	0.726	1.283	5.387	

TABLE V. Values of $\sigma_G\sigma_B$

Unit is feet in original scene × density. All values of $\sigma_G\sigma_B$ are to be divided by 100.

Kodak film	ω, rad/min	Focal length of lens, in.				
		2 1/2	4 1/2	8 5/8	18 1/4	33
Tri-X Aerial Recon	0	563	178	50.9	12.0	4.71
Plus-X Aerecon	0	202	63.7	17.7	5.01	2.38
Panatomic-X	0	115	36.1	10.2	3.20	1.67
Micro-File	0	24.4	7.62	2.24	0.829	0.475
Experimental document-recording	0	5.97	1.85	0.567	0.241	0.141
Tri-X Aerial Recon	1	563	178	59.1	13.0	10.2
Plus-X Aerecon	1	202	63.8	19.0	14.9	
Panatomic-X	1	115	36.5	14.3	20.9	
Micro-File	0.05	24.5	8.56	7.82	15.6	

number) in the camera than is needed for the negative materials so that the exposure time may be kept sufficiently short to reduce significantly the effect of image motion. Even though the Micro-File Film has a smaller spread function than the negative materials, it is not small enough to make up for the shorter focal length of the lens that must be used to obtain the necessary relative aperture. Consequently, the value of $(\sigma_G\sigma_B)_0$ is definitely higher than the optimum values for the negative materials.

Values of ρ, the relative detail rendition, were determined for each of the pictures in Figs. 10 and 11. Since relative detail rendition is a subjective quantity, the only way in which such values can be assigned to the various pictures is by a psychometric technique. The pictures differ widely in their relative detail rendition, and therefore the more precise techniques of obtaining psychometric quantities cannot be used. We were thus forced to use a ranking system, in which we simply asked twenty observers to line up the pictures in the order of the detail which they could see in the barn. This procedure gives, directly, a rank order to the pictures for each observer.[16] Then these rank orders were averaged.

TABLE VI. Optimum Values (Calculated)

Kodak film	ω, rad/min	f_0, in.	$(\sigma_G)_0$, density	$(\sigma_B)_0$, ft	$(\sigma_G\sigma_B)_0$, density × ft
Tri-X Aerial Recon	1.0	26.1	0.151	0.599	0.090
Plus-X Aerecon	1.0	13.0	0.186	0.665	0.124
Panatomic-X	1.0	9.2	0.195	0.666	0.130
Micro-File	0.05	5.9	0.092	0.711	0.065
Micro-File	1.0	2.1	0.262	1.718	0.450

The intervals between the average values of rank order thus obtained, which will be called ρ' since they are not the final values to be used, tend to be compressed at the high and the low ends of the scale. In consequence of the fact that there are a total of 42 pictures in the series that were ranked, the maximum possible value for ρ' is 42 and not infinity, and the minimum possible value is unity and not zero.

It was suggested by Hans Zweig, of these Laboratories, that this scale could be made more uniform by applying the conversion

$$\rho = (\rho' - 1)/(42 - \rho') \qquad (12)$$

16. J. P. Guilford, *Psychometric Methods*, 2nd ed., McGraw-Hill Book Co., New York, 1954. p. 178.

TABLE VII. Values of Detail Rendition in Terms of Subjective Rank ρ

Kodak film	ω rad/min	Focal length of lens, in. $2^1/_2$	$4^1/_2$	$8^5/_8$	$18^1/_4$	33
Tri-X Aerial Recon	0	0.017	0.125	0.289	1.27	2.69
Plus-X Aerecon	0	0.062	0.376	0.847	2.52	4.82
Panatomic-X	0	0.200	0.429	1.52	3.33	5.72
Micro-File	0	0.670	2.14	4.22	7.28	12.2
Experimental document-recording	0	3.14	9.38	21.2	53.7	102
Tri-X Aerial Recon	1	0.012	0.137	0.298	1.17	1.34
Plus-X Aerecon	1	0.072	0.378	0.851	1.05	
Panatomic-X	1	0.148	0.385	0.990	0.54	
Micro-File	0.05	0.716	1.84	1.69	0.46	

to the average values of rank order. In this way, ρ can vary from zero to infinity.

Values of ρ are listed in Table VII. These values are plotted as ordinates and the corresponding values of $\sigma_G\sigma_B$ are plotted as abscissas on logarithmic scales in Fig. 13. All the points fall on a straight line within the limits of experimental error, *thus demonstrating that detail rendition is inversely proportional to $\sigma_G\sigma_B$ not only when σ_B is convoluted with the lens and film spread-function, but also when the effects of image motion due to a uniform translational velocity of the camera are convoluted with these factors.*

Conclusions

It is shown that, in the case of aerial photography, parameters relating to the emulsion spread-function, which include the emulsion granularity, the lens spread-function, and a spread function related to the image motion introduced into the photographic system by the uniform velocity of the camera, can be combined so as to give a value which correlates with the subjectively determined amount of detail that can be seen in the final pictures produced by the photographic system. Combinations giving the maximum amount of detail can be calculated. The effects of lens aberrations, atmospheric turbulence, and vibration have not been included in this theory, but they are under study.

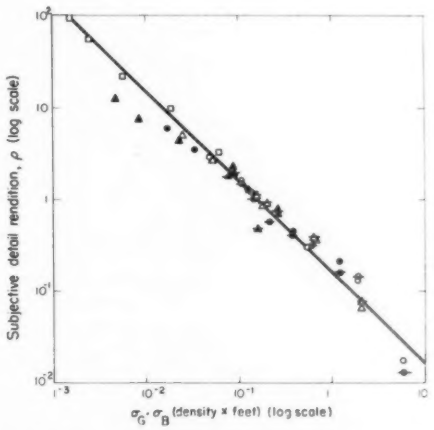

Fig. 13. Subjective detail rendition ρ from Eq. (12) plotted against $\sigma_G\sigma_B$ for all the pictures studied. The same symbols are used as in Fig. 12 except that dashes indicate pictures made during motion (Fig. 12, right). The straight line has a slope of practically -1.

PHOTOGRAPHIC SCIENCE AND ENGINEERING
Volume 4, Number 6, November–December 1960

Theoretical Considerations Concerning the Relationship between Characteristic Curves of Elementary and Thick Layers

E. KLEIN, *Scientific Photographic Laboratory, Agfa AG, Leverkusen, West Germany*

An integral equation is given which relates the elementary density curve to the density curve of a thick coating. A graphical method is used to obtain from this equation the elementary layer curve, starting with the given curve of a thick coating. The gradient of the elementary density curve has several maxima. Correspondingly, the grain-size distribution derived from the elementary density curve has several maxima. It is shown how the mean spread of the individual grain-size distribution affects the shape of the density curve of the thick coating and how it is related to the toe of the density curve.

Assuming[1] that light intensity within a photographic emulsion layer decreases exponentially, the following relation can be shown to exist between the characteristic curve of the elementary layer $s(\log E)$ and that of the thick layer $S(\log E)$, where E = exposure:

$$S(\log E) = \frac{1}{D}\int_{\log E-D}^{\log E} s(\log E)\,\partial \log E \qquad (1)$$

D is the optical density of the light scattering layer and:

$$D = \log(1+\rho)/\tau \qquad (2)$$

where ρ and τ are the reflection and transmission coefficients, respectively.[2] The characteristic curve of a thick layer is easily derived from the elementary layer by a graphic method using Eq. (1), but it is not easy to integrate Eq. (1) to obtain the elementary layer curve from a given curve of a thick layer. The following graphical method is based on the theoretical considerations of Zeitler.[3]

The measured function $S(\log E)$ is differentiated and we set:

$$D\cdot\frac{dS(\log E)}{d\log E} = Z(\log E) \qquad (3)$$

Next, a starting value, $\log E_0$, is located on the Z-curve so that: $Z(\log E) = 0$ in the range $\log E \leqq \log E_0 - D$ and $Z(\log E) \neq 0$ in the range $\log E > \log E_0$. $Z(\log E)$ is set equal to $S(\log E)$ for the range of $\log E \leqq \log E_0$. We then proceed in small increments beyond $\log E_0$ and set

$$s(\log E - D) + Z(\log E) = s(\log E) \qquad (4)$$

An accurate mathematical analysis of the integral Eq. (1) yields the following results:

1. For every function $s(\log E)$ which increases continuously from 0 to 1 within an exposure range $\log E_0$ to $\log E_{max}$ (with $s(\log E) \equiv 0$ for $\log E \leqq \log E_0$, and $s(\log E) \equiv 1$ for $\log E \geqq \log E_{max}$) there exists, according to Eq. (1), for every value of D a function, $S(\log E)$, which has an exposure range $\log E_0$ to $(\log E_{max} + D)$.

   This function, $S(\log E)$, again increases uniformly within the new exposure range and the following conditions apply: $S(\log E) \equiv 0$ for $\log E \leqq \log E_0$, and $S(\log E) \equiv 1$ for $\log E \geqq (\log E_{max} + D)$.

2. Conversely, a solution of the integral Eq. (1), $s(\log E)$, which satisfies the limiting conditions $S(\log E) \equiv 0$ for $\log E \leqq \log E_0$, and $s(\log E) \equiv 1$ for $\log E \geqq \log E_{max}$ does not exist for every function $S(\log E)$ which has the properties specified above. However, for physical reasons, there exists an elementary characteristic curve $s(\log E)$ for every characteristic curve of an actual thick layer $S(\log E)$. It makes sense, therefore, to strive for such functions of $S(\log E)$ even in theoretical investigations which yield a solution of the integral Eq. (1) and which fulfill the specified limiting conditions.

Other work[4] has already shown that the shape of the elementary characteristic curve is governed essentially by grain-size distribution. Factors that are neglected in this general case must be examined in specific instances, but their exclusion makes it possible to derive certain basic relations.

For example, for a given grain-size distribution, $\partial H/\partial d$ (H = frequency, d = diameter), a relative elementary density:

$$s_i = \frac{\int_{d_i}^{+\infty} d^2\partial H}{\int_0^{\infty} d^2\partial H} \qquad (5)$$

is obtained; furthermore, a certain exposure value,

Presented at the Annual Conference, Santa Monica, California, 13 May 1960. Received 9 May 1960.

1. C. E. K. Mees, *The Theory of the Photographic Process*, rev. ed., Macmillan, New York, 1954.
2. H. Frieser and E. Klein, *Z. Elektrochem.*, **62**: 874 (1958).
3. E. Zeitler, *Phot. Korr.*, **95**: 99 (1959).
4. H. Frieser and E. Klein, *Phot. Sci. & Eng.*, **4**: 264 (1960).

E_i, can be related to each diameter, d_i, the general condition being:

$$3 \log d_i = \log E_i \tag{6}$$

(expansion of the log d axis by a factor of 3).

Thus once the elementary characteristic curve is known, it is possible to compute the grain distribution $\partial H/\partial d$ for the accepted conditions by using Eq. (5). Moreover, with Eq. (1) and (5), we have the means for computing the grain distribution which corresponds to any arbitrarily selected characteristic curve of a thick layer.

The ideal goal for which we strive will be a characteristic curve that rises linearly within the range log E_0 to (log $E_{max} + D$). This curve will break at the abscissa values of log E_0 and of log $E_{max} + D$. Shown in Fig. 1 is a linear characteristic curve and its corresponding elementary characteristic curve, which was computed by means of Eq. (4), which is a solution of Eq. (1). In this example, [(log $E_{max} + D$) − log E_0], the exposure range, is an integer multiple of the optical density D.

This yields a stepped function with step width D. An elementary curve of the type given by Eq. (1) that satisfies the necessary limiting conditions cannot exist in the mathematical sense when the exposure range is not an integer multiple of D.

If we wanted to compute the grain-size distribution from the stepped type of the elementary characteristic curve by Eq. (5), we would obtain discrete values of grain size, and, in the case of Fig. 1, three discrete sizes. In other words, we would have to mix in proper proportion emulsions whose grains are without any size distribution. The logarithmic values of the grain diameters of these emulsions differ by additive values which are multiples of $D/3$. This means that perfectly linear characteristic curves can be obtained only through mixing of emulsions which do not have any grain-size distribution.

Of course, in practice it is not possible to make such emulsions and for this reason we want to examine what departures from linearity occur when separate emulsions are mixed that have grain-size distributions of selected dispersion. Our basic approach in this instance is that of substituting grain-size distributions for discrete values of grain size. The resultant characteristic curves of a thick layer can then be computed.

In general, we can define the grain-size distribution by means of a Gaussian function related to the logarithm of the grain diameter:

$$\frac{\partial H}{\partial \log d} = \frac{1}{\sigma\sqrt{2\pi}} e^{-\left(\log \frac{d}{d_0}\right)^2/2\sigma^2} \tag{7}$$

but it can be shown that the term $d^2\partial H$ which appears in Eq. (5) is itself a Gaussian function with the same standard deviation σ, although with a displaced mean value d'_0. Thus:

$$d^2 \frac{\partial H}{\partial d} = \frac{1}{\sigma\sqrt{2\pi}} d_0^2 \, e^{2(2.3)^2\sigma^2} e^{-\left(\log \frac{d}{d'_0}\right)^2/2\sigma^2} \tag{8}$$

where

$$d'_0 = d_0 \cdot 10^{2(2.3)\sigma^2} \tag{9}$$

Hence, we can easily determine the elementary characteristic curve once we know the grain-size distribution (see below).

The introduction of distributions in place of discrete values will be explained with the example given in Fig. 1; to this end, we have plotted in Fig. 2 the linear characteristic curve for values of log d (d increases to the left and the three logarithmic values of exposure correspond to appropriate log values of diameter). The stepped elementary characteristic curve is also shown (optical density = $\frac{1}{3}$ of the logarithmic unit).

Three values of d_0 (see Eq. (9)) can be determined immediately from the curves of Fig. 2:

$$d'_{01} = 10^{-4} \text{ cm} \qquad d'_{02} = 10^{-4.33} \text{ cm} \qquad d'_{03} = 10^{-4.67} \text{ cm}$$

We now introduce in place of these discrete values distributions of the form $d^2(\partial H/\partial \log d)$, in which the d'_0-values are the means and the σ values are 0.015, 0.05, 0.1, 0.2, and 0.3. These distributions are plotted in Fig. 3 on sum-frequency graph paper.

The new elementary characteristic curves can be determined directly from these graphs. For example, the density value of the elementary characteristic curve at log $d = -4.1$ is the sum of the individual densities which are contributed by the individual distributions, thus:

$$s = (s_1 + s_2 + s_3)/3 \tag{10}$$

Hence when $\sigma = 0.2$, we get (see Fig. 4):

$$\frac{s_1}{3} = \frac{1 - 0.31}{3}; \quad \frac{s_2}{3} = \frac{1 - 0.875}{3}; \quad \frac{s_3}{3} = \frac{1 - 0.9975}{3}$$

Thus we obtain a density $s = 0.272$ at the point log $d = -4.1$. The elementary characteristic curves of Fig. 2 were derived in this fashion. The results of the integration of the elementary curves according to Eq. (1) are presented in Fig. 4.

It is evident from Fig. 4 that increased spreading in the grain distribution of the individual emulsions leads to an extended toe at low densities and corresponding shouldering at high densities (departures from linearity). If the density at the inertia point S_{J_n} is taken as a measure of toe formation, an almost linear dependence of S_{J_n} on the σ value of the grain distribution is found to exist (see Fig. 5).

We compute next the grain distributions from the individual functions $d_1^2(\partial H/\partial \log d_1)$, $d_2^2(\partial H/\partial \log d_2)$, etc., which represent Gaussian functions about the mean values d_{01}, d_{02}, etc. The approximations that are used in this computation, as outlined before, yield distributions d_i^2 $(\partial H/\partial \log d_i)$ that are equal except for their mean values; this is evident in Fig. 6.

The grain-size distributions of the individual emulsions, shown in Fig. 7, have equal spreads about their means. Under these conditions, the frequencies must be inversely proportional to the squares of the mean values, in keeping with the relation given in Eq. (8), or:

$$\frac{\partial H_1}{\partial \log d_1} : \frac{\partial H_2}{\partial \log d_2} : \frac{\partial H_3}{\partial \log d_3} = \frac{1}{d_{01}^2} : \frac{1}{d_{02}^2} : \frac{1}{d_{03}^2} \tag{11}$$

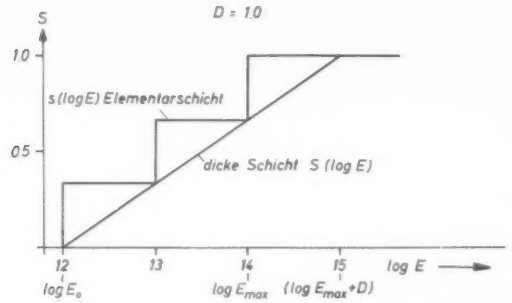

Fig. 1. A linear characteristic curve S(log E) and its corresponding elementary curve s(log E).

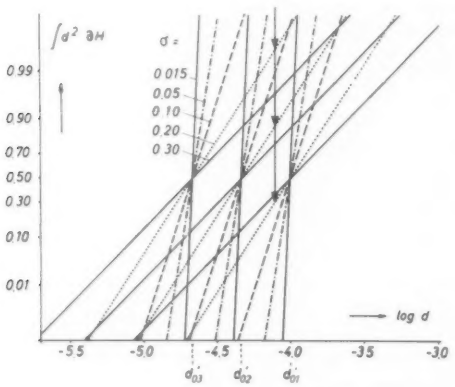

Fig. 3. Sum-frequency distributions of the individual emulsions.

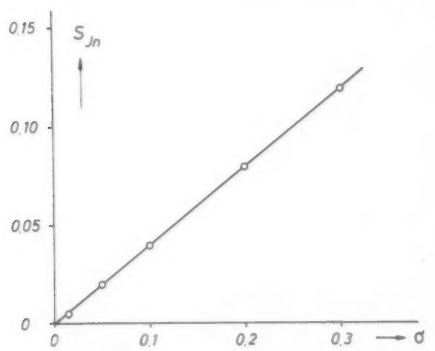

Fig. 5. Density at the inertia point as a function of the dispersion of grain-size distribution.

The mixture ratio of the individual emulsions is obtained from the volume distributions (see Fig. 8).

The integrals of this function $\int_{-\infty}^{+\infty} d^3 \partial H$ must be related to each other like the mean values of the grain distributions; hence, the relative amount contributed by each emulsion is defined by:

$$\int_{-\infty}^{+\infty} d_1^3 \partial H_1 : \int_{-\infty}^{+\infty} d_2^3 \partial H_2 : \int_{-\infty}^{+\infty} d_3^3 \partial H_3 = d_{01} : d_{02} : d_{03} = 1 : 10^{-D/3} : 10^{-2D/3} \quad (12)$$

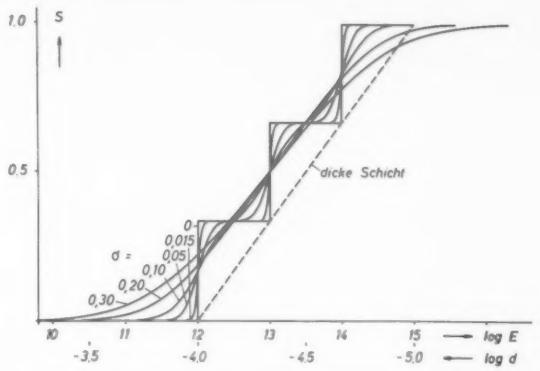

Fig. 2. Selected characteristic curve of a thick layer, and the elementary curves that are obtained for different dispersion of grain diameters of the individual emulsions.

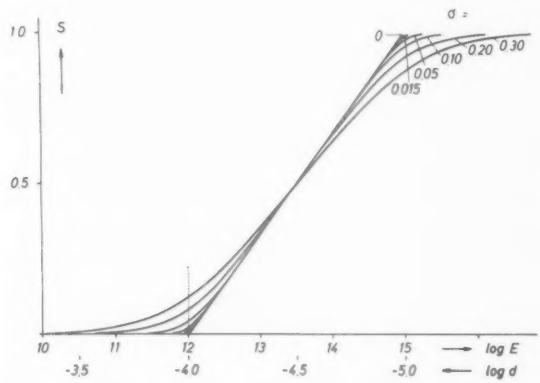

Fig. 4. Characteristic curves of a thick layer, obtained for different spreads in grain-size distribution of the individual emulsion.

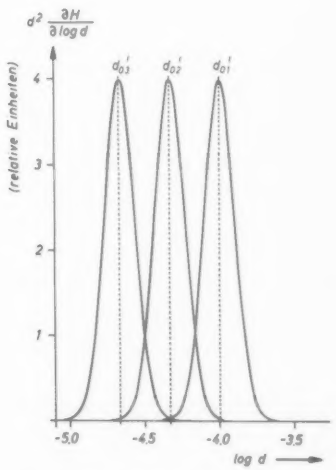

Fig. 6. Function $d^3(\partial H/\partial \log d)$ of three individual emulsions.

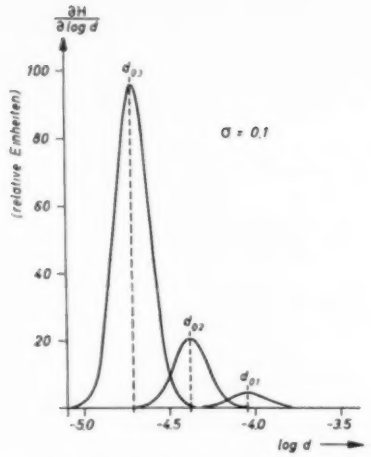

Fig. 7. Grain-size distribution of the individual emulsions.

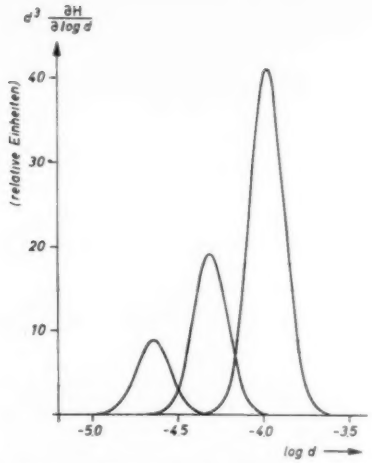

Fig. 8. Volume distributions of the individual emulsions.

Summary

This investigation deals with the problem of computing those conditions which promote essentially linear characteristic curves of a photographic layer. The well-known relationship between the characteristic curve of a thick layer and the elementary characteristic curve is utilized but is expanded to include the additional influence of the grain-size distribution curve. Other parameters that affect the characteristic curve, such as random quanta effects and sensitivity distribution, are purposely neglected since such omission permits a simpler means of gaining a few basic insights. Therefore, exact results are obtained only when random quanta effects and sensitivity distribution are of no consequence, but this is seldom true with regard to sensitivity distribution.[4]

Characteristic curves that are very nearly linear are best obtained by a build-up of elementary characteristic curves that are derived from the exposure $\partial\, s(\log E)/\partial \log E$ at periodic intervals within the exposure range.

If we start with just one emulsion having *one* grain-size distribution, a single elementary characteristic curve is obtained whose derivation can be represented as a Gaussian function with respect to $\log E_0$. The dispersion of these Gaussian functions is governed solely by the dispersion of the distribution function for grain diameter, when random quanta effects and sensitivity distribution are neglected. It seems appropriate, therefore, to approximate the above-mentioned periodic function that is used for deriving the elementary characteristic curve by a series of Gaussian functions that have equidistant mean values (distance between mean values = $1/n$ optical density D). This means that the number of necessary Gaussian distributions equals the quotient n of the exposure range and the optical density.

The theoretical requirement for a strictly linear characteristic curve of a thick layer can be fulfilled only by mixing emulsions that have no grain-size distribution at all. This requirement can only be approximated in practice by mixing in proper ratio emulsions with the narrowest grain distribution possible (in actual practice about 3 to 4 emulsions). Thus, the narrower the grain distribution, the better the linearity of the characteristic curve. It is observed in this connection that the toe of the characteristic curve increases with a widening in grain distribution.

The weight ratios of the necessary individual emulsions can be derived from the grain-size distribution values.

Nearly linear characteristic curves of any desired exposure latitude can be obtained, therefore, provided only that in actual practice very narrow grain distributions with predetermined mean grain diameters can be obtained.

However, a further deviation from the ideal, linear characteristic curve will occur whenever the dispersion of the sensitivity distribution is not negligible with respect to the dispersion of the grain-size distribution. In such instances, the individual distributions that make up the elementary characteristic curve have a total standard deviation σ which is computed from $\sigma = \sqrt{\sigma_\eta^2 + \sigma_\beta^2}$, where σ_η is the standard deviation of the grain distribution, and σ_β is the standard deviation of the sensitivity distribution (see Refs. 1 and 4).

It should be mentioned that the problem considered here is amenable to rigorous mathematical treatment; this will be undertaken in a future contribution.

My thanks are due Hans-Joerg Metz for his great assistance in this investigation.

PHOTOGRAPHIC SCIENCE AND ENGINEERING
Volume 4, Number 6, November–December 1960

A Photographic Process Using Persistent Internal Polarization in Phosphors

H. P. KALLMANN, JOSEPH RENNERT, AND M. SIDRAN,* *Department of Physics, New York University, New York, N.Y.*

The persistent internal polarization effect in a zinc cadmium sulfide phosphor was used to depict radiation in the visible and infrared to 2.5 μ. The image exposure was made either during the application of the polarizing voltage (polarizing method), or after the application of the voltage (depolarizing method). These methods yielded negative and positive copies, respectively. The latent image consisted of a polarization charge pattern corresponding to the object to be depicted. Alternately, a latent image of free charges could be formed on metallic dot electrodes sprayed on the surface of the layer. The latent images may be stored for an extended period before developing. Low-supply voltages are required in comparison with those used in electrophotography. The images were developed using dyed charged resin particles applied to the surface to form a permanent print. They could also be converted into transient pictures on a cathode-ray screen. The polarization was measured as a function of incident radiation intensity in order to determine the sensitometry for different spectral bands. The process is useful for line, halftone, and continuous-tone reproductions.

The possibility of using persistent internal polarization (p.i.p.) in phosphors for photography has been suggested by earlier work.[1] The present study was conducted to define conditions for which polarization densities in different area elements of a thin zinc cadmium sulfide phosphor layer would correspond to the energy distribution of an imaging beam and form a latent image.

It was found that either a negative or a positive latent polarization image could be produced by an appropriate choice of procedure. Two methods were developed for making such latent p.i.p. images visible. In the first method, dyed charged resin particles are applied to the phosphor plate, as in electrophotographic processes. A print is produced which can be permanently fixed by fusing the dyed resin to the surface. V. M. Fridkin[2] has used a similar method to produce photocopies on single crystals of anthracene and sulfur, as well as polycrystalline sulfur layers.

The second method permits a visible image to form on a cathode-ray screen when the phosphor plate bearing the latent p.i.p. image is mechanically traversed by a measuring probe or scanned by a moving light beam. In this way, the bound charges in each area element of the plate are freed for measurement and display.

Received 18 July 1960. The work described in this paper was performed at New York University Physics Dept., Washington Sq., New York 3, N.Y., under Contract 8-8546-704, National Carbon Company, December 1955–June 1957.

* Miss Sidran's present address is Research Department, Grumman Aircraft Engineering Corp., Bethpage, L.I., N. Y.

1. H. Kallmann and B. Rosenberg, *Phys. Rev.*, **97**, 1596 (1955). Patents applied for.
2. V. M. Fridkin, *Kristallografiya* (Translations), Vol. 2, Issue 1, 130–33 (1957).

The facsimile photoreproductions described here were made with radiation in the visible and near ultraviolet. It is known from other investigations that the action spectrum of p.i.p. extends from gamma rays to the infrared. P.i.p. photography using near and middle infrared radiation is described in a separate paper.[3]

Production and Development of the Latent P.I.P. Image

The persistent internal polarization effect is produced by placing a photoconductive layer between two electrodes, at least one of which is transparent, and applying a d-c field across the layer during or after light exposure. Electrons raised to the conduction band by the absorption of photons drift toward the positive electrode. Many are trapped in metastable energy levels at a distance from the atoms of their origin. Thus the layer becomes electrically polarized by the separation of trapped charges within the body of the phosphor.

Polarization can even be produced by an electric field applied a considerable period after light excitation. This is called dark polarization. The dark polarization can be reduced to a negligible value by de-exciting the phosphor with heat or infrared light before the polarizing field is applied.

If a polarized phosphor is stored in the dark, the charge separation decays very slowly; the half life of polarization is of the order of several thousand

3. H. Kallmann, J. Rennert, and M. Sidran, "Infrared Photography Using Persistent Internal Polarization in Phosphor Plates," to be published.

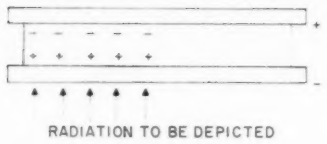

Fig. 1. Schematic diagram showing polarizing method. Plate is exposed to depicting radiation. An electric field is applied across the layer during or after light exposure. When light source and field are removed, the separated charges in the exposed areas remain trapped, thus forming a latent p.i.p. image.

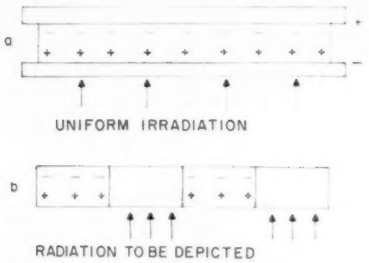

Fig. 2. Schematic diagrams showing depolarizing method. (a) Plate uniformly polarized. (b) Polarized plate exposed to the radiation to be depicted. This discharges the polarization in the exposed areas to form a latent p.i.p. image.

minutes. Irradiation of the polarized layer reduces the internal charge separation, according to the incident radiant energy.

Since light exposure can be used either to produce polarization, or to destroy it, two methods of forming a latent p.i.p. image are available. One gives a negative and the other a positive image. In the first, the polarizing method, the image-forming exposure is made on an unexcited phosphor plate either before or during the application of an electric field across the layer. This results in a latent p.i.p. image in which the polarization density in each area element corresponds to the incident radiant energy it has received (Fig. 1).

In the depolarizing method, the plate is first sensitized by polarizing it uniformly using light and a concomitant electric field. It is then exposed to the radiation to be depicted, and the polarization is annihilated according to the energy distribution in the incident radiation. Thus a latent p.i.p. image is formed (Fig. 2) which is the reverse of the preceding one. Areas of highest illumination are left depolarized.

The latent images prepared by both of these methods may be stored in the dark for a long time before they are developed. The dark storage life exceeds that of latent images prepared by other photocopying methods.

To transform the latent p.i.p. image into a permanent visible record, one electrode is removed, and a dyed coal-tar resin which acquires a static charge by the triboelectric effect is sprinkled on the surface of the phosphor bearing the latent image. The resin adheres to the polarized areas to form a print (Figs. 3 and 4).

Preparation of Phosphor Plates

Commercial zinc cadmium sulfide phosphors with average particle diameters of about 10 μ were deposited on electrically conductive glass plates by sedimentation from solutions of cellulose nitrate in amyl acetate. The supernatent liquid was withdrawn, and the remaining solvent driven off by heating. Layers of uniform thickness with an area density of about 25 mg/sq cm were prepared.

Most of these plates were made with K powder[4] (43.7% ZnS, 56.3% CdS, 0.01% Cu, 0.0025% Au, 0.003% Ag, 0.015% Pb, 0.0005% Ni). This phosphor was chosen because of its strong persistent internal polarization effect under visible light. Some prints were also made on commercial ZnO coated paper using p.i.p. photography. Many other phosphors were found to exhibit strong p.i.p. effects.[5] These could also be used in this application.

4. H. Kallmann and G. M. Spruch, *Phys. Rev.*, **103**, 94 (1956).
5. Report 6, Vol. I, June 1957, Air Force Contract No. AF 18-(600)-1004.

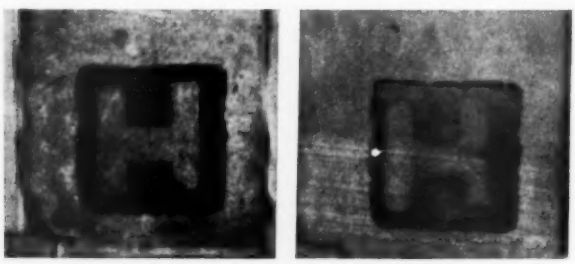

Fig. 3. Negative resin prints produced by the polarizing method. *Left:* Plate exposed to depicting radiation of 1.1×10^5 ergs/sq cm while 300 v were applied across the layer for 2 min. Resin development produced negative print. *Right:* Plate exposed to depicting radiation of 1.1×10^6 ergs/sq cm. After 15-hr dark storage, 450 v were applied across it for 5 min. Resin development produced negative print.

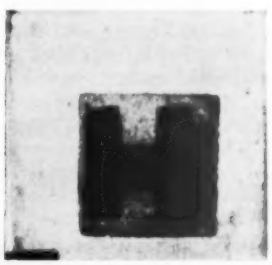

Fig. 4. Positive resin print produced by the depolarizing method. Plate uniformly polarized (4.4×10^5 ergs/sq cm, and 300 v for 2 min). Image exposure was made using 1.1×10^4 ergs/sq cm. Resin development produced positive print.

Experimental Techniques in the Production of Resin Prints on "Normal" Phosphor Plates

During the process of forming the latent image, the phosphor plate was housed in a light-protected chamber equipped with a shutter. The humidity inside the chamber was controlled by means of dessicants. This was necessary because the particular binder used was not impervious to moisture. The chamber was provided with a removable aluminum foil electrode to be placed in intimate contact with the rear face of the phosphor layer during polarization. Photographic exposures were made by projecting the image of an opaque letter "H" on a transparent backing onto the phosphor layer through the conductive glass electrode. A 50-w tungsten lamp was used as light source, with a lamp-to-phosphor-plate distance of about 8 in. Exposure times varied from seconds to minutes (see captions to figures).

After a latent p.i.p image had been produced by either the polarizing or depolarizing method (Figs. 1 and 2), the plate was removed from the dry chamber and resin P 648 (General Photo Products Co.) was sprinkled on the surface. The plate was then agitated and inverted to shake off excess resin. The resin, bearing a positive charge, adhered only to negatively charged areas. Finally the plate was heated to fuse the resin to the surface. Reproductions of resin images prepared in this manner are shown in Figs. 3 and 4; the maximum density of adhering resin produces a deep black image.

In preparing prints by the polarizing method, there should not be any background of adhering resin in unexposed areas, since these are unpolarized. However, the plates used in this work did not have very smooth surfaces so that some resin did adhere to unpolarized areas, including those not even covered by the square polarizing electrode (Fig. 3). Since the background is the same in all unexposed areas whether or not they were subjected to the electric field, it is clear that this is due to the rough surface, and not to dark polarization. This could be avoided by better techniques of plate preparation.

In the depolarizing method, some background of adhering resin may be expected in the exposed areas due to incomplete discharge of polarization (Fig. 4).

In both methods, during the image exposure, some light is scattered into the supposedly unexposed areas after internal reflections in the transparent electrode. This tends to create background effects which impair the contrast. At low exposures, these effects are negligible. At high exposures, they set an upper limit on the values of exposure time useful for photography. The effects can be minimized by using very thin transparent electrodes.

The polarizing and depolarizing methods are the basic methods of p.i.p. photography. It is sometimes advantageous to modify these methods. Several modifications will be discussed below.

Production of Latent Images Using Phosphor Plates with Conductive Dots on the Surface

It was found that removal of the external electrode affected the distribution of polarization in the plate to some extent. To avoid this effect, one face of the phosphor layer was provided with an array of small conductive dots of 0.05 cm diameter. This was done by spraying the plate with silver electroding paint through a perforated shield. These dots formed permanent electrodes in intimate contact with the surface and separated from each other. The dots did not interfere with exposure of the layer to light, since exposures were made through the transparent electrode to which the layer was permanently fixed. An external electrode placed on the dots could be removed without affecting any polarization in the layer.

The dots also provided a convenient method of measuring the distribution of polarization and displaying it on an oscilloscope screen as described below. In addition, they offered several advantages in making pictures by the resin technique using the polarizing and depolarizing methods. These are discussed later.

In p.i.p. photography using either bare phosphor layers or plates with dots on the surface, a latent polarization image is formed in the body of the phosphor. When dotted plates are used, a latent free charge image can also be formed on the dots. Thus the latter case involves the formation of two types of latent image, of which only the latent free charge image on the dots is utilized when resin is applied.

The sequence of operations used in the polarizing and depolarizing methods (Figs. 1 and 2) must be varied somewhat when plates with dots are used. The polarizing method for plates with dots is illustrated schematically in Fig. 5. The image exposure is made before or during the application of the

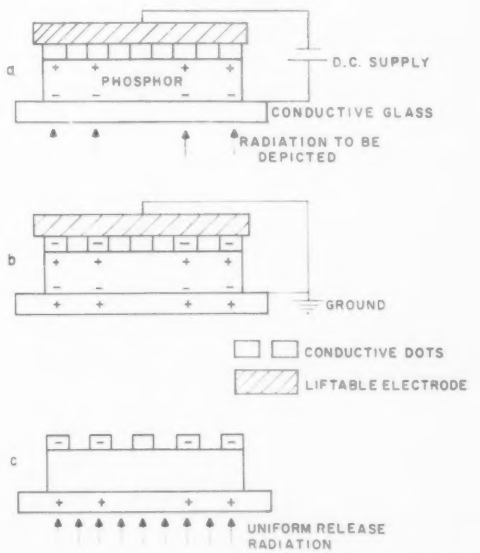

Fig. 5. Schematic diagram showing the polarizing method using plates with conductive dots. (a) Unexcited phosphor is exposed to depicting radiation, either before or during application of polarizing voltage. A latent p.i.p. image is formed in the phosphor. (b) Liftable electrode is grounded and dots acquire bound charges. (c) After removal of liftable electrode, plate is uniformly irradiated to free bound charges on the dots and form a latent free-charge image.

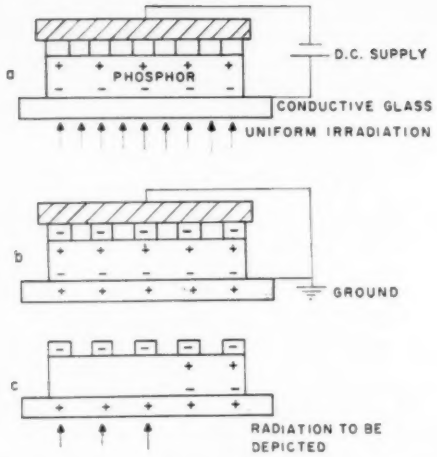

Fig. 6. Schematic diagram showing depolarizing method using plates with conductive dots. (a) Plate uniformly polarized. (b) Liftable electrode is grounded and dots acquire bound charges. (c) After removal of liftable electrode, depicting exposure is made to release polarization in exposed areas. Bound charge on the dots is freed to form a latent free-charge image.

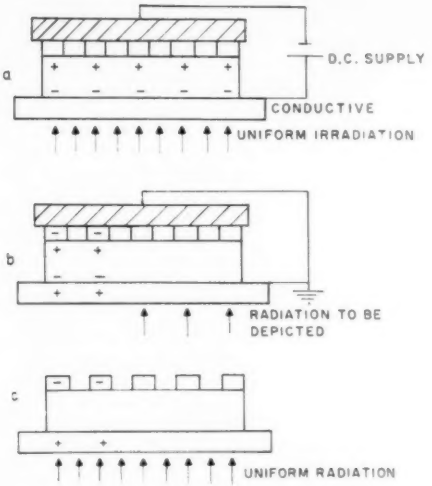

Fig. 7. Schematic diagram showing modified depolarizing method using plates with conductive dots. (a) Plate uniformly polarized. (b) Liftable electrode is grounded and the dots acquire bound charges. The depicting exposure is made *with the liftable electrode in contact with the dots and grounded,* to permit bound charge on dots in exposed areas to be freed and to flow to ground. (c) Grounded electrode is removed and plate is exposed uniformly, to release all polarization, and convert the residual bound charge on the dots to free charge. A latent free-charge image is thus formed.

polarizing field, as before. The field is applied with the external electrode in contact with the dots. The electrode is then grounded, and the dots acquire a bound charge density equal in magnitude and opposite in sign to the polarization charge density of the adjacent phosphor layer. The grounded electrode is removed from the dots, which remain at ground potential, but without external connection to any part of the circuit and without any measurable charge. Thereafter the polarization in the plate is discharged by a uniform light exposure and the bound charge on the dots is converted into free charge. A latent image of free charges is thus formed on the dots.

In the depolarizing method with a dotted plate (Fig. 6), the plate is polarized by an electric field applied during or after uniform light exposure. The external electrode is grounded and lifted away, leaving bound charge on the dots. The radiation to be depicted is then used to depolarize the plate in exposed areas. Bound charge is released on dots in these areas so that a latent image of free charges is formed.

The latent free-charge image formed by either the polarizing or depolarizing method can be developed by the resin technique. With dotted plates, both methods give a negative photocopy. This is because in both methods the radiation to be depicted releases charge on the dots. Strongly exposed areas thus have a large free-charge density residing on the dots.

A positive resin copy can be obtained by a modification of the procedure used in the depolarizing method (Fig. 7). In this modification, the radiation to be depicted is again used for depolarizing the plate, but this time with the external electrode touching the dots and grounded. The charge on dots in exposed areas then flows away to ground. The external electrode is removed from the dots, and the plate is exposed to uniform depolarizing radiation. This frees the bound charge remaining on dots in areas not irradiated during the image ex-

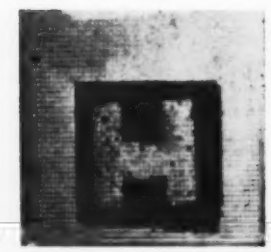

Fig. 8. Negative resin print produced on dotted plate by the polarizing method. 300 v were applied across the layer for 2 min. During this time, depicting exposure was made with 6.7×10^4 ergs/sq cm incident on exposed areas. Liftable electrode was grounded and removed. Releasing exposure was made using 1.1×10^4 ergs/sq cm. Resin development produced negative print.

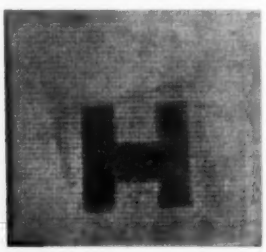

Fig. 9. Positive resin print produced on dotted plate by the modified depolarizing method. Plate uniformly polarized (4.4×10^5 ergs/sq cm and 300 v for 2 min). Liftable electrode was grounded and kept in contact with the dots during depicting exposure. Exposed areas received 2.2×10^5 ergs/sq cm. Liftable electrode was removed and plate uniformly irradiated with 1.1×10^4 ergs/sq cm. Resin development produced positive print

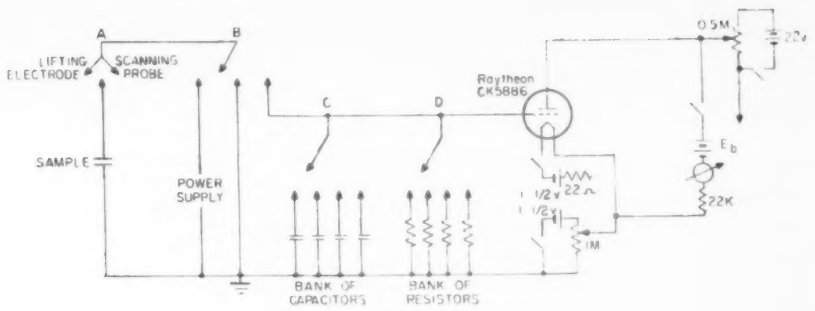

Fig. 10. Circuit diagram of electrometer. A,B,C,D: ROTARY CERAMIC SWITCHES

posure, so that a latent free-charge image is formed. This latent image is transformed by resin development into a positive copy of the depicted object.

The limitation on exposure times described above for use with "normal" plates also applied to all photographic methods using dotted plates.

Resin prints were prepared on dotted plates using the polarizing method (Fig. 8) and the modified depolarizing method (Fig. 9).

In order to determine the quantity of polarization charge produced in the plate during p.i.p. photography, the free charge on the dots was measured. These measurements are described below.

Measurement of Free Charge on the Conductive Dots

The circuit used in these charge measurements was a modification of the standard circuit for measuring polarization charges.[1] The circuit diagram and the experimental arrangement are shown in Figs. 10 and 11, respectively. A probe connected to the grid of the electrometer scanned the phosphor plate, making contact with individual dots in succession. A variable capacitance was connected between the grid and ground to introduce different sensitivity ranges. A variable resistance was connected in parallel with the capacitance to permit charges on the grid to decay as the probe moved from one dot to the next.

The free charge on each dot was measured as a voltage pulse on an oscilloscope. The output of the measuring circuit could also be fed into the Z-axis of the oscilloscope to form a visible image corresponding to the charge pattern on the dots.*

The capacitance of each dot depends, of course, on the capacitance per unit area of the phosphor layer, as determined by its thickness and composition. This dot capacitance is very small. Thus a small quantity of charge freed on a dot during a light exposure with the external electrode away produces enough voltage across the layer to prevent the polarization from being further discharged by light. Only a small fraction of the internal polarization can be released by each such light exposure of a dotted plate. The maximum charge which can be released on a dot is correspondingly limited. This free charge is removed from the dot by the scanning operation. A subsequent light exposure can therefore discharge part of the remaining polarization and release additional free charge. Thus if the internal polarization is strong, the plate can be scanned and the picture read off many times.

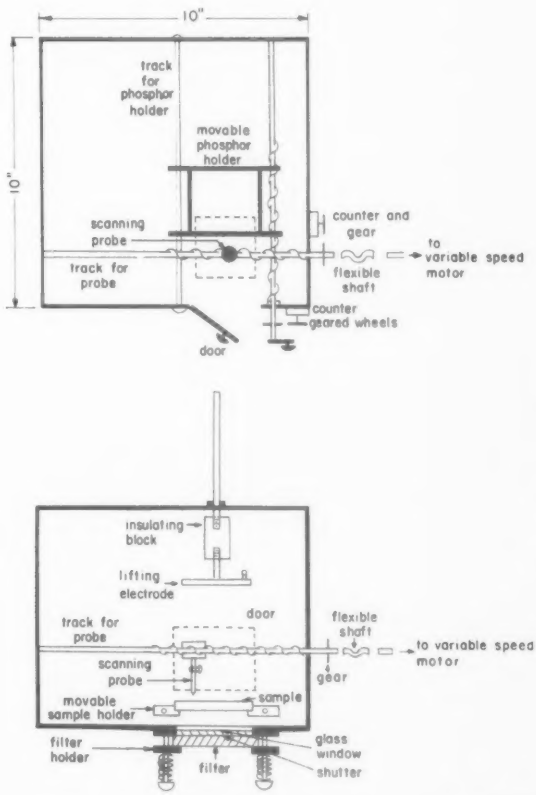

Fig. 11. Schematic diagrams showing sample housing and arrangement. *Top:* top view; *bottom:* front view.

* Performed by J. McNally, Department of Physics, New York University.

It was found that the maximum free charge which can appear on a dot of this size during a light exposure under these experimental conditions is 3×10^{-9} coulombs/sq cm, regardless of the intensity of polarization and the releasing light intensity.

Free Charge on the Dots as a Function of Polarizing Exposure

To determine the sensitometry of the polarizing method, the free charge on the dots was measured as a function of total incident energy of the polarizing radiation. The results of these measurements are plotted in Fig. 12. In this experiment, the polarizing exposure was varied by irradiating the plate through a step wedge with five steps which transmitted 0%, 17%, 46%, 74%, and 100% of the incident radiation, respectively. Thus different areas received different polarizing exposures at the same time.

The curve indicates that the variation of free charge with polarizing energy is not linear. The charge approaches a saturation value determined by the dot capacitance. (Due to dark decay, this saturation value is less than the maximum charge mentioned earlier.) However, there is a limited range of approximate linearity within which continuous tone photographs could be made. (In plates without dots, one would plot polarization density vs. polarizing exposure to determine suitability for continuous-tone work. The linear range for this relationship should extend to higher polarizing exposures, since the limitation due to dot capacitance does not apply.)

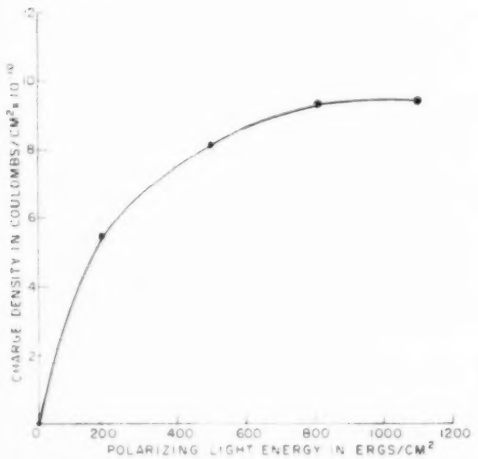

Fig. 12. Free-charge density on the conductive dots as a function of energy of polarizing light exposure. 300 v were applied across plate for 2 min. During this time, it was exposed through the step wedge upon which 1.1×10^3 ergs/sq cm were incident. After 30-min dark storage with the liftable electrode grounded, electrode was removed and plate uniformly exposed to 2.2×10^3 ergs/sq cm. The free charge on the dots was then measured. Each point on curve represents average of measurements on 20 individual dots exposed through same step of the step wedge.

The curve of Fig. 12 passes through the origin, indicating that no background of free-charge density was found in areas shielded from light during the image exposure.

If only line reproductions are desired, the polarizing image exposure can be much larger than the limiting value for continuous-tone reproductions. There is, however, an upper limit on useful polarizing image exposures due to light scattered into the unexposed areas by reflections in the transparent electrode, as discussed previously.

Free Charge on the Dots vs. Depolarizing Exposure

The sensitometry of the depolarizing method with dotted plates was determined by measuring the free charge, this time as a function of total incident energy of the depolarizing radiation. The depolarizing exposure was made with the external electrode removed from the dots. The step wedge was used to provide different exposures for different portions of the plate. These measurements (Fig. 13), show that the free charge on the dots increases uniformly with depolarizing energy for the experimental conditions described. It is therefore possible to make continuous-tone reproductions on dotted plates by the depolarizing method. As in the case of the polarizing method, the range of exposures useful for continuous-tone reproductions is limited by the capacitive effect of the dots. (Again, the limitation does not apply for plates without dots which should therefore have a more extended linear range suitable for continuous-tone work.)

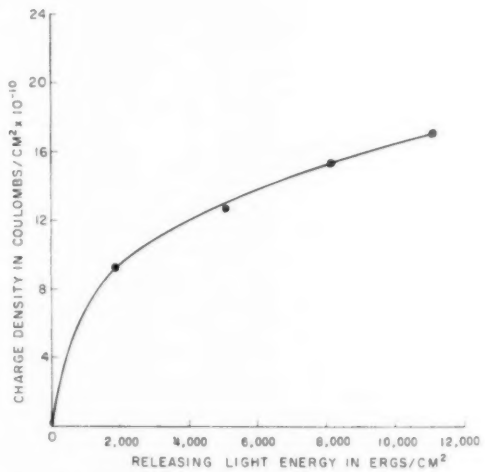

Fig. 13. Free-charge density on the conductive dots as a function of depolarizing light exposure. Plate uniformly polarized (4.4×10^5 ergs/sq cm and 300 v for 2 min). After 30-min dark storage with the liftable electrode grounded, the electrode was removed and the plate exposed through the step wedge upon which 1.1×10^4 ergs/sq cm were incident. The free charge on the dots was then measured. Each plotted value represents average of measurements on 20 individual dots exposed through same step of the step wedge.

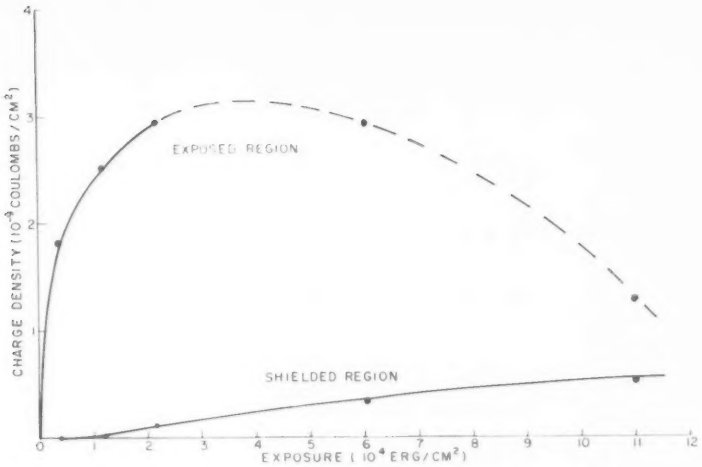

Fig. 14. Influence of high depolarizing exposures on the free-charge density on conductive dots. Plate uniformly polarized (4.4×10^5 ergs/sq cm and 300 v for 2 min). After 30-min dark storage with liftable electrode grounded, the elertrode was removed and the plate irradiated through a shield having alternate opaque and transparent strips, exposing about one half the total area. An intensity of 370 μw/sq cm was incident on exposed areas for a prescribed length of time. The free charge on the dots in exposed and unexposed areas was then measured. The experiment was repeated in the same way, using different periods of exposure to depolarizing radiation of the same intensity. Each plotted value represents average of measurements on about 50 individual dots.

The curve of Fig. 13 passes close to the origin, indicating that practically no background on free-charge density was found in areas shielded from light during the depolarizing exposure.

There is an upper limit of useful depolarizing exposures not shown on the curve. Two effects determine this maximum useful exposure. The first is the increase in photoconductivity at excessive exposures which causes the free charge on the dots to leak to ground through the phosphor layer. The second is the previously mentioned effect which limits all depicting exposures. In this case, the light scattered by multiple reflections inside the glass plate during the image exposure releases the polarization and produces background charge on dots in the supposedly unexposed areas. Both of these effects lower the contrast.

To determine the magnitude of these effects, the free charge was measured on dots in both shielded and illuminated areas, after various light exposures. In these experiments, the incident intensity was held constant, and the exposure time was varied. Figure 14 shows the results of these measurements. At excessive exposure times, the free charge on dots in exposed areas decreases due to photoconductive leakage, while the free charge on dots in shielded areas increases due to scattered light.

Photoconductive leakage can be a disadvantage in all methods of p.i.p. photography with dotted plates. The final depolarizing exposure is always made with the external electrode away from the dots. If this exposure is too high, photoconductive leakage reduces the free charge on the dots, and renders the method less sensitive. This is true even in the polarizing method, for which the final depolarizing exposure is not the depicting exposure.

For plates without dots, photoconductivity is not a disadvantage in photography.

Modified Depolarizing Method:

Free Charge on the Dots vs. First Depolarizing Exposure

The sensitometry of the modified depolarizing method was determined by measuring the charge on the dots as a function of the total incident energy of the depicting exposure, i.e., the first depolarizing exposure. Again the step wedge was used to vary the exposure of different portions of the plate. A typical result is plotted in Fig. 15. In this experiment, the external electrode remained in contact with the dots and grounded during the depicting ex-

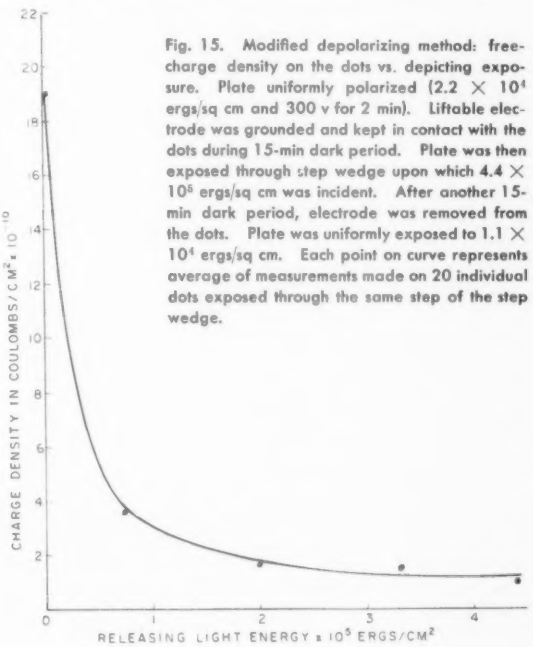

Fig. 15. Modified depolarizing method: free-charge density on the dots vs. depicting exposure. Plate uniformly polarized (2.2×10^4 ergs/sq cm and 300 v for 2 min). Liftable electrode was grounded and kept in contact with the dots during 15-min dark period. Plate was then exposed through step wedge upon which 4.4×10^5 ergs/sq cm was incident. After another 15-min dark period, electrode was removed from the dots. Plate was uniformly exposed to 1.1×10^4 ergs/sq cm. Each point on curve represents average of measurements made on 20 individual dots exposed through the same step of the step wedge.

posure. The charge on dots in exposed areas then flowed to ground according to the incident energy. The charge remaining on the dots after this exposure was liberated by the subsequent uniform exposure with the electrode away, and measured by the moving probe arrangement. Thus the areas receiving the largest depicting exposure had the smallest free charge on the dots after the uniform exposure.

The curve of Fig. 15 shows that the variation of free charge on the dots is nearly linear with depicting exposure, for low incident energies. Thus continuous-tone photographs could be obtained using this method. Maximum contrast is obtained for exposures in the range below 10^5 ergs/sq cm. The background free charge on the dots at this exposure is insufficient to cause a background of adhering resin.

The method gives excellent results in line reproduction work, as shown by the resin print of Fig. 9. The upper limit of useful depicting exposures is again determined by scattered light.

It should be noted that the light intensities given are those of the tungsten lamp. Only a fraction of this light is effectively utilized by the phosphor. The sensitivities quoted above would be considerably larger if the light fell in the region where the phosphor is most sensitive. Another way to increase the sensitivity would be to increase the polarizing voltage.

Resin Development Using Dotted Plates:

Density of Adhering Resin vs. Free Charge on the Dots

The use of phosphor plates with dots offers a number of advantages in p.i.p. photography with resin development. As mentioned above, the polarization pattern is not altered when the electrode is lifted away to apply the resin. Secondly, the resin adheres uniformly to the dots in any uniformly exposed area, thus eliminating edge effects. Thirdly, the charge on the dots is closer to the surface than the internal polarization charge, so that it can attract the resin particles more strongly. It is therefore possible to use the p.i.p. plate as a master, and transfer the image to an unsensitized layer such as paper.

The density of resin adhering to a charged dot depends on the free charge residing on the dot. This dependence was studied by observing the resin density visually, and measuring the free charge on the dots. Other factors influencing the resin density, such as the size of the dot, the size of the resin particles, and the nature of the resin were not investigated. Bound charges, of course, are not effective in attracting resin.

It was observed that no resin adhered to a dot with a free charge density less than 5×10^{-10} coulombs/sq cm. For dots with free charge densities between 5×10^{-10} and 12×10^{-10} coulombs/sq cm, the density of adhering resin varied from zero to a maximum. The maximum resin density produced a deep black region on the print (Figs. 8 and 9). For free-charge densities exceeding 12×10^{-10} coulombs/sq cm, up to the limiting free-charge density of 3×10^{-9} coulombs/sq cm, no increase in adhering resin density was observed.

If the resin and the dot size were suitably chosen, it should be possible to have the density of adhering resin depend linearly on the free charge density in the linear regions shown in Figs. 12 and 13. In that event, continuous-tone resin prints could be made, using either of these methods.

Factors Affecting Background in Photography Using Dotted Plates

The effects of excessive depicting exposures on background areas have been described earlier as being significant for all methods of p.i.p. photography on plates with and without dots. Those additional factors specifically affecting background areas in photography with dotted plates will now be considered. The corresponding factors for plates without dots have already been discussed.

In preparing latent free charge images on dotted plates by the polarizing method, no free charge is produced on dots in unexposed areas (Fig. 12). Therefore no background of resin adheres to the dots in these areas after development (Fig. 8).

In the normal depolarizing method with dotted plates, practically no charge is released on dots in unexposed areas (Fig. 13). Exposure to 10^4 ergs/sq cm of light releases 1.7×10^{-9} coulombs/sq cm on the dots, enough to attract the maximum density of resin. Thus, resin prints prepared on dotted plates by this method should have excellent contrast. However, it was observed that this contrast is completely erased by moisture in the air when the plate is removed from the dry chamber to apply the resin. The quantity of polarization discharged by atmospheric moisture in all parts of the plate is about the same as that released in light-exposed areas by the depicting exposure. It amounts to 3×10^{-9} coulombs/sq cm, which is the maximum that can be released, regardless of the method of release, as discussed previously.

Thus, to prepare resin prints on dotted plates by the normal depolarizing method, the phosphor layer must be protected from moisture by imbedding it in a moisture-resistant matrix. With the matrix used here, the same purpose can be accomplished by applying the resin in a dry atmosphere.

In the modified depolarizing method, the first depolarizing exposure leaves a small residual polarization in exposed areas. This is partly discharged by the uniform second depolarizing beam, producing background-free charge on dots in areas which should have been completely discharged by the previous exposure. This background-charge density of 10^{-10} coulombs/sq cm for large depicting exposures (Fig. 15) might introduce a slight background in direct display on a cathode-ray screen. However, in resin development, this charge density is insufficient to attract resin to exposed areas.

In unexposed areas, a free-charge density of 2×10^{-9} coulombs/sq cm resides on the dots (Fig. 15). This is sufficient to attract the maximum density of resin. Therefore, continuous-tone and line reproductions of high contrast may be obtained by this method using resin development (Fig. 9).

Comparison with Electrophotography

Although there is a superficial similarity between conventional electrophotography and p.i.p. photography using resin development, the mechanisms are fundamentally different. In electrophotographic methods, charges are sprayed on the surface of a photoconductor layer by means of corona discharges; d-c voltages in the range of several kilovolts are required. During the light exposure, which must be made soon after charging, the charges leak off wherever the radiation strikes.

In p.i.p. photography, the required polarizing voltage is small (50 to 500 v.). The picture may be taken any time before, during, or after the application of the voltage. The latent p.i.p. image is internal, in contrast to the surface-charge image in electrophotography. Therefore, the latent p.i.p. image can be protected from discharge induced by atmospheric moisture, by imbedding the phosphor in a moisture-insensitive matrix.

The polarization half life, which is in the order of 10^3 min, depends to some extent on the properties of the imbedding matrix. Thus with a suitable matrix, the charge separation can be fixed for a long time within the body of the phosphor, provided it is kept in the dark. Only a light exposure can destroy it. Both the sensitized plate and the latent image can be stored for a very long time compared to that used in electrophotography.

Summary

The p.i.p. effect was successfully used to produce photographs on phosphor layers. Two methods were developed for obtaining a latent p.i.p. image in the body of the phosphor. The latent image may be formed by a light exposure before or during the application of the field (polarizing method), or the exposure may be made after the application of the field (depolarizing method).

One may also use the polarizing or depolarizing method to form a latent free-charge image residing on metallic-dot electrodes sprayed on the surface of the layer.

Both the latent p.i.p. image and the latent free-charge image can be made visible by applying dyed charged resin powder to the respective plates. The latent image may also be converted to a visual display on a cathode-ray tube by scanning the plate optically or mechanically. In making visible images by the resin technique, or the display-tube technique, positive or negative reproductions may be obtained as desired.

The latent p.i.p. images have an extended storage life. They can be protected from discharge due to atmospheric moisture by imbedding the phosphor in a suitable matrix. The p.i.p. photographic process is useful for line, half tone and continuous-tone reproductions. Low supply voltages are required in comparison with those required in electrophotography.

The photographs described above were made using visible light. P.i.p. photography has also been successfully used to depict near and middle infrared radiation up to 2.5 μ on the same ZnCdS phosphor.[3] In principle, radiation in any part of the spectrum can be depicted by choosing a phosphor with suitable sensitivity in the given range.

• Coming Technical and Scientific Meetings

Optical Society of America, March 2–4, 1961, Pick-Roosevelt Hotel, Pittsburgh, Pa. To present a contributed paper, the author must submit by December 29 the title plus an abstract no longer than 200 words. Abstract forms available from OSA Executive Office, 1155 Sixteenth St., N.W., Washington 6, D. C., Attn. Mary E. Warga. Meeting to be held in part concurrently with the Pittsburgh Conference on Analytical Chemistry and Applied Spectroscopy at the Penn-Sheraton Hotel, where a large instrument exhibit will be on display.

89th Semiannual Convention, SMPTE, May 7–12, 1961, King Edward Sheraton, Toronto. Papers Committee Chairman, Rodger J. Ross, Canadian Broadcasting Corp., 354 Jarvis St., Toronto

1961 Annual Conference, SPSE, May 22-26, Binghamton, N.Y. Papers Committee Co-Chairmen, Dr. F. H. Gerhardt and Peter Krause, Ansco, Binghamton, N.Y.

90th Semiannual Convention, SMPTE, October 2–6, 1961, Lake Placid, N.Y.

1962 Annual Conference, SPSE, Boston

91st Semiannual Convention, SMPTE, April 30-May 4, 1962, Ambassador Hotel, Los Angeles

92nd Semiannual Convention, SMPTE, October 22–26, 1962, Drake Hotel, Chicago

PHOTOGRAPHIC SCIENCE AND ENGINEERING
Volume 4, Number 6, November–December 1960

Rapid-Drying Characteristics of Several Films for Aerial Photography

JAMES W. BOYD, *Film Testing Division, Eastman Kodak Company, Rochester, N. Y.*

Drying curves were obtained for six aerial films under several drying conditions in two dryers one an air impingement type and the other a Houston A-14 dryer. These curves show clearly the division of drying into two major periods: a constant-rate period in which drying is controlled by conditions of the dryer and a falling-rate period when characteristics of the film become a major factor.

In the equations governing the constant-rate period, the dryer coefficient describes the ability of the dryer to evaporate moisture from the film. In the falling-rate period, the rate of moisture evaporation from the film surface continuously diminishes in an exponential fashion; the rate depends upon emulsion characteristics prior to processing, the effects of the process on the emulsion, and also the drying conditions.

The ability of processed film to fulfill the purpose for which it is intended and its useful life often depend on the suitability of the drying process and the moisture content which is finally attained. Important physical characteristics, such as curl and brittleness, are affected by drying procedures.

The design and use of film dryers require a knowledge of the drying characteristics of the film to be dried. The increasing use of such rapid-drying devices as impingement-type dryers[1] makes the choice of drying conditions and times much more critical if a product with optimum qualities is to be obtained.

Because drying of porous and semiporous solids has wide application, much has been written on the subject. Chemical engineering texts and handbooks[2,3,4] develop the subject mathematically. This analytical approach has been used in a series of tests designed to obtain drying curves for six Kodak aerial films processed under a given set of conditions and dried in several different ways.

General Theory

The percentage of retained moisture in processed photographic film depends upon the type of film, the processing treatment it has received, and the relative humidity of the atmosphere with which it is in equilibrium.

Presented at the Annual Conference, Rochester, N. Y., 6 October 1958. Received 28 August 1959; revised 13 August 1960.

1. F. Dana Miller, *Jour. SMPTE*, **60:** 85 (1953).
2. W. C. Badger and W. L. McCabe, *Elements of Chemical Engineering*, McGraw-Hill, New York, 1936.
3. Walker, Lewis, McAdams and Gilliland, *Principles of Chemical Engineering*, McGraw-Hill, New York, 1937.
4. John H. Perry, Ed., *Chemical Engineer's Handbook*, 3d ed., McGraw-Hill, New York, 1950.

Figure 1 shows a typical plot of equilibrium moisture content versus environmental relative humidity for an aerial film.

Drying is the process of removing moisture from the film until the remaining moisture is equal to that for equilibrium with an atmosphere of chosen relative humidity. The drying process divides itself into two major periods. During the first, or constant-rate period, the rate of water evaporation from the wet emulsion surface is determined entirely by the flow of drying air and the thermodynamics of the evaporative process. The rate of diffusion of water within the emulsion and film base is sufficient to maintain the initial fully wet condition at the emulsion surface.

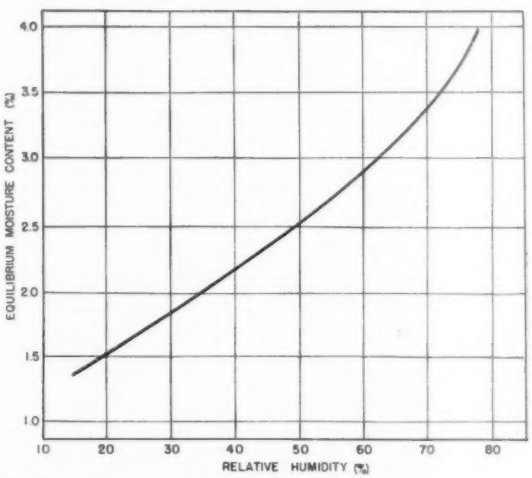

Fig. 1. Typical moisture equilibrium curve.

Eventually, as the quantity of water in the film diminishes, a point is reached where the rate of diffusion from within falls off and consequently the evaporation rate is reduced rather sharply. At this point of critical moisture content, the falling-rate period is entered. The evaporation rate continues to drop throughout the remainder of the drying period.

For the constant-rate period the following approximate equation holds:

$$dw/dt = k\,\mathrm{WBD} \qquad (1)$$

where

dw/dt = rate of water evaporation per unit surface area

WBD = degrees of wet-bulb depression of entering air in °F

The dryer coefficient, k, is given by the equation

$$k = D(M_0 - M_c) \times \frac{1}{T} \times \frac{1}{\mathrm{WBD}} \qquad (2)$$

where

D = absolute dry weight of film (typical unit: lb/100 sq ft)

M_0 = initial moisture content (fractional, dry weight basis)

M_c = critical moisture content (fractional, dry weight basis)

T = time of constant-rate period (typical unit: hours)

k = dryer coefficient (typical unit: lb water/hr/100 sq ft of gelatin surface/WBD)

The dryer coefficient, which specifies the ability of the dryer to remove water from a film during the

TABLE 1

Film	Temp.	WBD	Moisture content		Dryer coefficient		Drying time (sec) for:		
			Initial	Critical	Experimental	Theoretical	Const. rate period	Equil. with 60% R.H.	Equil. with 50% R.H.
Impingement Dryer									
Infrared Aerographic Film	120	40	25.4	5.0	3.40	3.30	20	46	——
	140	56	25.8	5.2	4.00	3.38	12	27	40
	160	72	25.2	5.2	3.18	3.38	11	20	27
Super XX Aerographic Film	120	44	28.6	7.0	2.97	3.15	22	51	——
	140	55	29.0	7.0	3.44	3.38	15	32	42
	160*	70	27.5	6.4	2.44	2.70	15	33	40
Aerographic Duplicating Film	120	42	17.2	5.0	3.40	3.15	11	——	——
	140	53	17.6	4.6	3.62	3.38	9	29	39
	160	70	17.8	4.4	3.66	3.38	6	20	29
Plus-X Aerecon Film	120	44	15.7	5.0	4.07	3.38	8	——	——
	140	58	15.8	5.2	3.36	3.38	7	40	——
	160	72	15.7	4.9	3.38	3.38	6	22	32
Tri-X Aerecon Film	120	40	21.4	6.2	3.26	3.30	17	——	——
	140	55	20.6	6.0	3.46	3.38	11	37	——
	160	72	20.4	6.0	3.12	3.38	9	22	——
Super-XX Aerial Recon R.P. Film	120	40	17.4	5.8	3.39	3.30	12	——	——
	140	61	18.6	5.8	3.72	3.45	9	32	44
	160	70	17.4	5.0	3.14	3.38	8	26	36
A-14 Dryer									
Infrared Aerographic Film	140	56	21.6	5.2	1.45	1.53	27	46	76
Super-XX Aerographic Film	140	56	24.2	5.2	1.51	(Average for all films)	32	40	47
Aerographic Duplicating Film	140	55	13.6	5.2	2.15		10	44	65
Plus-X Aerecon Film	140	56	8.3	5.0	1.57		6	48	69
Tri-X Aerecon Film	140	60	17.6	6.2	2.36		11	54	71
Super-XX Aerial Recon R.P. Film	140	56	12.6	5.5	1.74		9	48	66
Super-XX Aerographic Film Exhausted Hypo	140	57	24.2	6.0	1.60		28	61	83
Plus-X Aerecon Film Exhausted Hypo	140	58	10.7	4.9	1.71		8	55	79
85° F Exhausted Hypo	140	57	13.5	5.1	1.35		15	62	84

* Low drying coefficient and long drying time caused by low plenum pressure and therefore reduced air flow in dryer.

constant-rate period, is determined by the geometry of the dryer and operating characteristics affecting air flow over the film. It is useful for intercomparing the effectiveness of various dryers and dryer conditions during the initial period. This coefficient and the wet bulb depression maintained in the dryer establish the drying rate during the constant-rate period. Differences among film types having no gelatin coating on the back are insignificant. When these factors are known, along with the absolute dry weight of the film, the rectilinear portion of the drying curve can be drawn between the values for initial moisture content and the critical moisture content.

During the falling-rate period the drying rate is dependent not only on the characteristics of the dryer but on the properties of the photographic film. Moisture content falls approximately exponentially with time. Where precise determination of this portion of the curve is desired, experimental data representing each set of processing and drying conditions are necessary.

Experimental Procedure

A series of tests was made to obtain drying information under several drying conditions for six Kodak aerial films. Two dryers were used, one an impingement type, the other an Air Force A-14 Dryer of the so-called "squirrel-cage" type. The films investigated were:

Kodak Infrared Aerographic Film
Kodak Super-XX Aerographic Film
Kodak Aerographic Duplicating Film
Kodak Plus-X Aerecon Film
Kodak Tri-X Aerecon Film
Kodak Super-XX Aerial Recon R.P. Film

All films were processed in a Morse B-5 Portable Film Processor, 180 ft at a time in room light. One sample was processed at 85°F while the others were at 68°F. The 68°F process was:

Development	18 min	Kodak Developer D-19 (except Aerographic Duplicating Film)
	6 min	Kodak Developer DK-50 (Aerographic Duplicating Film)
Fixing	10 min	Kodak Fixing Bath F-10
Washing	20 min	
Soaking	15 min	(transit time to dryer)

All chemicals used in each test were fresh except in the three tests in which exhausted fixing bath was substituted. For one of the latter, a temperature of 85°F was maintained throughout the process with a development time of 10 min.

In the impingement dryer, the film passes between two perforated plates 2 in. apart. Air is blown through the perforations perpendicularly toward the film. The holes, $^1/_8$ in. in diameter, are spaced $^3/_4$ in. apart in rows $1^3/_8$ in. from each other. Rolls of each of the six films were dried at air temperatures of 120°F, 140°F, and 160°F. The film came from the processing-machine reel through a tank of wetting agent solution and a wringer-type squeegee to the dryer. Samples were cut from the film at the dryer entrance and at each of approximately ten intervals throughout the drying process and immediately put into special sample bottles having moisture-tight stoppers. These samples were weighed in the stoppered containers before and after prolonged exposure to high vacuum. This procedure gave dry-film weight and moisture-content weight. The quotient of these is the fractional moisture content.

Samples of dried processed film were conditioned in each of several atmospheres of different relative humidities to obtain moisture content data for plotting moisture equilibrium curves.

The A-14 dryer is part of an Air Force A-9 Aerial Film Processor. Squeegeeing in this machine is accomplished by a small blower and a series of rubber blades. In the dryer, the film travels around the periphery of a drum. Air is blown through slits in this drum by a fan in the center. The film is backed up by a series of rollers.

The sampling procedure was much the same as in the case of the impingement dryer. Tests were made on all films with a dryer temperature of 140°F.

For each test, a graph of moisture content versus drying time resulted. From the values for the initial and critical moisture content and the wet-bulb depression, the dryer coefficient was computed in accordance with Eq. (2). For the impingement dryer, this value was compared with the coefficient predicted by an empirical equation. Equilibrium with air of any given relative humidity could be chosen as the desired end point of drying. By reading the corresponding moisture content for each film from the moisture-equilibrium curves and evaluating the point on the drying curve when this value is reached, the drying time was obtained.

Results

Each test resulted in a drying curve characterizing the particular film, process, and drying conditions under investigation. The results of these tests

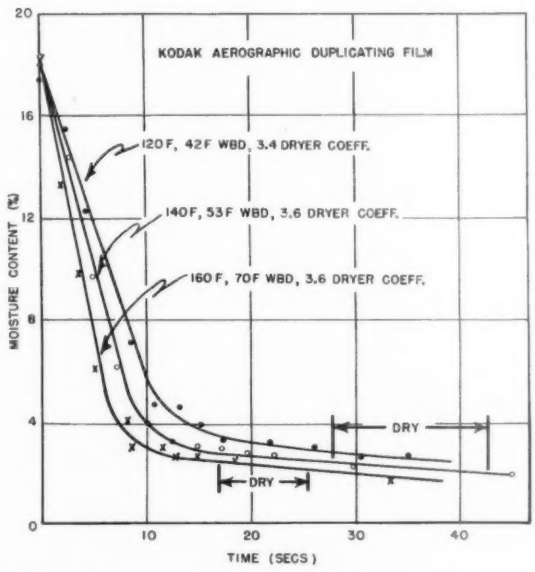

Fig. 2. Drying curves with variable wet-bulb depression.

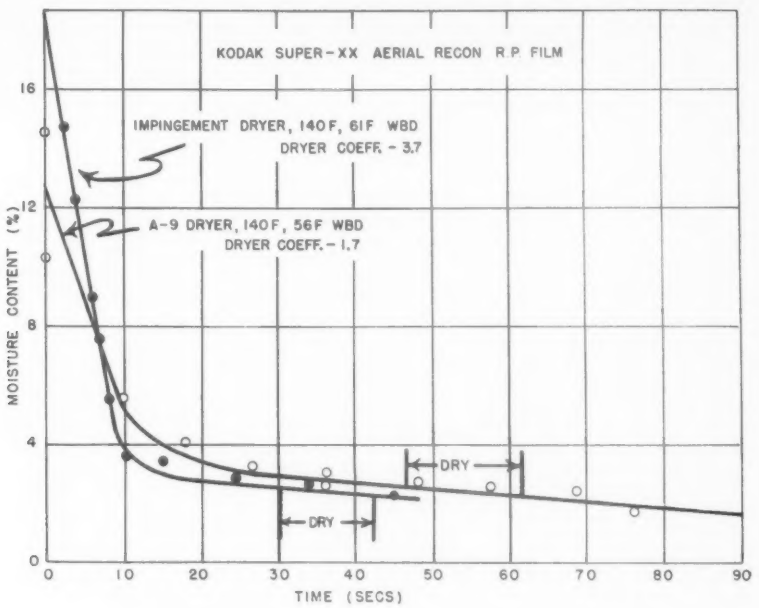

Fig. 3. Drying curves with variable dryer coefficient.

are summarized in Table I. A few of the curves are presented in the following figures to illustrate some of the relationships between them.

The particular drying curves in Fig. 2 show the effect of holding the dryer coefficient essentially constant and varying the wet-bulb depression in the dryer. The drying rate in the constant-rate period increases with an increasing wet-bulb depression. This and the more rapid drying in the falling-rate period decrease the total drying time as shown here. Critical moisture content remains much the same. Equilibrium with air of 50 to 60% R.H. is indicated as dry. The 120° F. drying curve did not reach 60% R.H. equilibrium in this experiment.

With the wet-bulb depression approximately constant and the different coefficients of the two dryers, curves such as those in Fig. 3 result. Despite the lower initial moisture content of the film entering the A-9 dryer because of more effective squeegeeing, the lower drying coefficient lengthens the constant-rate period and changes the curve shape of the falling-rate period so that the the total drying time is longer.

The films used to obtain the drying curves shown in Fig. 4 were given the same washing, squeegeeing, and drying procedure. Differences in the type of film result in different initial moisture contents. However, the fact that the constant-rate portions are parallel shows that the drying rate was constant during that period. The Aerographic Duplicating Film, having a thinner emulsion, has a relatively flat shallow curve in the falling-rate portion.

The effect of a variation in processing on drying is

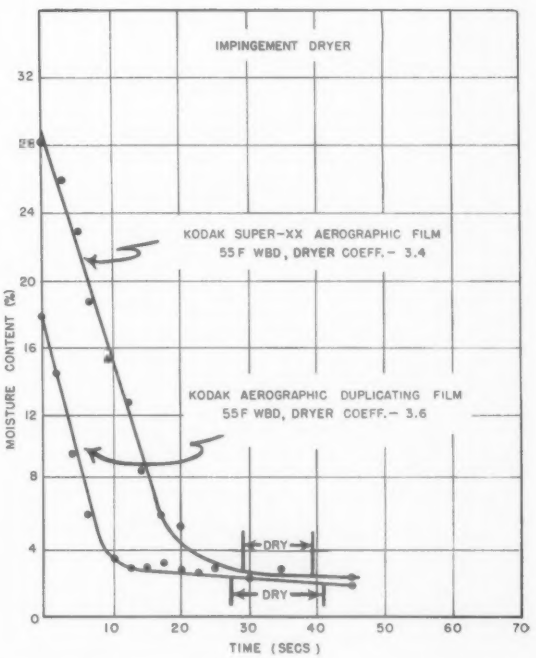

Fig. 4. Drying curves for two film types.

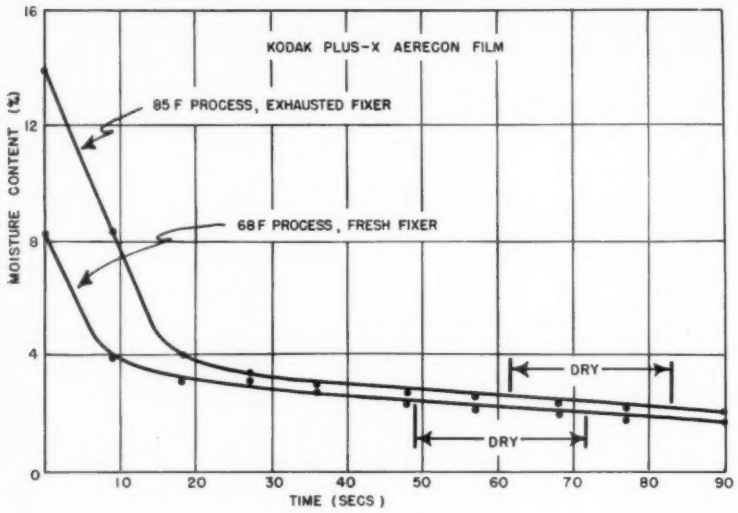

Fig. 5. Effects of processing variations on drying.

readily seen in Fig. 5. The 85°F processing temperature and the exhausted fixer both contribute to softening of the emulsion layer, thus increasing the initial moisture content and slightly affecting the shape of the falling-rate portion of the curve. Again the initial drying rate is constant due to constant dryer coefficient and wet-bulb depression.

Conclusions

Each of the drying-time curves showed typical constant-rate and falling-rate periods. The rate of drying during the initial constant-rate phase can be calculated from the dryer coefficient and the degrees of wet-bulb depression. Thus, if the initial moisture content and the critical moisture content are known, this curve portion may be drawn, and from this the duration of the constant-rate period can be read. Calculation of the dryer coefficient from this series of impingement drying tests showed an average error of 7.5% from the coefficients predicted by empirical equations.

Film characteristics do not affect the rate of initial drying; however, the film and the treatment which it receives prior to drying do determine the end points of this drying phase, i.e., the initial and critical moisture contents. Thus, it is important that values for these quantities be obtained under exactly controlled processing conditions. The initial moisture content can vary widely with processing variations, but in most circumstances the critical moisture content will vary only 10 to 15% with process changes.

The shape of the falling-rate portion of the curve is controlled by film characteristics such as emulsion thickness and hardness, by the dryer coefficient, and by the wet-bulb depression during drying. Moisture content falls approximately exponentially with time during this period. Small changes in any one of the determining factors do not usually result in major changes in curve shape, but for precise measurements or for radical changes in processing or drying conditions, it is advisable to obtain experimental data to establish each curve.

•Book and Journal Reviews

The Optical Industry Directory

The Optical Publishing Co., Lenox, Mass., 1960, paper covers, 200 pp., $7.50

Again the Optical Publishing Company has brought forth its invaluable annual list of American importers, designers, manufacturers, and distributers of optical instruments. Although the present edition is slightly less bulky than last year's, its coverage seems to be fully as extensive and, with respect to instruments used in space technology, the publishers claim the coverage to be even more extensive. The reduction in bulk seems to have been made by listing the firms alphabetically instead of grouping them by states and by abandoning the serial numbering of the types of apparatus. Although the review given in these pages a year ago (*P S & E*, **3**: 305 (1959)) applies equally to the current edition, the importance of annual revisions is made evident by a random comparison. Under the heading "Goniometers," six firms listed in 1959 have disappeared from that listing and nine new ones have appeared. Under "Microdensitometers and Microphotometers," seven firms have disappeared and ten have taken their places, leaving only four that are common to both editions.—*F. H. Perrin, Eastman Kodak Co., Rochester, N.Y.*

Control Techniques in Film Processing

WALTER I. KISNER (Chairman) and others, Society of Motion Picture and Television Engineers, New York, 181 pp., 74 illus., 6 by 9 in., $5.00

Thirty-two persons have collaborated as a committee to write this compact work. The joint authors represent manufacturers of photographic materials and equipment as well as processing establishments and others concerned with sensitized products.

The foreword indicates the aims of the book: "The text [was made] as fundamental as possible without being overly theoretical . . . . The principles and procedures outlined should be applicable to both the large and the small laboratory and should direct their efforts toward production of an end product of the highest quality. The book is not intended to be a handbook of detailed instructions; instead it is aimed toward furnishing a firm foundation for the understanding of proper process control techniques and to provide a guide for further work and study."

Methods for the control of continuous processing of black-and-white films are described in the six major sections of the book. After three short introductory chapters, typical processing machines are illustrated and described in terms of their functions. Recommendations are offered concerning control devices and their maintenance.

A review of sensitometric control methods includes illustrations of available densitometers (except the Welch Densichron) and sensitometers. Methods of evaluating sensitometric curves are briefly explained. A valuable section is devoted to sensitometric methods of controlling duplication processes.

The fundamental chemistry of the photographic process is explained in simple terms; this is followed by a mention of instruments useful for chemical control methods. An extensive list of references is given for the use of processors who may choose to adopt chemical analytical methods of control. Process adjustment and replenisher calculations are briefly discussed by means of examples.

A particular virtue of the book is the attention given to the variability of instruments and their proper maintenance, including trouble-shooting suggestions. Emphasis is placed on the factor of cost as it affects the decisions involved in control methods. Lists of useful references are appended to most chapters.

Persons involved in the continuous processing of films will find the book a unique and helpful guide. They will need to look elsewhere for a theoretical background and for specific methods for the determination of process variability and for the preparation of control charts. As a text book, considerable supplementation would be necessary.—*Hollis N. Todd, Rochester Institute of Technology, Rochester, N.Y.*

Kino—A History of the Russian and Soviet Film

JAY LEYDA, Macmillan, New York, 1960, 493 pp. + 32 plates, $9.50

This comprehensive history of motion pictures in Russia begins with the Lumières' filming of the coronation of Tsar Nikolai II in 1896, and covers the growth and vicissitudes of the Russian and Soviet film industry up to 1947, with a postscript on the period 1948–1958. Attention is given to the important Russian film industry before the revolution of 1917 and to its links with the emerging Soviet film. The film history is set against the background of Russia's social and artistic changes during the period considered.

Abridged Scientific Publications from the Kodak Research Laboratories

Volume XXXIV, 1952, Eastman Kodak Co., Rochester, N.Y., 1960, 253 pp.

This volume contains abridgments of 77 papers by members of the staff of the Kodak Research Laboratories. The original papers were published in scientific journals in 1952, except for two papers published in 1951.

Infrared Recording Today

C. E. ENGEL, *Brit. J. Phot.*, **105**:68–71, 73 (1958)

Methods of recording images by infrared radiation, based on volatilization, phosphorescence, and the image converter are reviewed. A survey of modern infrared photographic materials is given which sets out in tabular form: manufacturers, sizes, spectral sensitivity range, approximate emulsion speeds, recommended filters, safelights, and development conditions. The

tables given in the Russian paper on modern infrared sensitive materials, by S. M. Solov'ev, reviewed in *P S & E*, **4**: 179, are direct translations of the tables in Engel's paper.—*T. H. J.*

The Influence of the Rate of Development on the Reproduction of Picture Detail by a Photographic Material

G. V. Derstuganov, *Tekh. Kino i Televideniya*, **4**: 53–57, April 1960 (in Russian)

The "Photographic Information Volume" of Kardas (*Phot. Eng.* **5**: 91 (1954); **6**: 190 (1955)) is not suitable in its original form for the study of the reproduction of detail at low contrast. An index of the performance of a photographic material at a given contrast has therefore been obtained by taking the area of the cross-section of the volume at a given contrast of the test object. This corresponds to taking the area under the curve $R' = f(\log E)$ at a given constant contrast. A further refinement is to take the "useful" area lying above the ordinate $R' = 5\ \text{mm}^{-1}$, R' being the resolving power in lines per millimeter. This characteristic has been given the symbol U_p. Experiments were carried out by exposing a photographic material to a test object and studying the effect of time of development on U_p and sensitometric characteristics. It was found that increasing the rate of development, either by increasing the concentration of the developing agent or raising the temperature, produced a deterioration in the rendition of low-contrast detail, which was expressed quantitatively by a decrease in U_p. At the same time the properties of the photographic material markedly affected the decrease in U_p. When three different types of material were tested in Metol-hydroquinone developers, an increase in the rate of development produced a relatively greater fall in U_p for a high-speed coarse-grain film than for a slow-speed fine-grain film. For any given case, the smaller the detail contrast the greater is the decrease in U_p.—*S. C. Goddard*

Rapid Methods of Processing Aerial Photographic Materials

V. A. Vendenbakh, *Trudy Labor. Aerometodov. Akad. Nauk SSSR*, **7**: 32–36 (1959) (in Russian)

A short review is given of a number of methods of rapid processing of photographic materials suitable for aerial photography. The author has taken part in the working out of methods which depend on the use of viscous (containing agar-agar, starch, polyvinyl alcohol or Tylose) or alcoholic (ethylene glycol, glycerine) aqueous processing solutions for processing aerial photographic paper. At temperatures of 40–60°C the time of processing prints with satisfactory discrimination of detail is 20–30 sec. To obtain aero-negatives simultaneously with positives it is possible to use a rapid one-stage development of the Land type, while a better result is obtained with the so-called "deep" variant, in which the positive image is formed not in the surface of the developer on the positive material but in a special receptive layer of a film-forming substance which is insoluble in water. At 20°C, development of the negative is in general finished after 1 min, and the positive after 2–3 min. The negative is characterized by low values of gamma (0.4–0.45) and D_{max} (0.85–0.95), while the positive in gamma and in D_{max} directly corresponds to glossy paper No. 2 and exhibits a fairly low resolution (22–24 mm^{-1}), thus differing from the negative. A defect of this method of obtaining the image is the unavoidable narrowing of the useful exposure range.—*S. C. G.* (translated from *Referativnyi Zhur., Fizika*)

A Study of the Fundamental Parameters in the Jet Processing of Black-and-White Motion-Picture Film

B. V. Valuĭskiĭ, *Tekh. Kino i Televideniya*, **4**: 44–51, May 1960 (in Russian)

A theoretical hydrodynamic analysis is made of the development and fixing of moving motion-picture film by means of jets, the jets being applied vertically to a horizontal film. Confirmatory experiments are described. The major factors are the rate of application of the jets and the degree of overlapping of the streams on the film surface. The effect of temperature in this type of processing is similar to that of temperature in processing in tanks with agitation. Application normal to the surface of the film was found to be more effective than tangential application.—*S. C. G.*

A Study of the Physical Processes in a Shock Tube with the Aid of High-Speed Photography

L. A. Vasil'ev, S. S. Semenov and E. A. Tarantov. *Izvestia Akad. Nauk, SSSR, Otd. Tekhn. Nauk*: No. 11, pp. 186–188, 1957 (in Russian)

A method of high-speed shadow photography has been used for the study of phenomena taking place in a shock tube with a stream of gas flowing around a model. The IAB-451 was used as the shadow apparatus. Shots were made with the FP-22 ciné camera with a taking speed of 100,000 frames/sec. Constancy of the taking frequency during one shot was secured with an accuracy of greater than 0.2%. The problem of exposure in high-speed filming is considered. A relation between the real time of exposure and the latitude of the film is obtained. On the authors' evaluation, the real time of exposure of a frame for ciné films A_2, D_H, D_K, and A-35 correspond to 1.43, 1.62, 2.04, and 1.54 times less than full exposure time. Results have been obtained for the angles of connected discontinuities on a wedge-shaped model and the angles of separation of weak disturbances in the stream. A number of photographs are reproduced. —*S. C. G.* (translated from *Referativnyi Zhur., Fizika*)

Progress of Photography in Japan during 1958–1959

The Bulletin of the Society of Scientific Photography of Japan, No. 9, Dec. 1959 (Editorial Office: Chiba University, Matsudo-shi, Chiba Pref.)

This periodic report contains reviews (in English) of Japanese work during the period May 1958—May 1959 on photographic sensitivity, sensitive materials, special photographic agents, photographic raw materials, processing, equipment, evaluation of the photographic image, and applied photography. The reviews cover both published papers and papers presented at scientific meetings, as well as patents and new products. For reviews covering the period May 1956—May 1957, see the *Bulletin*, No. 7, Dec. 1957; for the period May 1957—May 1958, the *Bulletin*, No. 8, Jan. 1959.

A Method of Processing Multilayer Photographic Materials with Color Development

Avt. Svid. 113492 (in Russian), V. K. MILOSLAVOV, filed March 21, 1957

On coming out of the fixing solution after color development, the sound-track is coated separately from the remainder of the film with a viscous solution of a hypo-destroyer, e.g., an aqueous solution of iodine and potassium iodide, saturated with Tylose [methyl cellulose], after which it is immersed in a bleaching bath, and further separate processing of the sound-track and the image is carried out by one of the known methods. In order to eliminate the last hypo-solution on processing materials provided with a filter layer of metallic silver, they are coated following a short immersion of the film in a bleaching bath, after which the film is again immersed in the bleaching bath so as to finish the bleaching process. It is shown that if, on processing the film according to the method described in Avt. Svid. 82276, the optical density of the silver remaining in the sound-track does not exceed 0.5, on processing by the proposed method the optical density of the sound-track reaches 1.25.—*S. C. G.* (translated from *Tekh. Kino i Televideniya*)

Journal of the Society of Scientific Photography of Japan

Vol. 22, No. 4, December 1959 (in Japanese)

Résumés by S. Kikuchi and T. H. James

Processing and Properties of Polycarbonate and Dimensional Change of Films

MASAO ISOZAKI (*Govt. Chem. Ind. Research Inst., Tokyo Hiratsuka-shi, Kanagawa Pref.*), pp. 173–178

A review.

Solarization with Gamma-Rays and Electrons

AKIO MIYAUCHI AND YASUO SHIMIZU (*Fuji Photo Film Co., Ltd., Minamiashigara, Kanagawa, Japan*), pp. 179–184

Earlier studies on reciprocity failure in the region of solarization for exposures to γ-rays and electrons (*P S & E*, **4**: 117 (1960)) have been extended to obtain results of greater precision. The film was shielded from the action of stray radiation and from accumulation of static charge. Fuji X-ray film was used, and the emulsion on the side opposite to the direction of exposure was removed after development. Exposures were made in the electron microscope with accelerating potentials of 50, 80, and 100 kv. The electron density range was 10^{-6}–10^{-12} amp/sq cm and the time range 0.005–10,000 sec. A surface developer was used consisting of 2.0 grams Metol, 8.0 grams ascorbic acid, 4.0 grams hydroquinone, 28.0 grams sodium carbonate monohydrate, and 1.0 gram potassium bromide per liter. Characteristic curves and reciprocity curves are given for exposures to 50 and 80 kv electrons. No reciprocity failure was found for exposures in the normal region of increasing density, but marked high-intensity reciprocity failure was observed in the region of solarization. A high degree of solarization was obtained, showing that the vacuum in the electron microscope did not act as an effective halogen acceptor.

Exposures also were made to gamma rays from Co-60 and Cs-137. The distance of the source from the film was varied from 1 to 316 cm and the intensity from 0.003 to 3 r/sec. Various types of pretreatments of the film were tried: (1) It was soaked in sodium nitrite solution, 1 or 10 grams/liters, for 2 min and dried rapidly without washing. (2) It was soaked in sodium hydroxide solution (1, $^1/_4$, $^1/_{16}$, $^1/_{160}$ N) for 3 min, bathed in water, and dried naturally. (3) It was soaked in acetic acid solution (1, $^1/_4$, $^1/_{16}$, $^1/_{160}$ N) for 2 min and dried naturally without washing. (4) It was washed in running water for 5 min and dried naturally. Reciprocity curves are given for the controls and for the films (industrial and medical X-ray) with various treatments. Nitrite, which acts as a halogen acceptor, decreased solarization. The reciprocity failure curves for the nitrite and acetic acid treated film were shifted towards the high-exposure side along the constant-exposure time axis. Bathing in water decreased the low-intensity failure. A brief discussion of the results is given as they are explained by dependence of the destruction of latent image by positive holes on intensity and by the existence of reciprocity failure induced by the formation of latent subsurface image by γ-rays.

Studies on the Light Polarizer. 2. Infrared Polarizer

TSUTOMU YODA, HIROSHI NAKAMURA, HEIZABURO IDE, AND KAZUO NISHI (*Ofuna Factory, Mitsubishi Electric Mfg. Co., Ltd., Ofuna, Kamakura-shi, Kanagawa Pref., Japan*), pp. 185–189

Polarizers containing a relatively high concentration of linear polyiodine on oriented polyvinyl alcohol film have been used as dichroic film polarizers for infrared radiation (cf. R. P. Blake, A. S. Makas, and C. D. West, *J. Opt. Soc. Am.*, **39:** 1054 (1949); *Polaroid Reporter*, No. 1, p. 2 (1951)). Polarizers of this type can be prepared by treating a sheet of polyvinyl alcohol with a solution of iodine (e.g. 30 grams iodine, 30 grams KI, 200 cc water) and subsequently stretching the sheet to orient the molecules and heating it for a short time at 220–230°C. The authors have investigated modifications of this procedure in which the composition of the iodizing bath, the duration of treatment, and the temperature of heating were varied. They found that the use of a formaldehyde bath, either alone or added to the iodizing bath, permitted the preparation of the polarizer at a lower heating temperature and with less danger of tearing the stretched film. For example, they prepared a polarizer by treating a sheet of polyvinyl alcohol 0.05 mm thick with an iodizing solution consisting of 2 grams iodine, 20 grams KI, 20 cc formol, 20 cc sulfuric acid, and 160 cc water. The formol had a density of 1.085 and the sulfuric acid 1.826 at 28°C. The iodized film was stretched and heated at 120°C. Graphs showing the spectral polarizing characteristics of films prepared with iodizing baths of various compositions, and for various heat treatments are given for wavelengths extending from the visible to 2 μ. The best sheets showed a high transmittance for parallel light and nearly constant polarizing characteristics over the spectral range 0.8–2.0 μ.

The Effects of Stabilizers on the Production of Ag_2S by Labile Sulfur. II. The Inhibiting Action of Several Stabilizers on the Production of Ag_2S by Thiourea

TEIJI HABU (*Chemical Research Laboratory, Konishiroku Photo Ind. Co., Ltd., Hinomachi, Tokyo, Japan*), pp. 190–193

The inhibiting action of several stabilizers on the

formation of silver sulfide in the reaction between thiourea and silver bromide was studied by the procedure described earlier (*P S & E*, **4**: 58). The reactions were carried out in buffered solutions of pH 5.91, 6.47, 6.98, 7.38, and 8.01. When the ratio of the stabilizer, 5-methyl-7-hydroxy-1,2,3,4,6-pentazaindene, to thiourea was 100:1, the stabilizer substantially prevented sulfide formation at each pH, whereas when the ratio was only 10:1 it only decreased sulfide formation. Benzotriazole (100:1 ratio) also prevented sulfide formation, but 6-nitrobenzimidazole, benzimidazole, 4-ethoxy-6-methyl-1,3,3a,7-tetrazaindene, and bromotriazole had only slight or no restraining effect. The pentazaindene is considered to be the best stabilizer without showing desensitization.

Measurement of Relative Spectral Sensitivity of Photographic Materials

TERUO BABA AND KOHEI ITANO (*Chemical Research Laboratory, Konishiroku Photo Ind. Co., Ltd., Hinomachi, Tokyo, Japan*), pp. 194–197

Measurements were made of the relative spectral sensitivities of Konipan SS and SSS, Neopan SSS, on Plus-X films, using a series of narrow band filters. Exposures were given for 0.02 sec on the KSI sensitometer. One part of the film was exposed through a filter of the Kani-gelatin 801–820 series while the other part was exposed through a neutral step wedge. The density of the neutral wedge, D_w, which gave the same density as the filter on the developed film, was determined, and the corresponding transmittance, T_w, was calculated. Results are tabulated and equations are given for the calculation of the relative spectral sensitivities, and the relative sensitivities are plotted against wavelength.

Color Reproduction with Fuji Color Negative Film

SHIN FUJISAWA, SEIYA YAMAGUCHI, AND SHIGERU WATANABE (*Fuji Photo Film Co., Ltd., Research Lab.*), pp. 198–201

Both daylight and artificial light contain ultraviolet components to which color film is sensitive. This ultraviolet sensitivity has a harmful effect on color reproduction, particularly in the recording of yellow and green objects, and the use of a filter which absorbs radiation of wavelength shorter than 410 m μ is recommended. Spectral transmittance curves are given for four filters which show a sharp cutoff at 400 m μ or shorter, and three which show a medium cutoff. The effects of the two types could not be distinguished.

Nuclear Emulsion Technique. II.

AKIRA HIRATA (Konishiroku Photo Film Co.), pp. 202–208

A review (see *P S & E*, **4**: 241 (1960) for Part I). Tables are given listing: penetration times in minutes for Azol, D-19b, and amidol developers and emulsions of several thicknesses (105–1050 μ) at 20°C; penetration times for presoaked emulsions at developer temperatures of 5, 10, 15, and 20°C; formulas and procedures for processing by the Sakura two-bath development method; formulas and procedure for processing by Amidol developers of pH 6.7 and 7.2.

Zhurnal Nauchnoi i Prikladnoi Fotografii i Kinematografii

Vol. 5, No. 3, May–June 1960 (in Russian).

Résumés by S. C. Goddard

Polarization Absorption Spectra of Some Cyanine Sensitizing Dyes

K. S. LYALIKOV AND I. V. SEMENCHENKO, pp. 161–167

Polarization absorption spectra of stretched films of polyvinyl alcohol, weakly dyed with 1,1′-diethylquino-(2,2′)-cyanine chloride (I) or pinacyanol, show that molecules of these dyes absorb light preferentially with the electric vector parallel to the long axis of the molecule. The measured dichroism of the absorption band in the visible region is sufficiently close to unity to allow the molecules of these dyes within the limits of the above absorption band to be represented by linear oscillators directed along the length of the axis of the molecule. In the ultraviolet region spectra, the measured dichroism of dye I was lower than in the visible region; this is explained by the smaller anisotropy of the corresponding electronic transition.

In films of polyvinyl alcohol and polyvinyl acetate dyed with dye I in concentrations of the order of 0.1 mole/cu dm, J-aggregates of the dye are formed, characterized by an intense absorption band. Dye II (3,3′-dimethyl-9-ethyl-4,5,4′,5′-dibenzo-thiacarbocyanine iodide) does not form J-aggregates in polyvinyl acetate film. On stretching films dyed with dyes I and II, a shift of approximately 100 cm^{-1} in the maxima of the J-band towards the shortwave is observed.

For J-aggregates of dye I in stretched film of polyvinyl acetate, the following absorption bands are characteristic: (a) J-band with maximum 578 m μ, polarized along the J-aggregate axis; (b) bands with maxima 500 and 537 m μ, the direction of polarization of which forms with the J-aggregate axis an angle in all cases larger than 54° 14′. The J-aggregates of dye II in stretched polyvinyl alcohol film absorb light throughout the whole spectrum preferentially with the electric vector parallel to the direction of stretch of the film, i.e. the J-aggregate axis. In the absorption spectrum of J-aggregates of dye II, bands polarized at large angles to the aggregate axis are absent. (*Translation of authors' abstract*)

Fluctuations in the Density of Charged Particle Tracks in Nuclear Emulsions

K. S. BOGOMOLOV, pp. 168–172

An experimental study of the density fluctuations of charged particle tracks in type R nuclear emulsions—normal, with incomplete digestion, and normal hypersensitized—shows that a binomial distribution gives a better fit than a Gaussian. The theory of the binomial distribution of density fluctuations is worked out.

A Study of the Temperature Dependence of Photographic Development V. Some Problems of Method in the Determination of the Energy of Activation of Development of Photographic Materials

V. I. SHEBERSTOV, pp. 173–182

In earlier parts of the series, the author used the variation of the rate of development with temperature as a means of obtaining the energy of activation of development, E. The validity of this approach might be questioned on the grounds of the complexity of the

system and he has now made a study of possible disturbing factors. It is confirmed that over the range of temperatures used in practice the variation of rate of development with temperature agrees well with the Arrhenius equation. Variation in the rate of diffusion within the system is shown experimentally not to invalidate the calculation of E, provided E is larger than 8–10 kcal/mole. Different authors have used different methods of expressing the rate of development, but all methods give approximately the same value for E. The most convenient expression, however, is the reciprocal of the time required to obtain a given density. The experimental determinations give a value of E which is not corrected for the energy of ionization or the heat of adsorption of the developing agent onto the grains. In addition, E is a statistical average of the processes taking place within a population of emulsion grains.

The Elimination of Errors in the Internal Masking of Color Multilayer Films

YU. B. VILENSKIĬ, CHEN'KUAN-MIN, L. F. PATRIKEEVA, and E. I. TUL'CHINSKAYA, pp. 183–186

The unwanted absorption of a dye used for color photography should be independent of the wanted absorption. When the wanted absorption of a dye is plotted against the unwanted absorption, full correction is represented by a straight line parallel to the wanted absorption axis. In practice, the relation is frequently a curve, owing to insufficient correction at low wanted densities and over-correction at high wanted densities. Such distortion in masking occurs when correction is made by a mixture of masking and nonmasking couplers in a single layer and is due to their different reactivities. Full color correction can be obtained by putting the masking and nonmasking couplers into separate layers of emulsion, the sensitivity of which differs in such a way as to offset the difference in reactivities of the dyes.

The Measurement of the Diffusion of Sensitizing Dyes into Gelatin

B. VLČEK AND S. VLČKOVA, pp. 187–194

The diffusion of the dyes into a gelatin gel was measured by determining the optical densities along the path of diffusion and reading off the dye concentrations from a calibration curve. Twelve dyes were studied in this way: they all fully complied with the Fick diffusion equation. Their coefficients of diffusion varied widely. Since the dyes used possessed the properties of cationic surface-active agents the effect of anionic surface active agents on their coefficients of diffusion was studied. A color coupler having anionic surface-active properties caused a steady fall in the diffusion coefficients as its concentration was increased, but other anionic surface-active agents behaved in a more complicated fashion. There is some connection between the sensitizing properties of the dyes and their adsorption by silver bromide grains.

The Choice of the Optimal Parameters in Stereo-Cinematography

A. N. SHATSKAYA, pp. 195–206

Adherence to the physiological criterion—the zone of stereoscopic depth—is the most important factor in stereocinematography, determining a good stereo effect and stereo vision without strain. The optical base for photography must be chosen so as to maintain the zone of stereoscopic depth. Two formulas are derived which meet this condition. The position of the footlight plane (i.e., the apparent plane in the stereoscopic picture which appears to coincide with the plane of the screen) during shooting can be conveniently determined, starting from the distribution of important objects in the subject field and dividing the over-all difference in horizontal parallax into two. Two formulas are derived to allow the calculation of the distance of such a footlight plane. (*Adapted from author's abstract*)

The Electrophotography of Proton Beams

B. M. GOLOVIN, I. S. ZHELUDEV, N. T. KASHUKEEV, V. M. FRIDKIN, AND A. ANTONOV, pp. 207–208, 1 pl.

Proton beams (maximum intensity approximately 10^8 protons/cm^{2}sec, energy 680 mev) were recorded on electrophotographic layers of ZnO, ZnS, CdS, and polycrystalline sulfur in polyvinylbutyral as binder. Edge effects producing a nonuniform background were eliminated by giving the materials a preliminary exposure to a contact optical raster. The most sensitive materials were ZnO and sulfur, requiring an exposure of 5–10 sec for the 680 mev beams. Characteristic curves for ZnO were obtained. In comparison with X-ray film, electrographic paper with a ZnO coating has a similar threshold sensitivity to protons with a higher contrast but a smaller latitude. Electrographic materials can therefore be used as a quick and reasonably sensitive method of adjusting charged particle beams and testing their uniformity.

Image Movement in Time Magnification with Image Compensation

A. S. DUBOVIK, pp. 209–217

A mathematical analysis leads to the following conclusions. (1) The center of reflection of the scanning lens in systems with image compensation changes its position relative to the intermediate image in the time of exposure of one frame, leading to movement of the image. In choosing the general center of reflection (scanning) it is necessary to take into account the magnitude of image motion for different parts of the working angle of the camera. (2) Image shift in depth has no influence on the photographic quality of the picture. (3) The movement of the image on exposure of a frame is proportional to the speed of the camera lens and to a large degree is determined by the distance of the reflecting plane of the mirror from its axis of rotation. (4) Movement of the image for a given lens speed is proportional to the size of the intermediate image (size of the mirror). The present investigation makes it possible to take image movement into account in correctly choosing an optical system for constructing a high-speed camera with image compensation.—*Adapted from author's abstract*

Changes in the Photographic Properties and Resolving Power of Ultra-Fine-Grain Emulsions During Digestion

I. A. NOVIKOV AND B. B. TSYRILINA (Letter to the Editors), pp. 218–219

In some ultra-fine-grain emulsions, grain growth occurs to a certain extent during digestion. The effect of this has been studied for a silver chloride paper emulsion. The effect of grain growth during digestion is to superimpose a fall on the usual increase in resolving power and gamma, the curves for these two quantities plotted against time of digestion showing a maximum.

The Connection Between the Photographic and Photoelectric Sensitivities of an Emulsion Layer

L. G. Gross (Letter to the Editors), pp. 219–220

In both ammoniacal and neutral emulsion layers the photoconductivity increases with increase in the length of ripening, i.e., with increase in the mean grain sizes. In all cases, photoconductivity decreased with increase in the time of digestion. This relation is explained as due to the formation of sensitivity centers consisting of electron acceptors. A comparison has also been made between the spectral sensitivity of an unsensitized silver bromide emulsion and its spectral photoconductivity. Both curves fall with increasing wavelength.

The Elementary Composition of K.Ya-2 and T-3 Nuclear Emulsions

M. F. Rodicheva (Letter to the Editors), p. 221

The results of analyses of the above Soviet nuclear emulsions, all 1958 batches, are tabulated.

Qualitative Characteristics of the Latent Image Formed by the Action of Ionizing Particles

A. L. Kartuzhanskiĭ (Letters to the Editors), pp. 221–223

Three different emulsions, type R nuclear, electron recording, and lantern slide, were exposed to β-rays from C^{14} and P^{32}, at temperatures of 40° and 0°C. From the developed materials, reciprocity-law curves were constructed for a given density. The curves are in good agreement with an equation which was put forward by Meiklyar for exposures to light (*Zhur. Eksp. Teor. Fiz.*, **23**: 217, 1952). On the assumption that the constants in this equation have the same meaning for light and particles, calculations have been made of N_0, the minimum number of silver atoms in a development center, and U, the energy of activation of thermal dissociation of a center. The results are tabulated for the three emulsions for the two β-ray sources and light. It is concluded that N_0 for a given emulsion does not depend on the nature or energy of the exposing radiation. U, however, is higher for charged particles than for light. It is suggested that, with exposure to light, U is the characteristic of the thermal dissociation of an unstable monoatomic center while with particles U measures the dissociation energy of much larger centers forming the latent image. Reciprocity failure for particles with the emulsions studied is produced by latent image regression.

A Dropper for Making Nuclear Emulsions

O. P. Grigor'ev and L. I. Shur (Letter to the Editors), pp. 223–224

An apparatus is described for the controlled addition of solutions to an emulsion in the course of preparation. It is intended particularly for the preparation of nuclear emulsions by the method of Demers.

The Graininess of the Photographic Image. I.

W. Romer, pp. 225–230

A review.

Photographic Science and Technology in Czechoslovakia

K. S. Lyalikov, pp. 230–234

A survey is made of the institutions and organizations carrying out photographic research work in Czechoslovakia, with some indication of the subjects being studied. They comprise a number of establishments belonging to the Czechoslovak Academy of Sciences, including the Optical Laboratory, the Institute of Nuclear Physics, and the Institute of Theoretical Physics. In addition work is also being done in the Physical Institute of the Charles University, the Research Institute for Sound and Image, the Film Faculty of the Academy of Arts, and in laboratories connected with the photographic, gelatin, and chemical industries.

International Colloquium on Scientific Photography

K. V. Chibisov, pp. 234–238

A report is given of the conference held at Liège, Belgium, September 14–19, 1959.

Soviet Books on Photography, Cinematography, and Related Fields of Knowledge in 1959

Pp. 239–240

A bibliography of books produced in Russia during 1959 is given. It is the first of a series of periodic bibliographies.

PHOTOGRAPHIC SCIENCE AND ENGINEERING
Volume 4, Number 6, November–December 1960

• New Products and Developments

FRANK SMITH

• Cameras and Accessories

Analab Instrument Corp. Oscilloscope Cameras

Analab Instrument Corporation, Cedar Grove, N.J., has announced the availability of Types 3000, 3001, 3002, and 3003 Oscilloscope Cameras. The basic building block for all the cameras is the binocular-viewing periscope that fits on the CRT bezel of the oscilloscope and contains a dichroic mirror that reflects 80% of the light from the CRT screen to the camera and transmits 20% of the light for simultaneous binocular viewing without parallax. The camera unit mounts on top of the periscope by means of a slip hinge that permits the two units to be separated readily. The slip hinge arrangement also permits easy access to the lens and shutter. A Polaroid Camera back permits finished-print recording on paper in 1 min and on film in 2 min. A special adapter lens for the cameras provides off-scope recording. A complete series of Graflex backs may also be used with these cameras.

Electro-Optical Systems, Inc., Stressed-Plate Shutter

Development of a shutter for high-speed electrooptical modulation of light beams in space or under rugged environmental conditions was described by Stuart M. Hauser of Electro-Optical Systems, Inc., in a paper presented before the Society of Photographic Instrumentation Engineers on August 4, 1960.

The stressed-plate shutter, which is a mechanical analog of the Kerr cell, consists of a glass plate mounted between a pair of rigid beams. Placed at either end of the beams are stacks of piezoelectric drivers. Voltage applied to these driver stacks causes them to expand or contract, depending on the polarity. This strain is transmitted by the rigid beam assembly to the glass plate, and causes temporary double refraction which will change the state of polarization of a light beam passing through the shutter plate. If the shutter plate is mounted between a pair of crossed or parallel polarizers, and a voltage is applied to the driver stacks, the shutter will change from light-transmitting to light-absorbing in a time as short as 100 μsec. The stressed-plate shutter requires about 3000 v for operation, compared with 35,000 v for the Kerr cell.

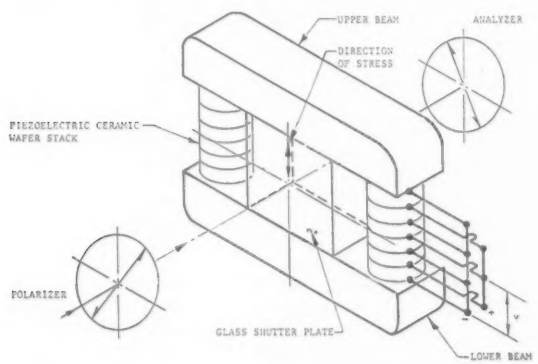

Although the information contained in this section is compiled from sources believed to be reliable, the author cannot assume responsibility for its accuracy. Publication of the information here is not to be construed as an endorsement or recommendation of the product or equipment described.

Geotechnical Corp. Auto-Processing Film Recorder-Viewer

A 16mm-film recorder-processor-viewer, called the Develocorder, for use with galvanometers or a cathode-ray tube, has been announced by the Geotechnical Corp., Garland, Texas. Data representing 4 to 32 hr of operation can be recorded on 200-ft reels of microfilm at speeds of 3 to 20 cm/min. Self-contained circulating chemicals are used to process the film automatically. The Develocorder displays the data magnified ten times on a 6 × 17-in. viewing screen within 2 to 20 min after recording. The date, time, and film number are optically printed on the film during recording. Time mark pulses are fed directly to the galvanometers. A plastic grid template can be placed over the viewing screen for data measurements. Film trace width is 0.5 mm.

Lockheed Take-Off and Landing Camera System

Lockheed Aircraft Corp., Burbank, Calif., has designed a one-camera airborne take-off and landing system for evaluation of the performance of these runs for any airplane or helicopter on an airfield or ground facility of known measurements. The system consists of a single motion-picture camera mounted in the aircraft so that the lens views the runway directly beneath the airplane and, through two canted mirrors, the runway boundaries. This produces a split-image recording, consisting of three images on each film frame.

Besides its use for take-off and landing performance, the system may be used for obtaining relative positions between airplanes, helicopters, and other objects in flight, and for obtaining information on approach path and landing techniques for simulator use.

• Processing Equipment & Techniques

Frigidheat Portable Thermal Unit

Frigidheat Industries, Box 6235, Nashville 12, Tenn., has developed a temperature control unit for photographic baths which consists of a reversible heat pump and a stainless coiled tubular spoon which is immersed in the bath. Correct solution temperature is obtained by adjusting a built-in percentage timer. The unit will change the temperature of 5 gal of solution 1° each 30 to 60 sec, depending on the starting temperature. The unit is shockproof and fast acting and operates in any type of tank or tray.

• Reproduction and Copying

Reproduction Engineering Corp. Rotary Contact Printer

Reproduction Engineering Corp., Essex, Conn., has announced a contact printer, called the Photo-Ray, for exposing black-and-white developing-out papers. The printer, which weighs 19 lb., is a continuous rotary-type machine using a single, rheostat-controlled fluorescent lamp and will expose contact proof paper at a rate of 16 ft/min. Negative and contact proof paper are placed in contact and fed into the electrically operated printer. Measuring 27 in. in over-all length, the unit can accommodate 14-in. wide negatives of any length.

• Sensitized Materials

Kodak Graphic Arts Films

Kodalith Royal Ortho Film, Estar Base, is four to five times faster than Kodalith Ortho Film, Type 3, Estar Base, and is recommended for making halftone images from color separations. The film is on 0.007-in. support for maximum dimensional stability. Kodalith Contact Film, Estar Base, is designed for making contact prints from various types of original material. The film has high safelight tolerance, permitting it to be handled under bright yellow safelights. The following five films have also been announced: Kodalith Ortho Matte Film, Type 3, Estar Base; Kodalith Ortho Film, Type 3, Estar Thick Base; Kodalith Pan Film, Estar Base; Kodak Pan Masking Film, Estar Base; and Kodak Auto-positive Film, Estar Base.

Ozalid Diazo-Sensitized Continuous-Tone Film 111CTF

A diazo-sensitized continuous-tone film for use in copying continuous-tone silver film originals has been introduced by the Ozalid Division of General Aniline and Film Corp., Johnson City, N.Y. The film has a sufficiently high specular density to be used in projection applications. To make a copy, the diazo-sensitized film is placed in emulsion-to-emulsion contact with the silver film, and the two sheets are fed through a diazo process machine. The continuous-tone duplicate is automatically exposed, developed, and delivered out of the machine in less than 30 sec.

• Miscellaneous

PROOF—Optical Fingerprint Recorder

Chance Vought Aircraft Inc., Box 5907, Dallas 22, Texas, has developed a compact, box-like optical instrument that records fingerprints without the use of ink or chemicals. Officially known as Precision Recording (Optical) of Fingerprints, but called, briefly, PROOF, the recorder uses a small glass area against which a finger is pressed, permitting the print pattern to be permanently recorded or projected on a screen for visual observation.

Recordak Reliant 500 Microfilmer

The Recordak Reliant 500 Microfilmer was introduced at the National Microfilm Association Show in New York on April 19, 1960.

The Reliant 500 will record on microfilm up to 500 checks or 185 letters in 1 min. This microfilmer retains many of the features of previous Recordak models, including Kodamatic Indexing to facilitate rapid retrieval of data, high-speed feeder, and document counter.

A feature of the Reliant 500 is the removable and interchangeable film unit. By changing film units, reduction ratios can be varied in seconds. In addition, this feature allows different departments within an organization to use a single microfilmer, yet retain their record continuity. Additional film units will be sold as accessories. Three reduction ratios will be available: 40 : 1, 32 : 1, and 24 : 1.

Tutor — An Automated Teaching Machine

Western Design, Div. of U.S. Industries, Inc., Goleta, Calif., has announced an automated teaching machine for military, industrial, and educational training programs.

Called Tutor, the machine is basically a random-access, recording microfilm–motion-picture projector. It presents either microfilmed or motion-picture material to the student, examines him on each point presented, and requires the student to demonstrate understanding of each point before it will pass to the next.

The material is handled on 35mm film and the machine has a capacity of 10,000 images, any of which may be called up, in any order, by entering the appropriate image number to the keyboard. Motion-picture sequences may be intermixed with still (microfilm) material, but the film moves only when a motion-picture sequence is desired.

Mast Radar Test Equipment

The LM-56A Radar Recording Camera Test Set, from Mast Development Co., Davenport, Iowa, performs four tests which completely check shutter, film movement, and control operations of five different radar recording cameras and their controls. These are: 0–15, 0–23, KS-30 (formerly 0–20), KS-31 (formerly 0–30) and KS-32 (formerly 0.32) Cameras. The LM-56A is also used for testing the M1 and M2 Control Systems and the LD-6 Exposure Frequency Control.

The four basic test phases are facilitated by a series of mechanical-optical displays. Phase I provides a simulated sweep display which is photographed by the camera being tested to check the shutter operation and to check film shift.

Phase II, similar to Phase I, also involves the photographing of a display with the camera being tested. The resulting exposures are of a graduated, circular scale with a superimposed light path created by a rotating light spot. The exposure can be read directly to determine the "shutter open" and "shutter closed" time periods with 0.001-sec accuracy.

Phase III utilizes a display of stationary lights to simulate an optical "bombsight." The display is photographed, and the exposed film is inspected to check camera accuracy for alternate photographing of a radar scope display and the target, simultaneously viewed through a bombsight.

Phase IV provides electrical pulses which are used to check camera controls. It also provides a means for visually checking camera shutter operation and for checking camera range lights.

The Radar Target Folder Viewer is designed to help bomber navigators find their way by means of PPI radar. It permits a fast visual comparison of a marked reconnaissance radar picture with the current scope image. Looking through the usual rubber face hood at his PPI, the navigator not only sees the scope but just below it a projected picture of the same size that was made during a reconnaissance run and subsequently marked for key points. It is installed with three screws without modification of the periscope.

Photographic
SCIENCE AND ENGINEERING

Volume 4 • 1960

Numbers 1–6

Official publication of the

Society of Photographic Scientists and Engineers

Box 1609, Main Post Office, Washington, D.C.

Photographic
SCIENCE AND ENGINEERING

official publication of the

Society of Photographic Scientists and Engineers

Volume 4, 1960

EDITORIAL STAFF

T. H. James
Editor

Jennie H. Allen
Managing Editor

H. F. Nitka
Associate Editor

Norman A. Exley
Assistant Editor

S. C. Goddard
Feature Editor

Frank Smith
Feature Editor

EDITORIAL REVIEW BOARD

J. H. Altman
R. S. Barrows
Richard L. Bent
B. R. Harriman
John H. Jacobs
R. Clark Jones
Peter Krause
John H. Ladd
K. G. Leistner
Marilyn Levy
C. S. McCamy
J. A. Maurer
F. W. H. Mueller
H. F. Nitka
W. S. Shoemaker
Thomas D. Smith
William West
Deane R. White

Photographic Science and Engineering is published six times a year by the Society of Photographic Scientists and Engineers.

• Address remittances, orders for subscriptions and for single copies, claims for missing numbers, and notices of change of address to the Society at Box 1609, Main Post Office, Washington, D.C. Subscription to nonmembers of the Society, $12.00 per year; subscription cost to members included in $8.00 annual dues; single copies, $2.00 each.

• The publication office is at 20th and Northampton Streets, Easton, Pa. Second-class mail privileges authorized at Easton, Pa. This publication is authorized to be mailed at the special rates of postage prescribed by Section 132.122.

• The Society is not responsible for the accuracy of statements made by authors and does not necessarily subscribe to their views.

© Copyright 1961 by the Society of Photographic Scientists and Engineers, Inc. Permission to reprint any part of the contents, except in reviews and abstracts, must be obtained in writing from the Editorial Vice President.

to penetrating electromagnetic radiation. The film is practically always surrounded by some material, if nothing more than the camera itself. When high-energy beta particles are stopped in matter, electromagnetic radiation (bremsstrahlung), physically identical to gamma and x-rays, is produced. Bremsstrahlung is much more penetrating than the beta radiation which gives rise to it, and thus can reach the film and affect it even when the beta radiation is entirely absorbed before it reaches the film.

To sum up, photography in the presence of gamma rays is quite feasible, and good records can be obtained by proper choice of film, camera exposure, and printing paper. Graininess may be a problem in some phases of photography, since the fogging gamma radiation inherently produces a much higher graininess than does visible radiation, and since comparatively long development times may be used. When there exists the possibility of fogging by gamma rays, particularly where very high gamma-ray exposures are anticipated, a film should be chosen which has a high ratio of light sensitivity to gamma-ray sensitivity, a high contrast, and a long scale of useful gradient. Long printing times can be expected for gamma-ray-fogged negatives but this may be of minor significance.

Photographic Science and Engineering deeply regrets the omission from page 296, Volume 4, Number 5 (September-October 1960), of the last 26 lines of "The Effect of Gamma-Ray Exposure on Camera Films," by G. M. Corney. The lines are supplied above for pasting into copies of *P S & E* or binding in when volumes are bound.

Photographic Science and Engineering

VOLUME 4—1960; NUMBERS 1–6

TITLE INDEX

Abridged Color-Projection Systems, A Demonstration of Color Perception with
C. S. McCAMY No. 3, p. 155

Addition Agents, Influences of Some on the Color of Developed Silver from Liquid Photographic Emulsion
K. FUTAKI, Y. OHYAMA, AND T. IWASAKI No. 2, p. 97

Addition Agents, The Influence of Some, on the Rate of Development of Liquid Photographic Emulsion
K. FUTAKI AND Y. OHYAMA No. 5, p. 257

Additive Color Photography, Reappraisal of
L. H. WHEELER No. 5, p. 302

Advance Program, 1960 Annual Conference No. 2, p. 122

Aerial Photography, Rapid-Drying Characteristics of Several Films for
JAMES W. BOYD No. 6, p. 354

Aerosol Development, High-Resolution Xerography by
J. T. BICKMORE, M. LEVY, AND J. HALL No. 1, p. 37

3-Aminopyrazoline Derivatives, The Superadditivity of Mixtures of Hydroquinone and
H. ULRICH AND H. SCHUELER No. 4, p. 225

Ammonia-Complex Solutions, Saturated Bromide- and, Experiments on the Formation and Crystallographic Stability of Silver Bromide Grains in
R. MATEJEC No. 5, p. 281

Ammonium Thiosulfate Solutions, Concentrated, The Stability of, at High Temperature
G. I. P. LEVENSON No. 2, p. 101

Awards and Citations
Journal Awards: William West and Vernon I. Saunders No. 4, p. 248
New Honorary Member Douglas A. Spencer No. 4, p. 185

Ballistic Plates, Interference Comparators for Coordinate Measurement of
A. CHITAYAT No. 5, p. 249

Book Reviews
The Audio Cyclopedia, by H. M. Tremaine, rev. by C. J. BARTLESON No. 2, p. 115
Control Techniques in Film Processing, by Walter I. Kisner and others, rev. by HOLLIS N. TODD No. 6, p. 359
Electronic Flash Photography, by Ralph L. Aspden, rev. by H. G. MORSE No. 3, p. 178
The Elements of Style, by William Strunk, Jr., rev. by T. H. JAMES No. 2, p. 116
Eye, Film, and Camera in Color Photography, by Ralph M. Evans, rev. by H. K. HOWELL No. 2, p. 115
Fundamentals of Photographic Theory, by T. H. James and G. C. Higgins, rev. by W. S. SHOEMAKER No. 3, p. 178
Keemag Graphic Solutions in the Use of Lenses, by Joseph D. Brubaker, rev. by J. W. GOSLING No. 4, p. 239
Kino—A History of the Russian and Soviet Film, by Jay Leyda No. 6, p. 359
Modern Geometrical Optics, by Max Herzberger, rev. by D. C. GILKESON No. 2, p. 114
The Optical Industry Directory, rev. by F. H. PERRIN No. 6, p. 359
The Study of Elementary Particles by the Photographic Method, by C. F. Powell, P. H. Fowler, and D. H. Perkins, rev. by T. H. JAMES No. 5, p. 305

Bromide- and Ammonia-Complex Solutions, Saturated, Experiments on the Formation and Crystallographic Stability of Silver Bromide Grains in
R. MATEJEC No. 5, p. 281

Bromination of Gelatin, The
WALTER COOPER No. 3, p. 160

Changes in pH in Photographic Coatings during Development, Measurement of
J. EGGERS No. 5, p. 284

Characteristic Curve, Contribution to the Theory of the
H. FRIESER AND E. KLEIN No. 5, p. 264

Characteristic Curves of Elementary and Thick Layers, Theoretical Considerations Concerning the Relationship between
E. KLEIN No. 6, p. 341

Chemical Ripening, Effect of, on the Photographic Response to Light, X- and Gamma Radiation
D. A. NEPELA AND H. F. NITKA No. 1, p. 12

Cinemicrography, High-Speed, of Electrically Exploded Tungsten and Molybdenum Wires
L. ZERNOW, G. WOFFINDEN, AND K. N. KREYENHAGEN No. 1, p. 31

Cloud Undercast Presentation for Flight Simulator Operation
W. B. KLEMPERER AND J. E. EKSTROMER No. 5, p. 296

Color Balance and Camera Lens Color
F. C. WILLIAMS AND F. GRUM No. 2, p. 113

Color Correction and Frequency Response, On the Relation between, in the Central Part of the Image of a Group of Photographic Systems
T. MALINOWSKI AND W. MANDLER No. 6, p. 317

Color Film for Automatic Exposure Controlled Cameras —Measuring and Judging Photographic Exposure of
ALLEN STIMSON No. 4, p. 203

Color Films, Reversible, Speed Rating of
S. R. ALBRO AND I. B. CURRENT No. 2, p. 65

Color Perception with Abridged Color-Projection Systems, A Demonstration of
C. S. McCAMY No. 3, p. 155

Color Photography at 400,000 Frames Per Second
WINSTON O. S. JOHNSON No. 5, p. 300

Color Photography, Reappraisal of Additive
L. H. WHEELER No. 5, p. 302

Color Printer, A High-Speed
A. M. GUNDELFINGER, E. A. TAYLOR, AND W. R. YANCEY No. 3, p. 141

Color Slides, Projected, Two Psychophysical Methods for Evaluating the Quality of
W. WOODBURY No. 2, p. 69

Comparators, Interference, for Coordinate Measurement of Ballistic Plates
A. CHITAYAT No. 5, p. 249

Computer Memory, Photographic Problems Associated with the Construction of a Large
M. B. PURVIS AND G. V. DEVERALL No. 2, p. 90

Contrast Transfer Function of Photographic Layers, Spread Function and
H. FRIESER No. 6, p. 324

Crystallographic Stability of Silver Bromide Grains, Experiments on the Formation and, in Saturated Bromide- and Ammonia-Complex Solutions
R. MATEJEC No. 5, p. 281

Detail Rendition, The Effect of the Variables of a Photographic System on, with Special Reference to Camera Motion
ROBERT N. WOLFE AND SAM A. TUCCIO No. 6, p. 330

Developed Silver from Liquid Photographic Emulsion, Influences of Some Addition Agents on the Color of,
K. FUTAKI, Y. OHYAMA, AND T. IWASAKI No. 2, p. 97

Developers, 1-Phenyl-3-Pyrazolidone-Hydroquinone, A Study of the Oxidation of, by Infrared Analysis
G. R. VAN VEELEN AND H. RUYSSCHAERT No. 3, p. 129

Developing Agents, Photographic: 2. Quinones
R. W. HENN, J. F. TINKER, AND H. L. FIELDING No. 3, p. 167

Development by the Ferro-EDTA Complex Ion, Kinetics of
T. H. JAMES No. 5, p. 271

Development Kinetics of a p-Phenylenediamine-Type Developer and a Metol-Hydroquinone Developer, Comparison of
R. B. PONTIUS, R. M. COLE, AND R. J. NEWMILLER No. 1, p. 23

Development, Measurement of Changes in pH in Photographic Coatings during
J. EGGERS No. 5, p. 284

Development of Liquid Photographic Emulsion, The Influence of Some Addition Agents on the Rate of,
K. FUTAKI AND Y. OHYAMA No. 5, p. 257

Development, Photographic, by Hydroquinone Compounds with Positively Charged Groups
J. F. WILLEMS No. 2, p. 101

Discussion and Evaluation
Is There a Future for Photooptical Instrumentation for Metric Purposes in Missile Testing?
C. W. BEMISS No. 3, p. 176

Eyepieces in Photography
G. H. MATTER No. 4, p. 234

Reappraisal of Additive Color Photography
L. H. WHEELER No. 5, p. 302

Distortion, Nonlinear, Caused by Photographic Lenses, A Method of Measuring
K. KINOSHITA, H. SATO, AND S. TATUOKA No. 2, p. 86

Dodging Printers, A Sensitometric Method of Measuring the Masking Effect of
KARL LEISTNER No. 1, p. 44

Effect of the Variables of a Photographic System on Detail Rendition, with Special Reference to Camera Motion
ROBERT N. WOLFE AND SAM TUCCIO No. 6, p. 330

Electric Fields, Enhancement of Photographic Speed and Sensitivity by
JEROME ROTHSTEIN No. 1, p. 5

Electrothermography—A New Electrostatic Printing Technique
P. M. CASSIERS No. 4, p. 199

Emulsion, Print-Out, with a Component of Silver Azide
YOSHITADA TOMODA No. 4, p. 196

Enhancement of Photographic Speed and Sensitivity by Electric Fields
JEROME ROTHSTEIN No. 1, p. 5

Enlarger, The 20× Precision
R. D. PICKERING No. 4, p. 213

Exposure, Gamma-Ray, The Effect of, on Camera Films
G. M. CORNEY No. 5, p. 291
Erratum No. 6, facing p. 367

Exposure, Photographic, of Color Film for Automatic Exposure Controlled Cameras, Measuring and Judging
ALLEN STIMSON No. 4, p. 203

Exposures, Camera, Safety Factors in
C. N. NELSON No. 1, p. 48

Eyepieces in Photography
G. H. MATTER No. 4, p. 234

Ferro-EDTA Complex Ion, Kinetics of Development by the
T. H. JAMES No. 5, p. 271

Film Thickness Variations, The Effect of, on Coherent Light
ARTHUR L. INGALLS No. 3, p. 135

Flight Simulator Operation, Cloud Undercast Presentation for
W. B. KLEMPERER AND J. E. EKSTROMER No. 5, p. 296

Formation and Crystallographic Stability of Silver Bromide Grains in Saturated Bromide- and Ammonia-Complex Solutions, Experiments on the
R. MATEJEC No. 5, p. 281

Frequency Response and Color Correction, On the Relation between, in the Central Part of the Image of a Group of Photographic Systems
T. MALINOWSKI AND W. MANDLER No. 6, p. 317

Gamma Radiation, Effect of Chemical Ripening on the Photographic Response to Light, X-, and
D. A. NEPELA AND H. F. NITKA No. 1, p. 12

Gamma-Ray Exposure, The Effect of, on Camera Films
G. M. CORNEY No. 5, p. 291
Erratum No. 6, facing p. 367

Gamma-Ray Sensitometer, An Automatic, Using Cobalt-60 Foil Sources
V. G. MCININCH AND H. M. CLEARE No. 2, p. 78

Gelatin, Photographic, A Novel Method for Characterizing
F. W. H. MUELLER AND C. B. ROTH No. 3, p. 151

Gelatin, The Bromination of
WALTER COOPER No. 3, p. 160

Glass Screen Halftone Sensitometer, A
RAYMOND ALFAYA No. 2, p. 74

High Polymers, New Types of Photography Involving
GERALD OSTER No. 4, p. 237

High-Resolution Xerography by Aerosol Development
J. T. BICKMORE, M. LEVY, AND J. HALL No. 1, p. 37

High-Speed Cinemicrography of Electrically Exploded Tungsten and Molybdenum Wires
L. ZERNOW, G. WOFFINDEN, AND K. N. KREYENHAGEN No. 1, p. 31

High-Speed Color Printer, A
A. M. GUNDELFINGER, E. A. TAYLOR, AND R. W. YANCEY No. 3, p. 141

High-Speed Motion Pictures, Magnesium, A New Light Source in Flashlamps for Sequence and
W. C. FINK No. 4, p. 208

Hydroquinone and 3-Aminopyrazoline Derivatives—The Superadditivity of Mixtures of
H. ULRICH AND H. SCHUELER No. 4, p. 225

Hydroquinone Compounds with Positively Charged Groups, Photographic Development by
J. F. WILLEMS No. 2, p. 101

Infrared Analysis, A Study by, of the Oxidation of 1-Phenyl-3-Pyrazolidone-Hydroquinone Developers
G. F. VAN VEELEN AND H. RUYSSCHAERT No. 3, p. 129

Interference Comparators for Coordinate Measurement of Ballistic Plates
A. CHITAYAT No. 5, p. 249

Interferometer Patterns, Resolving Power of Photographic Materials as Determined from
H. THIRY No. 1, p. 19

Kinetics, Development, of a p-Phenylenediamine-Type Developer and a Metol-Hydroquinone Developer, Comparison of
R. B. PONTIUS, R. M. COLE, AND R. J. NEWMILLER No. 1, p. 23

Kinetics, Monobath, An Approach to
R. E. SWING AND S. A. BARRY No. 3, p. 173

Kinetics of Development by the Ferro-EDTA Complex Ion
T. H. JAMES No. 5, p. 271

Lens Color, Camera, and Color Balance
F. C. WILLIAMS AND F. GRUM No. 2, p. 113

Lenses, Photographic, A Method of Measuring Nonlinear Distortion Caused by
H. SATO AND S. TATUOKA No. 2, p. 86

Light Source, Magnesium, A New, in Flashlamps for Sequence and High-Speed Motion Pictures
W. C. FINK No. 4, p. 208

Light, X- and Gamma Radiation, Effect of Chemical Ripening on the Photographic Response to
D. A. NEPELA AND H. F. NITKA No. 1, p. 12

Magnesium, A New Light Source in Flashlamps for Sequence and High-Speed Motion Pictures
W. C. FINK No. 4, p. 208

Masking Effect of Dodging Printers, A Sensitometric Method of Measuring
KARL LEISTNER No. 1, p. 44

Measuring and Judging Photographic Exposure of Color Film for Automatic Exposure Controlled Cameras
ALLEN STIMSON No. 4, p. 203

Mees, C. E. K.—Obituary and Bibliography
T. H. JAMES No. 6, p. 313

Metol-Hydroquinone Developer and a p-Phenylenediamine-Type Developer, Comparison of Development Kinetics of a
R. B. PONTIUS, R. M. COLE, AND R. J. NEWMILLER No. 1, p. 23

Monobath Kinetics, An Approach to
R. E. SWING AND S. A. BARRY No. 3, p. 173

New Products and Developments
FRANK SMITH No. 1, p. 62; No. 2, p. 120; No. 3, p. 183; No. 4, p. 245; No. 5, p. 310; No. 6, p. 364

Nonlinear Distortion Caused by Photographic Lenses, A Method of Measuring
K. KINOSHITA, H. SATO, AND S. TATUOKA No. 2, p. 86

Notes from the Editor
T. H. JAMES No. 3, p. 175; No. 4, p. 248

Obituary and Bibliography—C. E. K Mees
T. H. JAMES No. 6, p. 313

Oxidation of 1-Phenyl-3-Pyrazolidone-Hydroquinone Developers, A Study by Infrared Analysis of the
G. F. VAN VEELAN AND H. RUYSSCHAERT No. 3, p. 129

Persistent Internal Polarization in Phosphors, A Photographic Process Using a
H. P. KALLMANN, JOSEPH RENNERT, AND M. SIDRAN No. 6, p. 345

pH in Photographic Coatings during Development, Measurement of Changes in
J. EGGERS No. 5, p. 284

Phosphors, A Photographic Process Using a Persistent Internal Polarization in
H. P. KALLMANN, JOSEPH RENNERT, AND M. SIDRAN No. 6, p. 345

Photographic Problems Associated with the Construction of a Large Computer Memory
M. B. PURVIS AND G. V. DEVERALL No. 2, p. 90

Photographic System, An Equation of State for the
R. W. SWENSON No. 4, p. 219

Photography Involving High Polymers, New Types of
GERALD OSTER No. 4, p. 237

Photooptical Instrumentation for Metric Purposes in Missile Testing, Is There a Future for
C. W. BEMISS No. 3, p. 176

Polarization in Phosphors, A Photographic Process Using a Persistent Internal
H. P. KALLMANN, JOSEPH RENNERT, AND M. SIDRAN
No. 6, p. 345

Polymers, High, New Types of Photography Involving
GERALD OSTER No. 4, p. 237

p-Phenylenediamine-Type Developer and a Metol-Hydroquinone Developer, Comparison of Development Kinetics of a
R. B. PONTIUS, R. M. COLE, AND R. J. NEWMILLER
No. 1, p. 23

Precision Enlarger, The 20×
R. D. PICKERING No. 4, p. 213

Printer, A High-Speed Color
A. M. GUNDELFINGER, E. A. TAYLOR, AND W. R. YANCEY No. 3, p. 141

Printer Integrating Circuits, Analysis of
ROBERT K. RICKARD No. 5, p. 288

Printers, Dodging, A Sensitometric Method of Measuring the Masking Effect of
KARL LEISTNER No. 1, p. 44

Print-Out Emulsion with a Component of Silver Azide
YOSHITADA TOMODA No. 4, p. 196

Processing with Saturated Paper
SEYMOUR SCHRECK No. 5, p. 298

Program, Advance, 1960 Annual Conference
No. 2, p. 122

Projected Color Slides, Two Psychophysical Methods for Evaluating the Quality of
W. WOODBURY No. 2, p. 69

Quinones, Photographic Development Agents: 2.
R. W. HENN, J. F. TINKER, AND H. L. FIELDING
No. 3, p. 167

Radiation, Light, X- and Gamma, Effect of Chemical Ripening on the Photographic Response to
D. A. NEPELA AND H. F. NITKA No. 1, p. 12

Rapid-Drying Characteristics of Several Films for Aerial Photography
JAMES W. BOYD No. 6, p. 354

Reciprocity Characteristics of AgBr and AgCl Emulsions
A. HAUTOT No. 5, p. 254

Resolving Power of Photographic Materials as Determined from Interferometer Patterns
H. THIRY No. 1, p. 19

Reversible Color Films, Speed Rating of
S. R. ALBRO AND I. B. CURRENT No. 2, p. 65

Review: New Types of Photography Involving High Polymers
GERALD OSTER No. 4, p. 237

Safety Factors in Camera Exposures
C. N. NELSON No. 1, p. 48

Sensitization of Photographic Emulsions to X-Rays by Thallous Salts, Studies on the
YASUO WAKABAYASHI No. 1, p. 1

Sensitometer, A Glass Screen Halftone
RAYMOND ALFAYA No. 2, p. 74

Sensitometer, An Automatic Gamma-Ray, Using Cobalt-60 Foil Sources
V. G. MCININCH AND H. M. CLEARE No. 2, p. 78

Sensitometric Method of Measuring the Masking Effect of Dodging Printers, A
KARL LEISTNER No. 1, p. 44

Sequence and High-Speed Motion Pictures, Magnesium, A New Light Source in Flashlamps for
W. C. FINK No. 4, p, 208

Silver Bromide and Silver Chloride Emulsions, Reciprocity Characteristics of
A. HAUTOT No. 5, p. 254

Silver Bromide Grains in Saturated Bromide- and Ammonia-Complex Solutions, Experiments on the Formation and Crystallographic Stability of
R. MATEJEC No. 5, p. 281

Speed and Sensitivity, Photographic, Enhancement of, by Electric Fields
JEROME ROTHSTEIN No. 1, p. 5

Speed Rating of Reversible Color Films
S. R. ALBRO AND I. B. CURRENT No. 2, p. 65

Spread Function and Contrast Transfer Function of Photographic Layers
H. FRIESER No. 6, p. 324

Stability of Concentrated Ammonium Thiosulfate Solutions at High Temperature, The
G. I. P. LEVENSON No. 2, p. 101

Superadditivity of Mixtures of Hydroquinone and 3-Aminopyrazoline Derivatives, The
H. ULRICH AND H. SCHUELER No. 4, p. 225

Thallous Salts, Studies on the Sensitization of Photographic Emulsions to X-Rays by
YASUO WAKABAYASHI No. 1, p.1

Thiourea and Its Derivatives in Photographic Stabilization Processing
ROLF S. BRUENNER No. 4, p. 186

Tropical Storage of Processed Negatives
R. W. HENN AND I. A. OLIVARES No. 4, p. 229

Xerography, High-Resolution, by Aerosol Development
J. T. BICKMORE, M. LEVY, AND J. HALL
No. 1, p. 37

X-Rays, Studies on the Sensitization of Photographic Emulsions to, by Thallous Salts
YASUO WAKABAYASHI No. 1, p. 1

AUTHOR INDEX

ALBRO, S. R., AND CURRENT, I. B.
Speed Rating of Reversible Color Films No. 2, p. 65

ALFAYA, RAYMOND
A Glass Screen Halftone Sensitometer No. 2, p. 74

BARRY, S. A., AND SWING, R. E.
An Approach to Monobath Kinetics No. 3, p. 173

BEMISS, C. W.
Is There a Future for Photooptical Instrumentation for Metric Purposes in Missile Testing? No. 3, p. 176

BICKMORE, J. T., LEVY, M., AND HALL, J.
High-Resolution Xerography by Aerosol Development No. 1, p. 37

BOYD, JAMES W.
Rapid-Drying Characteristics of Several Films for Aerial Photography No. 6, p. 354

BRUENNER, ROLF S.
Thiourea and Its Derivatives in Photographic Stabilization Processing No. 4, p. 186

CASSIERS, P. M.
Electrothermography—A New Electrostatic Printing Technique No. 4, p. 199

CHITAYAT, A.
Interference Comparators for Coordinate Measurement of Ballistic Plates No. 5, p. 249

CLARK, WALTER
Citation—New Honorary Member Douglas A. Spencer No. 4, p. 185

CLEARE, H. M., AND MCININCH, V. G.
An Automatic Gamma-Ray Sensitometer Using Cobalt-60 Foil Sources No. 2, p. 78

COLE, R. M., PONTIUS, R. B., AND NEWMILLER, R. J.
Comparison of Development Kinetics of a p-Phenylenediamine-Type Developer and a Metol-Hydroquinone Developer No. 1, p. 23

COOPER, WALTER
The Bromination of Gelatin No. 3, p. 160

CORNEY, G. M.
The Effect of Gamma-Ray Exposure on Camera Films No. 5, p. 291
Erratum No. 6, facing p. 367

CURRENT, I. B., AND ALBRO, S. R.
Speed Rating of Reversible Color Films No. 2, p. 65

DEVERALL, G. V., AND PURVIS, M. B.
Photographic Problems Associated with the Construction of a Large Computer Memory No. 2, p. 90

EGGERS, J.
Measurement of Changes in pH in Photographic Coatings during Development No. 5, p. 284

EKSTROMER, J. E., AND KLEMPERER, W. B.
Cloud Undercast Presentation for Flight Simulator Operation No. 5, p. 296

FIELDING, H. L., HENN, R. W., AND TINKER, J. F.
Photographic Developing Agents: 2. Quinones No. 3, p. 167

FINK, W. C.
Magnesium, A New Light Source in Flashlamps for Sequence and High-Speed Motion Pictures No. 4, p. 208

FRIESER, H.
Spread Function and Contrast Transfer Function of Photographic Layers No. 6, p. 324

———, AND KLEIN, E.
Contribution to the Theory of the Characteristc Curve No. 5, p. 264

FUTAKI, K., AND OHYAMA, Y.
The Influence of Some Addition Agents on the Rate of Development of Liquid Photographic Emulsion No. 5, p. 257

———, OHYAMA, Y., AND IWASAKI, T.
Influences of Some Addition Agents on the Color of Developed Silver from Liquid Photographic Emulsion No. 2, p. 97

GRUM, F., AND WILLIAMS, F. C.
Color Balance and Camera Lens Color No. 2, p. 113

GUNDELFINGER, A. M., TAYLOR, E. A., AND YANCEY, R. W.
A High-Speed Color Printer No. 3, p. 141

HALL, J., BICKMORE, J. T., AND LEVY, M.
High-Resolution Xerography by Aerosol Development No. 1, p. 37

HAUTOT, A.
Reciprocity Characteristics of Silver Bromide and Silver Chloride Emulsions No. 5, p. 254

HENN, R. W., AND OLIVARES, I. A.
Tropical Storage of Processed Negatives No. 4, p. 229

———, TINKER, J. F., AND FIELDING, H. L.
Photographic Developing Agents: 2. Quinones No. 3, p. 167

INGALLS, ARTHUR L.
The Effect of Film Thickness Variations on Coherent Light No. 3, p. 135

IWASAKI, T., FUTAKI, K., AND OHYAMA, Y.
Influences of Some Addition Agents on the Color of Developed Silver from Liquid Photographic Emulsion No. 2, p. 97

JAMES, T. H.
Kinetics of Development by the Ferro-EDTA Complex Ion No. 5, p. 271

———
C. E. K. Mees—Obituary and Bibliography No. 6, p. 313

———,
Notes from the Editor No. 3, p. 175; No. 4, p. 248

JOHNSON, WINSTON O. S.
Color Photography at 400,000 Frames Per Second No. 5, p. 300

KALLMANN, H. P., RENNERT, JOSEPH, AND SIDRAN, M.
A Photographic Process Using a Persistent Internal Polarization in Phosphors No. 6, p. 345

KINOSHITA, K., SATO H., AND TATUOKA, S.
A Method of Measuring Nonlinear Distortion Caused by Photographic Lenses No. 2, p. 86

KLEIN, E.
Theoretical Considerations Concerning the Relationship between Characteristic Curves of Elementary and Thick Layers No. 6, p. 341

———, AND FRIESER, H.
Contribution to the Theory of the Characteristic Curve No. 5, p. 264

KLEMPERER, W. B., AND EKSTROMER, J. E.
Cloud Undercast Presentation for Flight Simulator Operation No. 5, p. 296

KREYENHAGEN, K. N., ZERNOW, L., AND WOFFINDEN, G.
High-Speed Cinemicrography of Electrically Exploded Tungsten and Molybdenum Wires No. 1, p. 31

LEISTNER, KARL
A Sensitometric Method of Measuring the Masking Effect of Dodging Printers No. 1, p. 44

LEVENSON, G. I. P.
The Stability of Concentrated Ammonium Thiosulfate Solutions at High Temperature No. 2, p. 110

LEVY, M., BICKMORE, J. T., AND HALL, J.
High-Resolution Xerography by Aerosol Development No. 1, p. 37

MALINOWSKI, T., AND MANDLER, W.
On the Relation between Color Correction and Frequency Response in the Central Part of the Image of a Group of Photographic Systems No. 6, p. 317

MANDLER, W., AND MALINOWSKI, T.
On the Relation between Color Correction and Frequency Response in the Central Part of the Image of a Group of Photographic Systems No. 6, p. 317

MATEJEC, R.
Experiments on the Formation and Crystallographic Stability of AgBr Grains in Saturated Bromide- and Ammonia-Ccmplex Solutions No. 5, p. 281

MATTER, G. H.
Eyepieces in Photography No. 4, p. 234

MCCAMY, C. S.
A Demonstration of Color Perception with Abridged Color-Projection Systems No. 3, p. 155

MCININCH, V. G., AND CLEARE, H. M.
An Automatic Gamma-Ray Sensitometer Using Cobalt-60 Foil Sources No. 2, p. 78

MUELLER, F. W. H., AND ROTH, C. B.
A Novel Method for Characterizing Photographic Gelatin No. 3, p. 151

NELSON, C. N.
Safety Factors in Camera Exposures No. 1, p. 48

NEPELA, D. A., AND NITKA, H. F.
Effect of Chemical Ripening on the Photographic Response to Light, X- and Gamma Radiation No. 1, p. 12

NEWMILLER, R. J., PONTIUS, R. B., AND COLE, R. M.
Comparison of Development Kinetics of a p-Phenylenediamine-Type Developer and a Metol-Hydroquinone Developer No. 1, p. 23

NITKA, H. F., AND NEPELA, D. A.
Effect of Chemical Ripening on the Photographic Response to Light, X- and Gamma Radiation No. 1, p. 12

OHYAMA, Y., AND FUTAKI, K.
The Influence of Some Addition Agents on the Rate of Development of Liquid Photographic Emulsion No. 5, p. 257

———, FUTAKI, K., AND IWASAKI, T.
Influences of Some Addition Agents on the Color of Developed Silver from Liquid Photographic Emulsion No. 2, p. 97

OLIVARES, I. A., AND HENN, R. W.
Tropical Storage of Processed Negatives No. 4, p. 229

OSTER, GERALD
New Types of Photography Involving High Polymers No. 4, p. 237

PICKERING, R. D.
The 20× Precision Enlarger No. 4, p. 213

PONTIUS, R. B., COLE, R. M., AND NEWMILLER, R. J.
Comparison of Development Kinetics of a p-Phenylenediamine-Type Developer and a Metol-Hydroquinone Developer No. 1, p. 23

PURVIS, M. B. AND DEVERALL, G. V.
Photographic Problems Associated with the Construction of a Large Computer Memory No. 2, p. 90

RENNERT, JOSEPH, KALLMANN, H. P., AND SIDRAN, M.
A Photographic Process Using a Persistent Internal Polarization in Phosphors No. 6, p. 345

RICKARD, ROBERT K.
Analysis of Printer Integrating Circuits No. 5, p. 288

ROTH, C. B., AND MUELLER, F. W. H.
A Novel Method for Characterizing Photographic Gelatin No. 3, p. 151

ROTHSTEIN, JEROME
Enhancement of Photographic Speed and Sensitivity by Electric Fields No. 1, p. 5

RUYSSCHAERT, H., AND VAN VEELEN, G. F.
A Study by Infrared Analysis of the Oxidation of 1-Phenyl-3-Pyrazolidone-Hydroquinone Developers No. 3, p. 129

SATO, H., KINOSHITA, K., AND TATUOKA, S.
A Method of Measuring Nonlinear Distortion Caused by Photographic Lenses No. 2, p. 86

SCHRECK, SEYMOUR
Processing with Saturated Paper No. 5, p. 298

SCHUELER, H., AND ULRICH, H.
The Superadditivity of Mixtures of Hydroquinone and 3-Aminopyrazoline Derivatives No. 4, p. 225

SIDRAN, M., KALLMANN, H. P., AND RENNERT, JOSEPH
A Photographic Process Using a Persistent Internal Polarization in Phosphors No. 6, p. 345

SMITH, FRANK
New Products and Developments (Technicalia Photographica) No. 1, p. 62; No. 2, p. 120; No. 3, p. 183; No. 4, p. 245; No. 5, p. 310; No. 6, p. 365

STIMSON, ALLEN
Measuring and Judging Photographic Exposure of Color Film for Automatic Exposure Controlled Cameras No. 4, p. 203

SWENSON, R. W
An Equation of State for the Photographic System No. 4, p. 219

SWING, R. E., AND BARRY, S. A.
An Approach to Monobath Kinetics No. 3, p. 173

TATUOKA, S., KINOSHITA, K., AND SATO, H.
A Method cf Measuring Nonlinear Distortion Caused by Photographic Lenses No. 2, p. 86

TAYLOR, E. A., GUNDELFINGER, A. M., AND YANCEY, R. W.
A High-Speed Color Printer No. 3, p. 141

THIRY, H.
Resolving Power of Photographic Materials as Determined from Interferometer Patterns No. 1, p. 19

TINKER, J. F., HENN, R. W., AND FIELDING, H. L.
Photographic Developing Agents: 2. Quinones No. 3, p. 167

TOMODA, YOSHITADA
Print-Out Emulsion with a Component of Silver Azide No. 4, p. 196

TUCCIO, SAM A., AND WOLFE, ROBERT N.
The Effect of the Variables of a Photographic System on Detail Rendition, with Special Reference to Camera Motion No. 6, p. 330

ULRICH, H., AND SCHUELER, H.
The Superadditivity of Mixtures of Hydroquinone and 3-Aminopyrazoline Derivatives No. 4, p. 373

VAN VEELEN, G. F., AND RUYSSCHAERT, H.
A Study by Infrared Analysis of the Oxidation of 1-Phenyl-3-Pyrazolidone-Hydroquinone Developers No. 3, p. 129

WAKABAYASHI, YASUO
Studies on the Sensitization of Photographic Emulsions to X-Rays by Thallous Salts No. 1, p. 1

WHEELER, L. H.
Reappraisal of Additive Color Photography No. 5, p. 302

WILLEMS, J. F.
Photographic Development by Hydroquinone Compounds with Positively Charged Groups No. 2, p. 101

WILLIAMS, F. C., AND GRUM, F.
Color Balance and Camera Lens Color No. 2, p. 113

WOFFINDEN, G., ZERNOW, L., AND KREYENHAGEN, K. N.
High-Speed Cinemicrography of Electrically Exploded Tungsten and Molybdenum Wires No. 1, p. 31

WOLFE, ROBERT N., AND TUCCIO, SAM A.
The Effect of the Variables of a Photographic System on Detail Rendition, with Special Reference to Camera Motion No. 6, p. 330

WOODBURY, W.
Two Psychophysical Methods for Evaluating the Quality of Projected Color Slides No. 2, p. 69

YANCEY, R. W., GUNDELFINGER, A. M., AND TAYLOR, E. A.
A High-Speed Color Printer No. 3, p. 141

ZERNOW, L., WOFFINDEN, G., AND KREYENHAGEN, K. N.
High-Speed Cinemicrography of Electrically Exploded Tungsten and Molybdenum Wires No. 1, p. 31

Back Issues Available

Photographic Engineering—1950–1956

Volumes 1 through 6 (4 issues each volume)	$5.00 per volume	$1.50 per issue
Volume 7 (2 single issues, Nos. 1 and 2, plus two issues, Nos. 3 and 4, combined under one cover)	5.00 per volume	1.50 per single issue 3.00 for combined issue

Photographic Science and Engineering—since 1957

Volumes 1 and 2 (4 issues each volume)	Members—$6.00 per volume	$1.75 per issue
Volume 3 (6 issues)	Nonmembers—8.00 per volume	2.00 per issue
Subscription to current volume (6 issues)	Nonmembers	$12.00
	Members	Included in $8.00 annual dues

An index appears in the final issue of each volume except Volume 6 of *Photographic Engineering*. This index was published separately and is included with the issues when Volume 6 is ordered.

Order from:

Edward S. Cobb, *Managing Secretary*
Society of Photographic Scientists and Engineers
Box 1609, Main Post Office
Washington, D.C.

The Society of Photographic Scientists and Engineers

Box 1609 • Main Post Office • Washington, D.C.

OFFICERS

President	GEORGE T. EATON, Building 59, Kodak Park, Rochester 4, New York
Executive Vice President	STEVEN LEVINOS, Ansco, Binghamton, New York
Engineering Vice President	JOHN A. MAURER, 116–118 West 29th Street, New York 1, New York
Editorial Vice President	R. CLARK JONES, Polaroid Corporation, 730 Main Street, Cambridge 39, Mass.
Financial Vice President	HERBERT MEYER, 325 Sequoia Drive, Pasadena 2, California
Secretary-Treasurer	FRANCIS J. HEYDEN, S.J., Georgetown College Observatory, Washington 7, D.C.
Managing Secretary	EDWARD S. COBB, Box 1609, Main Post Office, Washington, D.C.

CHAPTERS *and* CHAPTER OFFICERS

Binghamton, New York	*President*	HARRY G. MORSE, 326 Riverside Drive, Binghamton, New York
	Secretary	E. SCUDDER MACKEY, Stone Road, MR-98, Binghamton, New York
Boston, Massachusetts	*President*	JOHN B. TAYLOR, 290 Davis Road, Bedford, Massachusetts
	Secretary	MRS. SHEILA BARRY PATRAIKO, 1 Kilby Street, Woburn, Massachusetts
Chicago, Illinois	*President*	ROBERT W. MAZOR, Standard Studios, Inc., 540 North Michigan Avenue, Chicago 11, Illinois
	Secretary	NELSON W. RODELIUS, 2749 Reese Avenue, Evanston, Illinois
Cleveland, Ohio	*President*	HARRY L. FICHTER, JR., 1256 Overlook Road, Lakewood 7, Ohio
	Secretary	JOHN N. PIKE, 1480 Belle Avenue, Lakewood 7, Ohio
Monmouth, New Jersey	*President*	D. L. CASTELLINI, 98 Leland Terrace, New Shrewsbury, New Jersey
	Secretary	MISS MARILYN LEVY, 100 McLaren Street, Red Bank, New Jersey
New York, New York	*President*	HENRY CROIX, Industrial Photo Products, Inc., 86 Worth Street, New York 13, New York
	Secretary	JAMES W. HOWARD, Interchemical Corporation, 432 West 45th Street, New York 36, New York
Northern California	*President*	PHILIP B. CARNAHAN, Building 47, University of California, Berkeley 4, California
	Secretary	PETER L. CICCARELLO, Ansco Division, General Aniline & Film Corporation, 640 Second Street, San Francisco 8, California
Rochester, New York	*President*	JOHN F. ENGLERT, JR., Sales Service Division, Eastman Kodak Company, Rochester 4, New York
	Secretary	WOODLIEF THOMAS, JR., Color Technology Division, Eastman Kodak Company, Rochester 4, New York
Southern California	*President*	L. L. BUNNING, 9045 Fairview Avenue, San Gabriel, California
	Secretary	JOHN N. HARMAN, JR., 550 West Colorado Street, Glendale 4, California
Washington, D.C.	*President*	JOSEPH A. SCHANTZ, 5409 24th Avenue, S.E., Washington 21, D.C.
	Secretary	LOUIS WERNER, 3610 North Powhatan Street, Arlington 13, Virginia

Sustaining Members / Society of Photographic Scientists and Engineers

Abrams Instrument Corporation
Lansing 1, Michigan

Aero Service Corporation
Philadelphia 20, Pennsylvania

Ansco Division, General Aniline & Film Corporation
Binghamton, New York

Atkinson Laboratory, Incorporated
Hollywood 38, California

Atlantic Gelatin Div., General Foods Corporation
Woburn, Massachusetts

Bar-Ray Products, Incorporated
Brooklyn 32, New York

Bausch & Lomb Incorporated
Rochester 2, New York

Bell & Howell Company
Chicago 45, Illinois

Charles Beseler Company
East Orange, New Jersey

Bulova Watch Company, Inc., Photographic Division
Woodside 77, New York

Burke & James, Incorporated
Chicago 4, Illinois

Byron Motion Pictures, Incorporated
Washington 7, D.C.

Chicago Aerial Industries, Incorporated
Melrose Park, Illinois

Consolidated Film Industries
Hollywood 38, California

De Jur-Amsco Corporation
Long Island City 1, New York

E. I. du Pont de Nemours & Company
Parlin, New Jersey

Eastman Kodak Company
Rochester 4, New York

Edgerton, Germeshausen & Grier, Incorporated
Boston 15, Massachusetts

Elgeet Optical Company, Incorporated
Rochester 6, New York

Fairchild Camera & Instrument Corporation
Syosset, Long Island, New York

Farrand Optical Company, Incorporated
New York 70, New York

Oscar Fisher Company, Incorporated
MD-27, Newburgh, New York

FMA, Incorporated
El Segundo, California

The F-R Corporation
New York 56, New York

General Electric Company
Schenectady, New York

General Film Laboratories Corporation
Hollywood 28, California

Graflex, Incorporated
Rochester 8, New York

W. & L. E. Gurley Company
Troy, New York

Haloid Xerox Incorporated
Rochester 3, New York

Hardale Associates
New York 22, New York

Hi-Speed Equipment, Incorporated
Waltham 54, Massachusetts

Houston Fearless Corporation
Los Angeles 64, California

Charles A. Hulcher Company, Incorporated
Hampton, Virginia

Philip A. Hunt Company
Palisades Park, New Jersey

Hycon Manufacturing Company
Pasadena, California

Itek Corporation
Waltham 54, Massachusetts

The Kalart Company, Incorporated
Plainville, Connecticut

Kollmorgen Corporation
Northampton, Massachusetts

LogEtronics Incorporated
Alexandria, Virginia

L-W Photo Products Company
Northridge, California

J. A. Maurer, Incorporated
Long Island City 1, New York

The Morse Instrument Company
Hudson, Ohio

National Research and Chemical Company
Hawthorne, California

North American Aviation, Incorporated
Los Angeles 45, California

Pako Corporation
Minneapolis 11, Minnesota

Photogrammetry, Incorporated
Silver Spring, Maryland

Polaroid Corporation
Cambridge 39, Massachusetts

Rolor Industrial Corporation
New York 17, New York

Simmon Brothers, Incorporated
Long Island City 1, New York

Technicolor New York Corporation
New York 19, New York

Viewlex, Incorporated
Long Island City 1, New York

Wollensak Optical Company
Rochester 21, New York

Zoomar, Incorporated
Glen Cove, New York